UNIVERSITÀ DEGLI STUDI DI PADOVA

DIPARTIMENTO DI INGEGNERIA INDUSTRIALE

CORSO DI LAUREA MAGISTRALE IN INGEGNERIA CHIMICA E DEI PROCESSI INDUSTRIALI

Tesi di Laurea Magistrale in
Ingegneria Chimica e dei Processi Industriali

EXPERIMENTAL INVESTIGATION OF THE COMBINED EFFECT OF LIGHT AND TEMPERATURE ON MICROALGAE GROWTH IN MILLI-PHOTOBIOREACTORS

Relatore: Prof. Fabrizio Bezzo
Correlatrici: Prof.ssa Eleonora Sforza
Ing. Beatriz Felices Rando

Laureanda: ANGELA LOTTI

ANNO ACCADEMICO 2022-2023

Ai tuoi sogni e alla tua forza.
So che avresti brillato qui con me.

Abstract

Microalgae are emerging as highly promising and sustainable alternatives for energy production and the creation of environmentally friendly products. However, production costs still pose limitations for various applications. In this context, photobioreactors play a vital role in understanding the factors, including temperature, light conditions and nutrient availability that influence microalgal growth and its metabolic responses. The objective of this study is to present a suitable model for large-scale cultivation for investigating the combined effect of light and temperature and identify optimal growth conditions. For this purpose, a series of experiments were conducted using the microalga *Acutodesmus obliquus* in a small-scale photobioreactor of 45 mL with a 15 mm thickness, on its concentration, content and morphology. The outcomes emphasize the milli-PBRs capability to effectively capture and represent the same phenomena observed in large-scale microalgal growth. The biomass displayed its peak productivity at 30°C and 600 μmol m^{-2} s^{-1}, yielding a concentration of 2.49 g L^{-1}, consistent with literature studies, and a decline in growth rate as the conditions distance from the optimum. It is intriguing that the combined impact of light and temperature shows variations depending on the aspect being studied. The influence of temperature appears to be slightly more pronounced under high light conditions when considering concentration, under low light conditions when examining chlorophyll content and under moderate irradiance when evaluating cell size. It is worth noting that the utilized model of Bernard and Rémond (2012) which does not account for the joined effect, showed a bad fitting, especially under high light and low-temperature conditions, leading to the conclusion that the strongest interaction appears to manifest in these circumstances.

Riassunto esteso

Nell'arco dell'ultimo decennio, le microalghe hanno attirato sempre più interesse nell'ambito industriale, rappresentando una potenziale risposta alla crescente richiesta di fonti rinnovabili e sostenibili. Con lo sviluppo di sistemi efficienti di coltivazione su larga scala, la biotecnologia delle microalghe può rispondere alle esigenti richieste di alimenti, integratori alimentari, farmaci e biofertilizzanti. Tuttavia, l'accessibilità a tecnologie avanzate per la produzione di biodiesel a base di microalghe, rimane ancora troppo costosa. Sebbene si sia osservato un aumento della produttività a livello di laboratorio e su scala pilota utilizzando sistemi di fotobioreattori (PBRs), la loro implementazione su larga scala è limitata dalle sfide legate allo *scale-up* e ai costi elevati coinvolti. La crescita della biomassa in un PBR è un processo complesso, risultato di molteplici effetti, tra cui la luce, la disponibilità di nutrienti e la temperatura. Trovare un modello efficace che permetta di considerare l'influenza di queste variabili sulla crescita delle microalghe è essenziale sia per ottimizzare la crescita che per prevedere il comportamento in diverse condizioni operative. L'obiettivo di questa tesi è di investigare l'effetto combinato della temperatura e dell'intensità luminosa sulla crescita della microalga *Acutodesmus obliquus,* mantenendo un eccesso di disponibilità di nutrienti. Gli esperimenti sono stati condotti utilizzando un fotobioreattore da 45 mL operato in modalità continua e valutando le variazioni nella concentrazione (in termini di peso secco), nella composizione della biomassa (contenuto di pigmenti) e nella morfologia cellulare (dimensione e forma) al variare di luce e temperatura.

Confrontando i risultati con quelli ottenuti da studi passati in letteratura, essi hanno mostrato sia una coerenza a livello numerico sia a livello di andamento rispetto all'intensità di luce e alla temperatura, raggiungendo un picco di produttività in stato stazionario a 600 μmol m^{-2} s^{-1} e 30°C. Inoltre, alla temperatura di 36°C, la competizione con altri microorganismi che prosperano in condizioni di alta temperatura, è diventata più intensa. Questo ha provocato episodi di contaminazione più frequenti, limitando l'acquisizione di dati. Per quanto riguarda il contenuto di pigmenti, l'influenza della temperatura ha dimostrato una incoerenza rispetto ad alcune ricerche: il contenuto di clorofilla aumentava al diminuire della temperatura fino a intensità di luci circa 600 μmol m^{-2} s^{-1}. A luci più elevate, la temperatura non mostrava nessuna influenza rilevante sul contenuto di clorofilla. Questa osservazione è supportata da altri studi che hanno dimostrato un comportamento simile in alcune specie di alghe, tra cui *A. obliquus*, implicando che l'effetto della temperatura sul contenuto di clorofilla varia a seconda della specie. Inoltre, l'analisi respirometrica è stata uno strumento molto utile per valutare rapidamente l'influenza della temperatura sull'attività fotosintetica della microalga. Essa ha confermato i risultati ottenuti a lungo termine: i tassi di crescita più elevati sono stati raggiunti a temperature di circa 30°C, almeno per una coltura acclimatata a 30°C e 1200 μmol m^{-2} s^{-1}.

L'introduzione dell'analisi delle immagini come tecnica di monitoraggio quotidiano ha consentito la valutazione delle dimensioni e della forma delle cellule in diverse condizioni sperimentali. I risultati indicano che, a ciascun livello di intensità luminosa, l'aumento delle temperature porta a una riduzione delle dimensioni cellulari (con una riduzione del diametro fino a 1 μm). Questo effetto è particolarmente accentuato ad intensità luminose moderate, mentre l'impatto della temperatura sulla forma delle cellule è più evidente a luci molto basse o molto alte. Inoltre, considerando il modello implementato, costruito da Bernard e Rémond (2012), i risultati mostrano che offre una buona aderenza dei dati a 30°C (R^2>0,95), temperatura in prossimità dell'optimum trovato. Tuttavia, considerando temperature più basse e livelli di luce più elevati, l'aderenza del modello è compromessa, suggerendo un livello maggiore di interazione tra i fattori luce e temperatura. Questa situazione porta a parametri ottimizzati per questo scenario specifico, ma che potrebbero non catturare pienamente i processi fisici, chimici o biologici effettivi.

Table of contents

INTRODUCTION **1**
CHAPTER 1 - STATE OF ART AND THESIS OBJECTIVE **3**
1.1 Microalgae industrial utilizations 3
1.1.1 Classification 4
1.1.2 Acutodesmus obliquus 5
1.2 Photosynthetic process 6
1.2.1 Photosyntethic efficiency 8
1.3 Algal growth 8
1.3.1 Light 9
1.3.2 Nutrient availability 12
1.3.3 Temperature and pH 14
1.3.4 Culture mixing 15
1.4 Production systems 16
1.4.1 Open systems 16
1.4.2 Closed systems 19
1.4.3 Batch and continuous mode 21
1.4.4 Industrial scale-up 23
1.5 Mathematical models for microalgae growth 25
1.5.1 Models considering light as a single factor 25
1.5.2 Models considering light and temperature 27
1.6 Constraints to microalgae applications 28
1.7 Aim of the thesis 29
CHAPTER 2 – MATERIALS AND METHODS **31**
2.1 Microalgae strain and culture medium 31
2.2 Cultivation system 32
2.2.1 Milli-photobioreactors 34
2.3 Monitoring protocols 35
2.3.1 Optical density 35
2.3.2 Dry weight 36
2.3.3 Front and back irradiance measurements 37

2.3.4 Cell counting 37
2.3.5 Image analysis 38
2.3.6 Pigments 39
2.3.7 Orthophosphates 39
2.3.8 Respirometry 40
2.4 Mathematical model 42
CHAPTER 3 - RESULTS AND DISCUSSION 45
3.1 Biomass concentration and productivity at steady state 45
3.1.1 Dry weight results 46
3.1.2 Washout condition 49
3.1.3 Assessment of the self-shading effect 50
3.1.4 Biomass productivity 51
3.2 Pigment content 53
3.2.1 Temperature dependency on pigment content 56
3.3 Respirometry results 57
3.4 Image analysis results 59
3.5 Model simulation 65
CONCLUSIONS 47
REFERENCES 70

Introduction

Microalgae represent a promising sustainable source for various valuable products and processes, such as food, supplements, biofuels, and water purification. However, the challenges of making their production economically viable and suitable for large-scale industrial use, persist. Photobioreactors serve as critical tools for comprehending the intricate interplay of factors as temperature, light conditions and nutrient availability that shape microalgal growth and metabolic reactions. Achieving process optimization necessitates an in-depth understanding of how microalgae respond physiologically to various factors. Mathematical modeling plays a pivotal role in expanding the industrial applications of microalgae by elucidating the impacts of different process conditions, including nutrients, light, pH, and temperature. Modeling the kinetics of algal growth is instrumental not only for estimating and fine-tuning operational parameters but also for maintaining optimal process conditions. An effective model should encompass the influences of all process variables and their interactions. Furthermore, when integrated with a reactor model, it should be capable of forecasting the performance and productivity of a growing system under diverse operational scenarios. The primary goal of this thesis is to collect data from microalgae cultures of *A. obliquus* in continuous milli-scale photobioreactors. Cultivation in continuous allows for the analysis on acclimated cultures, facilitating the monitoring of variables that, once steady state is attained, remain constant. The data acquired will be utilized to construct a model that investigates the potential combined effect of temperature and light on microalgal growth and composition in order determine optimal cultivation conditions applicable to larger scales. The strain of *A. obliquus* was chosen due to its rapid growth and undemanding cultivation. The thesis is structured as follows:

In Chapter 1, a comprehensive background on microalgal cultures is provided, exploring their industrial applications along with the associated benefits and limitations of their cultivation. The biological aspects of microalgae and their photosynthetic processes are detailed, including an examination of operational modes, in particular on photobioreactors. Furthermore, this chapter analyses the factors influencing microalgae growth, followed by an examination of the mathematical models present in the literature that aim to portray microalgal growth.

Chapter 2 focuses into the cultivation conditions and the setup created to carry out the experiments. It also takes a closer look at the monitoring analysis, protocols to follow and laboratory equipment used for these studies. Finally, the chapter outlines the equations applied to develop a mathematical model aimed at scaling up the outcomes.

In Chapter 3, the experimental results are presented and discussed. This section specifically investigates the combined impact of light intensity and temperature on various aspects of the microalgae: biomass concentration, pigment content, cell morphology and dimensions. Additionally, the outcomes of modeling simulations and their parametric estimation are showcased and analyzed.

The thesis concludes with final remarks and perspectives for future research, providing a comprehensive closure to the study.

Chapter 1
State of art and thesis objective

This chapter will give a background on microalgal cultures, the industrial application with the benefits and limits related to their cultivation. Microalgae from a biological point of view and their photosynthetic process will be described, as well as the modes of operation with a particular focus on the photobioreactors. Furthermore, a comprehensive review of the mathematical models available in the literature for the microalgal growth will be provided.

1.1 Microalgae industrial utilizations

The need for finding economically competitive renewable energy sources as alternatives to fossil fuels is gaining more and more relevance. Countries around the world are struggling with environmental concerns such as global warming and climate change, as well as pressure from dwindling fossil fuel reserves. For instance, the objective at the heart of the European Green Deal and in line with the EU's commitment to global climate action under the Paris Agreement is to be climate-neutral by 2050 – an economy with net-zero greenhouse gas emissions (Wolf *et al*., 2021).

As a result, various forms of bioenergy are currently being developed and implemented worldwide, aiming at potentially replacing traditional fossil fuels in the medium-long term (Barbera *et al.*, 2015). These bioenergy sources include wood, agricultural crop residues, municipal solid waste (e.g., paper, cotton, and plastic), animal waste and industrial waste. Marine resources are raising big expectations in the context of the EU bioeconomy and microalgae are particularly attractive as source of a wide variety of high-value molecules for diversified uses (Pulz & Gross, 2004) and as feedstocks to develop biofuels and achieve carbon neutrality (Khan *et al.,* 2023).

Microalgae are photosynthetic organisms with the potential to serve as source of third-generation biofuels. The latter do not have the drawbacks of the first-generation ones (land use competition, loss of biodiversity, environmental pollution through pesticides and fertilizers) and of second-generation biofuels, such as straw or forest residues (Haase, Rösch, & Ketzer, 2016). Microalgae became one of the most promising alternatives for biofuel production in the transportation sector because of their high lipid content, high growth rate, ability to rapidly improve strains, and capability to produce co-products without competing for arable land (Hannon *et al.,* 2010). For instance, microalgae have been studied for producing bioethanol, biodiesel, biocrude oil, bio-jet fuels, pyrolytic bio-oil, biohydrogen and biomethane (Khan *et al.*, 2023).

Besides as biofuel feedstock, the chemical, pharmaceutical, wastewater treatment, cosmetic and energy industries are exploring the potential of microalgae (Pulz & Gross, 2004). In particular, due to microalgae reservoir of essential nutrients (carbohydrates, proteins and vital vitamins, potassium), some nations like China, Japan, and Korea, have been integrated green microalgae into their diets as nutritional supplements and food sources. Moreover, pigments extracted from microalgae are used in a variety of applications, such as food coloring, skin care products and hair care products. Microalgae can be also used to remove pollutants from wastewater by binding toxic metals, nitrates, phosphates to their surface (Zainith *et al*., 2021). Research has highlighted the remarkable efficacy of algae-based biosorption, surpassing other biomass types by 15.3% and outperforming alternative microbial biosorbents by a significant margin of 84.6% (Kanamarlapudi *et al*., 2018).

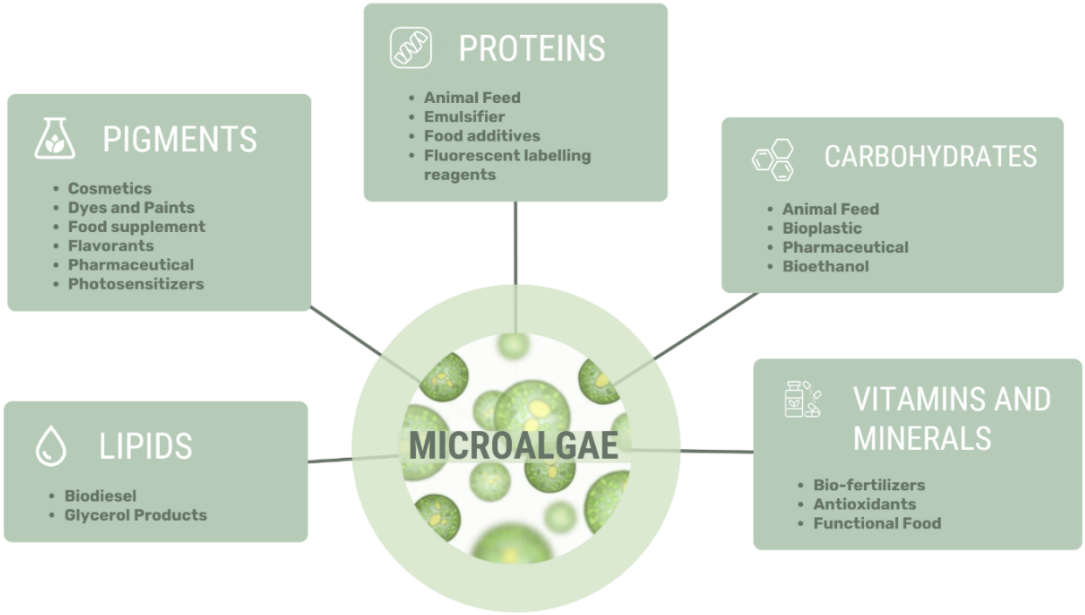

Figure 1.1. *Industrial applications of microalgae.*

1.1.1 Classification

Microalgae size ranges from about 5 µm to more than 100 µm and are classified under eukaryotic organisms. They are usually unicellular in nature, but some multicellular microalgae exist as free-living individual entities, colonies, or in symbiosis with other microorganisms (Becker, 2013; Shaikh *et al.*, 2022,).

Currently, although there is uncertainty about which organisms should be considered algae, the conservative approach has resulted in an estimated 72,500 species of algae (Guiry, 2012). They are classified into several groups based on various characteristics such as structural features, pigments and their composition, product storage, etc.

The main division of microalgae includes the eukaryotic ones in which the largest *phyla* of *Dinophyta, Chlorophyta, Rhodophyta* are present, and the prokaryotic division which includes *Prochlorophyta* and *Cyanophyta.* Each *phylum* contains, in turn, many classes and species. One of the most cultivated microalgae at an industrial level, *Spirulina sp.* (*Arthrospira platensis*) belongs to *Cyanophyta*: it has a high nutritional value, chemical composition and product safety (Sili *et al.*, 2012). However, the species under study is *Acutodesmus obliquus* and belongs to *Chlorophyta*, also called "green algae".

1.1.2 Acutodesmus obliquus

Acutodesmus obliquus, previously known as *Scenedesmus obliquus* is a unicellular microalga that belongs to the green algae. It thrives at temperatures ranging from 15°C to 40 °C and it exhibits its best growth in conditions with a neutral to alkaline pH (Zhang *et al.*, 2019).
During favorable conditions, the cells divide rapidly, leading to population growth and the formation of small colonies or aggregates. Each individual cell has a characteristic shape, which gives rise to its name "obliquus" (meaning slanting or inclined) as shown in Figure 1.2. The cells contain a single cup-shaped chloroplast, which is responsible for photosynthesis, and one or more flagella, aiding in motility.
A. obliquus, like many other microalgae, contains various pigments that play essential roles in its photosynthetic processes and overall physiology, giving the characteristic green color to these microorganisms (Metting Jr, 1996).

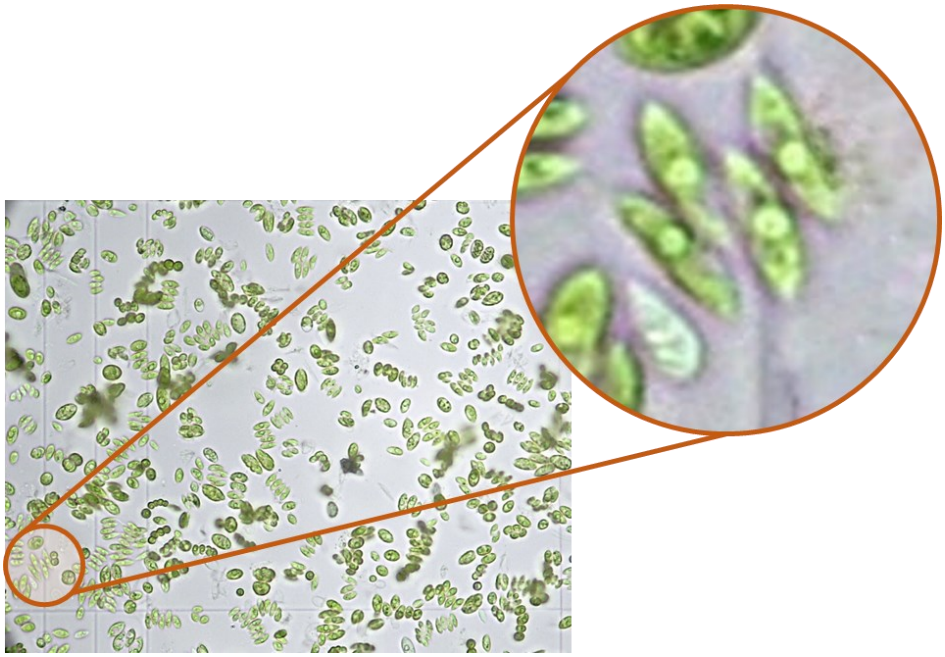

Figure 1.2. *A. obliquus captured under optical microscope as described in §2.3.5*

In *A. obliquus*, the dominant pigments are chlorophyll *a* (Chl *a*) and chlorophyll *b (*Chl *b)*. Chl *a* is crucial for capturing light energy and initiating the photosynthetic reactions, while Chl *b* helps to broaden the range of light wavelengths that can be absorbed.
Carotenoids are accessory pigments that protect the photosynthetic machinery from excess light compounds and have antioxidant properties, making them useful in the food and cosmetic industries. Some species of *A. obliquus* may contain phycobiliproteins, which are water-soluble pigments found in cyanobacteria and certain algae which can provide additional photosynthetic flexibility in environments with varying light conditions. The combination of these pigments allows *A. obliquus* to efficiently capture light energy from the surrounding environment converting it into chemical energy through photosynthesis (Lurling, 2016).
Specifically, this microalga has proven to be particular interesting for industrial exploitation due to its consistent lipid production, which occurs independently of the need for meticulous management of light conditions or even in the absence of stressing conditions factors (Ma *et al.*, 2019).
A. obliquus proved to have the capability of: (i) generating a substantial quantity of biomass which is rich in proteins (10-45 % w/w in DW), lipids (30-50%), and carbohydrates (20-40%) (Sajjadi *et al.*, 2018); (ii) growing in wastewaters and in non-sterile medium (Barbera *et al.*, 2015): (iii) removing nitric oxide (NOx) and fixing CO_2 of flue gas (Ma *et al.*, 2019). The attributes outlined earlier render *A. obliquus* promising for large-scale production of lipids and biomass (Gris *et al.*, 2014).

1.2 Photosynthetic process

Microalgae, as photoautotrophs microorganisms, are involved in the process known as photosynthesis, where they convert inorganic substances and light into organic substances. This process occurs within their specialized chloroplast structures, where pigments like chlorophyll, carotenoids, and phycobiliproteins capture light energy, initiating a series of molecular reactions. The chloroplast is composed of an outer membrane that allows molecules to pass through, an inner membrane that is more selective and a structure called the *granum*, which is, in turn, made up of flattened membrane stacks called thylakoids (Staehelin, 1986).
Oxygenic photosynthesis can be depicted as a redox reaction driven by light energy (captured by chlorophyll molecules), wherein carbon dioxide and water are transformed into carbohydrates and oxygen (Masojídek *et al.*, 2013). In particular, water is oxidized and CO_2 is reduced to the level of energy-rich carbohydrates (Witt, 1996) as shown in Equation 1.1.

$$CO_2 + 2H_2O + photons \rightarrow CH_2O + H_2O + O_2 \quad (1.1)$$

The overall reaction can be divided into 2 phases: the light phase where light energy is captured and converted into chemical energy, and the subsequent dark phase, which focuses

on utilizing this energy to assimilate carbon dioxide and synthesize valuable organic compounds. The process is depicted schematically in Figure 1.3. The light phase is characterized by the activities of two crucial complexes: photosystem I (PSI) and photosystem II (PSII) which are placed inside thylakoid membranes aiming to capture light energy and transfer it from a lower redox potential to a higher one (Masojídek *et al.*, 2021).

In the light phase, photosystem II absorbs light energy and uses it to power the splitting of water molecules. This process, called water photolysis, releases oxygen molecules as byproducts. The energized electrons from the water molecules are then transferred through an intricate chain of molecules, known as the electron transport chain. This chain generates energy that is harnessed to pump protons across the thylakoid membrane, creating a proton gradient which serves as the driving force to produce adenosine triphosphate (ATP), the cell's energy currency. Simultaneously, the energized electrons reach photosystem I, where they are further energized by light and eventually used to reduce nicotinamide adenine dinucleotide phosphate (NADP+) to form NADPH, another vital energy-rich molecule.

As the light phase culminates, the dark phase, also known as the Calvin-Benson cycle, takes place. In this phase, ATP and NADPH produced during the light phase are employed to facilitate the biochemical reduction of carbon dioxide into carbohydrates. This intricate dance of light absorption, energy conversion, and biochemical transformations forms the cornerstone of oxygenic photosynthesis, a process that not only sustains the life of microalgae but also contributes significantly to Earth's biosphere and energy balance.

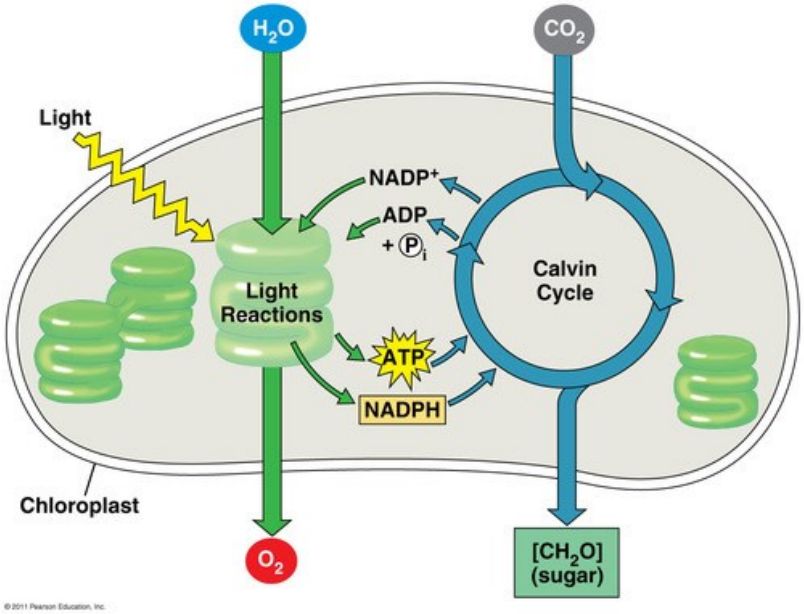

Figure 1.3 *Schematic representation of the light and dark phase of the oxygenic photosynthesis and its reactions*

1.2.1 Photosyntethic efficiency

Photosynthetic efficiency (PE) refers to how effectively these organisms convert light energy into chemical energy through the process of photosynthesis. It quantifies the ability of microalgae to capture and utilize light energy for the production of organic compounds, primarily carbohydrates, which are essential for their growth and survival (Masojídek *et al.*, 2013). Efficiency can be influenced by various factors, including the type of microalgae, the intensity and penetration of light, the availability of nutrients, temperature, and even the presence of any stressors. High photosynthetic efficiency is desirable in applications such as biofuel production, wastewater treatment, and carbon dioxide mitigation, where microalgae are utilized to convert light energy into valuable products. The strategies suggested to enhance PE primarily involve boosting the metabolic performance of microalgae, for instance through the utilization of genetic engineering and modifications to the photosynthetic apparatus (Vecchi *et al.*, 2020). Moreover, in some studies it was noticed that blue wavelengths (400-450 nm) promote the accumulation of lipids in general (Habibi *et al*., 2019) while red light affects photosynthesis and cell division, and green light stimulates chlorophyll production (Mohammed *et al*., 2014). Therefore, altering lighting conditions and LED colors can enhance growth and productivity with respect to fluorescent lamps since there are no unnecessary wavelengths present (Borella *et al*., 2022).

1.3 Algal growth

As a result of their photosynthetic nature, with numerous microalgae being particularly proficient at converting solar energy, these microorganisms are cultivated in naturally illuminated environments or through artificial means. Presently, the prevalent method for cultivating microalgae is autotrophic growth, wherein cells capture light energy and employ CO_2 as a source of carbon (Perez-Garcia *et al*., 2011).

As an attainable alternative, heterotrophic growth involves microalgae obtaining their energy and nutrients from external organic sources. Instead of relying solely on photosynthesis, heterotrophic microalgae consume organic compounds like sugars, acetate, or other microorganisms to meet their metabolic demands. This strategy is particularly advantageous when light availability is limited or when microalgae are grown in the dark. Thus, by utilizing organic carbon sources, microalgae can bypass the need for photosynthesis and still achieve growth and reproduction. Both autotrophic and heterotrophic growth have their benefits and drawbacks. Autotrophic growth leverages the inherent efficiency of photosynthesis, but it requires suitable light and nutrient conditions; heterotrophic growth, on the other hand, offers flexibility but may necessitate additional organic substrates, may encounter the risk of contamination and competition from other microorganisms and might not be suitable for all microalgal species (Perez-Garcia *et al.,* 2011).

In the context of this work, *A. obliquus* was grown using autotrophic metabolism. Nonetheless, certain investigations have indicated that merging heterotrophic and photoautotrophic cultivation (mixotrophy) of *A. obliquus* at a pilot scale, not only proved to be economically viable but also increased lipid production of microalgal cells compared to those grown under autotrophic conditions (Jin *et al.,* 2019).

Microalgal growth is a complex phenomenon driven by a web of interconnected factors that orchestrate their development and metabolic activities. Among these factors, light intensity, nutrient availability, temperature, pH, CO_2 and culture mixing play pivotal roles in shaping the growth trajectory of microalgae. In addition to carbon, microalgae also require nitrogen and phosphorus, which are crucial macronutrients essential for their growth (Khan *et al.* 2018).

1.3.1 Light

Light is pivotal for microalgae because they utilize it for photosynthesis, their energy production process. The optical actions within microalgae rely on the wavelength of the incoming light. Visible light spans from roughly 390 nm (violet) to 780 nm (red) across the electromagnetic spectrum, closely matching the photosynthetically active radiation (PAR) range (400–700 nm) (Lehmuskero *et al.*, 2018).

Various light sources including the sun, LED lamps, and fluorescent bulbs, exhibit a distinctive intensity distribution dependent on wavelength (emission spectrum). Another significant aspect of light is its polarization, which refers to the alignment of the electric field in relation to its propagation direction. In general, the way microalgae scatter and diffract light relies on the polarization of the incoming light (Lehmuskero *et al.*, 2018).

The intensity, spectrum, and duration of light exposure significantly influence their growth rate. Typically, the growth rate of microalgae rises as light intensity increases, but it eventually reaches a threshold and varies based on the species of microalgae. In order to describe the photosynthetic activity, the measured evolution of oxygen in function of light intensity is shown in the so-called light–response (P/I) curve (Masojidek *et al.*, 2013). Figure 1.4 shows, indeed, the variation of the photosynthetic rate (based on how quickly photons are absorbed and how effectively they are transformed into chemical energy) vs the irradiance to which the culture is subjected. In conditions of zero light exposure (dark) only respiration takes place, while photosynthesis remains dormient, so consequentially, there is a net consumption of oxygen (O_2 uptake) (Masojidek *et al.*, 2013).

Increasing irradiation, an equilibrium point (compensation point, I_c) between oxygen consumed and produced is reached and then, when is overcome with the rising of light energy, O_2 evolution (net photosynthesis) can be detected (Tredici, 2010). The first region identified is the light-limited region: at low light intensity, the rate of photosynthesis shows a linear

dependency on irradiation. The initial slope (α) shows the maximum photosynthetic efficiency and is calculated as:

$$\alpha = \frac{P_{max}}{I_s} \tag{1.2}$$

where P_{max} indicates the maximum rate of photosynthesis and I_s is the saturation irradiance. While light intensity is low (below the saturation level), the growth will be limited by light since cellular respiration utilizes high-carbon compounds more rapidly than they are generated through photosynthesis, and there is no net accumulation of new biomass (Lee *et al.,* 2015).

The shift from the light-limited zone to the photo-saturation range is marked by a decline in photosynthetic efficiency. As a result, the correlation between light intensity and photosynthetic rate no longer follows a linear pattern.

An additional increase in light intensity brings to the decline of the photosynthetic rate: at the point Ip (inhibitory light level), the growth will be inhibited by light and the cultivation will be "stressed" (Difusa *et al*., 2015). This phenomenon is known as photoinhibition: photosystem II generates free radicals that can result in photo-oxidative harm and, in more extreme instances, cell mortality (Lehmuskero *et al.,* 2018).

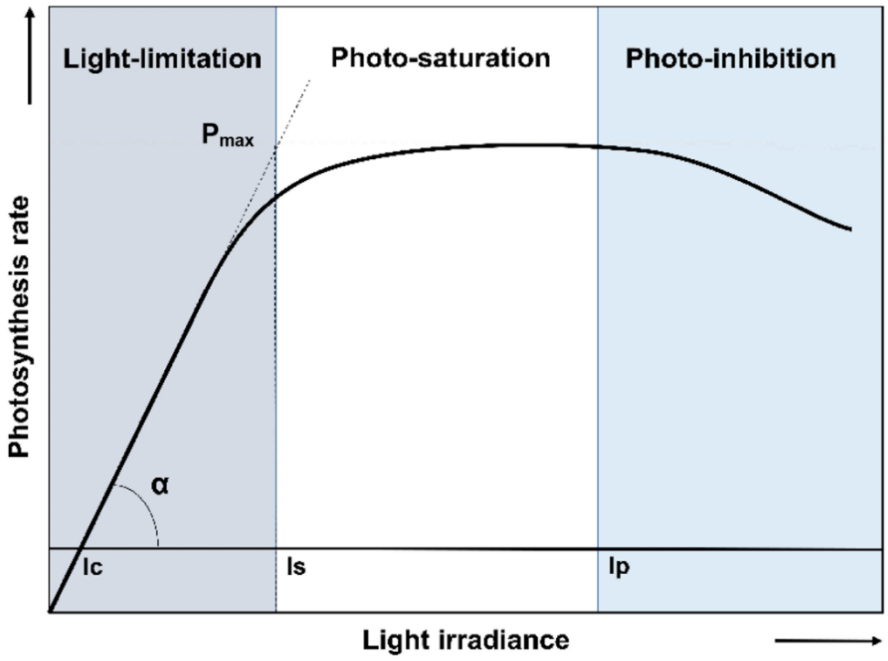

Figure 1.4. *Photosynthetic light-response curve. α: slope of the curve, i.e. max light conversion efficiency; Pmax: maximal rate of photosynthesis; Ic: compensation irradiance; Is: saturation irradiance; Ip: inhibition irradiance (Ferro, 2019).*

The light-response curve is used in microalgae physiology to characterize the light-acclimation status of microalgae cell (Torzillo *et al.,* 2013). Photoacclimation is a dynamic

process through which microalgae fine-tune their pigment content and composition in response to varying light intensities impacting directly on the rate of photosynthetic production (Nikolaou *et al*., 2016). Specifically, when light intensity decreases, there is an observable increase in the concentration of Chl *a* and other pigments responsible for capturing light. Conversely, when irradiance levels rise, Chl *a* content decreases (Andersen, 2013). Thus, the aim of acclimation processes is to balance the light and dark photosynthetic reactions, i.e., energy intake and utilization, avoiding the harmful effects of excessive light exposure (Masojidek *et al.*, 2013).

Comparing photoacclimation and photoinhibition, they act on different time scales: photoinhibition occurs on a time scale of minutes, whereas photoacclimation acts on a time scale of days (Nikolaou *et al*., 2016). Given its central role in determining productivity, light profoundly governs the resources accessible to cells within the culture, and the density of cells significantly shapes this dynamic (Tredici, 2010). In dense cultures, especially in closed photobioreactors (§1.4.2), the irradiance shows a decreasing gradient from the surface, deeper into the culture, which subsequently impacts the growth of microalgae. This is known as *self-shading* effect (Janssen, 2016). Light attenuation divides the culture into several zones, with two extremes: a highly illuminated top layer where cells are exposed to light irradiance that is higher than they need, and a bottom layer where cells are in darkness. The light decreases exponentially through the culture (light attenuation curve), as Figure 1.5 shows, according to the Lambert–Beer law (§2.4) which takes into account only light absorption (Wang *et al*., 2014).

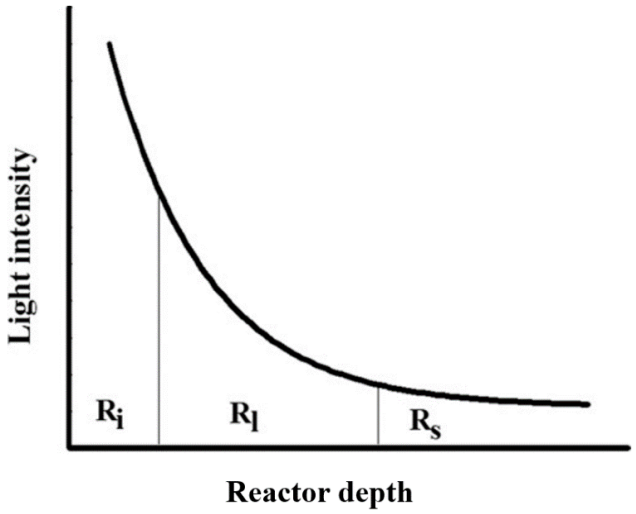

Figure 1.5. *Typical light attenuation curve in microalgae cultivation. R_i: photoinhibition region, R_l: light-limited region, R_s: stagnant region (Modified by Wang et al., 2014).*

This heterogeneous distribution is unfavorable and brings to a decreasing in biomass productivity (Sforza *et al.,* 2014). Thus, light intensity has to be balanced with the cell density and culture layer (Masojídek *et al.,* 2015). Certain researchers have examined artificial

lighting setups that utilize LED technology. These systems are aimed at producing carefully controlled pulsating light flashes, intended to sustain elevated photosynthetic rates while preventing photoinhibition, as discussed by Zarmi *et al*., (2020).

1.3.2 Nutrient availability

In addition to light, there are also other non-living factors that affect the growth of microalgae (Lehmuskero *et al.,* 2018). Besides macronutrients, such as carbon, nitrogen and phosphorous, which are crucial, microalgal population also requires micronutrients (e.g. Fe, Mn, Zn, Ni) (Procházková *et al.,* 2013). However, the line between a nutritional boost and cell toxicity for microalgae is often razor-thin, as they require essential elements in minuscule amounts, up to picograms per litre (Becker, 1994).

Carbon is the main element present in microalgae biomass, amounting about 50% for the majority of the species. However, photosynthetic microorganisms use inorganic carbon dioxide (CO_2) as their main source of carbon for growth (Markou *et al*., 2014). Since microalgae are aquatic microorganisms, CO_2 is dissolved in water forming a weak acid-base buffer system, so it is strictly related to the pH of the solution. CO_2 is mainly supplied in gaseous form, leading to a limitation related mostly to the mass from the gas to the liquid phase solution (Markou *et al*., 2014). A common way to face this problem, namely suppling cultures with a CO_2-rich gas, which has higher solubility at high pH, and so, mass transfer is enhanced (Zuccaro *et al.,* 2020).

Moreover, since an increase in time of exposure to light resulted in an increase in CO_2 uptake rates, some studies have shown that due to their high biomass yields, microalgae cultivation can be an effective method for capturing carbon dioxide from the atmosphere, which could potentially reduce the costs of CO_2 supply, making them promising candidates for large-scale production (Gonçalves *et al*., 2014).

Nitrogen is the second most abundant component in microalgal biomass, and its content varies from 1% up to 14% (Grobbelaar, 2007), so it represents a critical macronutrient for metabolism and biochemical composition of microalgae (Zarrinmehr, 2020). Nitrogen can be absorbed by microalgae in a variety of forms, including nitrate, nitrite, urea, ammonia and ammonium (Xu *et al*., 2001). The prevalence of free ammonia at pH values greater than 9.25 (at 25°C) can be toxic to some microalgae species (Azov & Goldman, 1982). Conversely, ammonium is the preferred form of nitrogen for microalgae, and its formation can be induced by adjusting the pH of the culture medium. This is due to the equilibrium system of dissolved ammonia in water shifts from one side to the other as the pH changes (Jeanfils *et al*., 1993).

Changes in nitrogen concentration can have a dramatic impact on the production of proteins, lipids, and carbohydrates (Pancha *et al.,* 2014). Even though nitrogen limitation can lead to increased lipid production, it can also come at the cost of lower biomass productivity (El-

Kassas, 2013). In the study by Yang *et al*. (2008), it was found that nitrogen deficiency in microalga *Chlamydomonas reinhardtii* led to an inhibition of biomass accumulation by up to 31.7%, but a simultaneous increase in total fatty acid yield by up to 93% and a significant enhancement in lipid production. These results suggest that nitrogen concentration favours higher biomass productivity, while depletion of nitrogen shifts the metabolic flux towards lipid production (Yaakob *et al.,* 2021).

Phosphorus (P) is another critical nutrient that all algae require for growth. Algal biomass typically contains less than 1% phosphorus by dry weight, while the medium used to culture algae typically contains from 0.001 g/L to 0.179 g/L of P (Roopnarain *et al*., 2014). In natural aqueous environments, phosphorus is often a growth-limiting nutrient because it can bind to other ions (such as carbonate and iron) and precipitate, making it unavailable for algal uptake (Procházková *et al.,* 2013).

Similar to nitrogen, the restriction of phosphorus is an effective environmental factor that prompts the accumulation of lipids (Xin *et al*., 2010). Yang *et al*. (2018) exhibited that *Scenedesmus* sp. experienced a rise in lipid content when phosphorus levels in the medium were lowered: the lipid content increased to 22.3% at 50 mg/L phosphorus, while up to 42.5% at 1 mg/L phosphorus.

Furthermore, a deficiency in phosphorus can lead to diminished growth rates and decreased levels of proteins and chlorophylls. This can result in a respiration rate that is five times lower and a notable reduction in the rates of both photosynthetic CO_2 fixation and O_2 evolution (Theodorou *et al*., 1991). Nonetheless, there are reports suggesting that certain species, such as *Nostoc* sp., exhibit the ability to sustain slow growth even after 16 days in a medium devoid of a phosphorus source. This suggests that microalgae could potentially adapt to low-phosphorus environments to a certain extent by absorbing and storing phosphorus in significant amounts (Xing *et al*., 2021). So, in this condition of "luxury uptake", P content can reach up to 3% by dry weight (Procházková *et al*., 2013) and this aspect can be harnessed for the purpose of removing phosphorus from wastewater (Brown & Shilton, 2014).

Understanding the distribution and transformation of phosphorus in wastewater is important for improving the performance of microalgae-based P removal and biofuel production (Wu *et al*., 2021). Microalgae primarily retrieve phosphorus from wastewater through absorption into their cells (Xing *et al*., 2021), but this uptake can become saturated due to factors such as light limitations and reductions in carbon dioxide and oxygen levels within the culture medium (Yaakob *et al.,* 2021).

Since the cultivation of microalgae and cyanobacteria consumes considerable quantities of nutrients, strategies to improve the nutrient application efficiency are needed, such as the recycle of the medium (Gonçalves *et al*., 2022).

1.3.3 Temperature and pH

Temperature is one of the most important environmental factors that affects microalgae growth. Due to seasonal and diurnal fluctuations, temperature represents one of the important biological limitations for outdoor mass production of microalgae (Masojidek *et al*., 2021).
In general, the optimum temperature for microalgae growth ranges between 25 and 35 °C (Ranglová *et al*., 2019). However, temperatures vary depending on the species of microalgae: some species can grow at temperatures as low as few Celsius degrees, while others can grow at temperatures up to 40°C. At temperatures below the optimum range, microalgae growth will slow down, while for temperatures above the optimum range, microalgae growth will stop and the cells may even die (Khan *et al*., 2018). Thus, typically, a bell-shaped growth curve is employed to characterize the temperature-dependent response of microalgae growth rate, but it is important to notice that distinct species exhibit considerable variation in the specific shapes of these curves (Figure 1.6). This behaviour can be explained considering that optimal growth rates indicate a healthy energy balance within a cell: growing microalgae attempt to maintain equilibrium between the energy supplied through photosynthesis in their thylakoid membranes and the energy they use in the Calvin cycle within the cell. When environmental conditions are ideal, cells can perform photosynthesis without changing their inherent biochemical or physiological functions. However, changes in the environment can upset this balance, causing an energy supply-demand mismatch, often due to temperature shifts. Indeed, lower temperatures tend to decrease carboxylase activity, so, reduced efficiency in converting carbon dioxide which can impact the overall rate of photosynthesis and inhibit microalgal growth. Thus, if light conditions remain constant, an excess of energy supply can occur (Ras *et al*., 2013). Moreover, if temperatures exceed the optimal range, photosynthesis, respiration, and growth decrease, mainly due to an imbalance between the energy needed and the ATP produced, as well as the disruption or deactivation of proteins crucial for photosynthesis (Ras *et al*., 2013).
In addition to the optimum temperature, the rate of microalgae growth is also affected by the rate of temperature change: if the temperature changes too quickly, the microalgae cells may not have time to adapt and they may die. This is why it is important to gradually increase or decrease the temperature of the culture medium when growing microalgae.
Microalgae can tolerate temperatures below their optimal point, but their tolerance decreases as temperatures rise above the optimum (Ras *et al*., 2013). Over longer periods, strategies for adapting to temperature increases have revealed that certain species can indeed acclimate to temperatures beyond their optimal range. Overall, temperature is an important environmental factor that needs to be carefully controlled when growing microalgae: by understanding the temperature requirements of a particular species of microalgae, it is possible to optimize productivity and reduce the cost of PBR cooling (Masojidek *et al*., 2021).

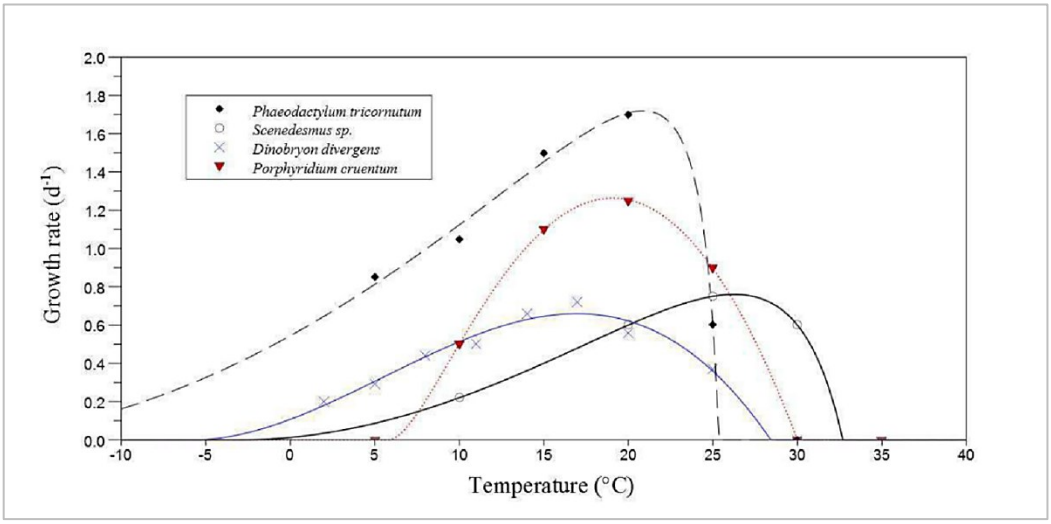

Figure 1.6. *Temperature effect on microalgae growth rate for different species (Ras et al., 2013).*

The pH level of the growth medium is one of the most important environmental factors that affects the microalgal growth and physiology. Microalgae are sensitive to changes in pH, as it affects various biochemical and physiological processes within their cells.

Different species of microalgae have varying pH tolerances, with some thriving in acidic conditions (lower pH) and others in alkaline conditions (higher pH). The optimal pH for most microalgae species is in the range of 6 to 8.6. with a slight variation depending on the species (Lam & Lee, 2012). According to Goldman *et al.* the optimum pH condition for the microalgae growth allows intense culture photosynthesis, which responds to an increase in pH of the medium condition towards the stationary phase and which lowers the microalgae growth rate (Difusa *et al*., 2015). The pH of the surrounding environment influences the solubility of nutrients and the availability of carbon dioxide. At low pH (<6) and high pH (>9), the solubility of CO_2 decreases, which can limit the growth of microalgae. In addition, low pH can also damage the cell membranes of microalgae, leading to cell death, while algal cultivation at high pH can suppress undesired biological contaminants (Bartley *et al*., 2013).

Maintaining a stable and suitable pH level within the growth medium is essential for achieving optimal microalgae productivity in various applications, including biotechnology, biofuel production, and wastewater treatment.

1.3.4 Culture mixing

Effective mixing is essential for the growth of microalgae. It ensures the uniform distribution of nutrients, gases, and light throughout the culture medium, preventing nutrient gradients and sedimentation. This is important because nutrient gradients can lead to localized depletion or excess, both of which hinder optimal growth. Sedimentation can cause microalgae to settle to the bottom of the culture medium, where they may die.

Mixing also promotes the removal of oxygen-depleted zones around the microalgae, which can arise due to their high oxygen production during photosynthesis. Mixing can also create an optimal light/dark regime for the cells to increase the biomass culture yield (Borowitzka, 2016). Moreover, mixing improves light penetration by breaking up the surface of the culture medium and creating turbulence. This allows more light to reach the bottom of the culture medium, where the algae are growing, reducing the self-shading effect in well-mixed dense cultures (Masojidek *et al*., 2021).

However, it is difficult to isolate the contribution of the different factors influenced by mixing, especially when it is more difficult to separate the effect of single environmental factors. In addition, the degree of culture mixing can be potentially limited both by the shear sensitivity of the microalgae cells and the cost of the energy provided for the mixing (Masojidek *et al*., 2021).

1.4 Production systems

There are two main approaches for cultivating microalgae on a large scale: open cultivation and closed cultivation. The main difference between these two systems is how they operate and their vulnerability to outside influences (Jerney & Spilling, 2018).

1.4.1 Open systems

Open cultivation systems are the most common and cost-effective way to grow microalgae. Their exposure to the atmosphere allows for the unimpeded exchange of gases such as carbon dioxide and oxygen, which are essential for microalgae growth. However, open systems are also more susceptible to contamination from other organisms, such as bacteria and algae, and can be challenging to manage. The most commonly used systems include raceway ponds (RP), circular ponds (CP) and thin layer cascades.

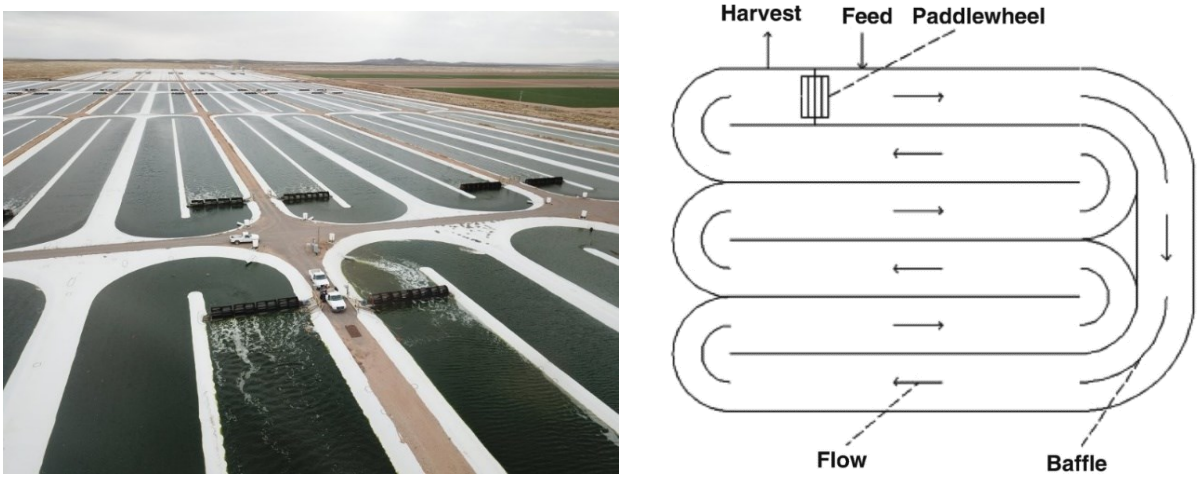

Figure 1.7. *A field of algae raceway ponds and an aerial schematic view (Chisti, 2007).*

Raceway ponds (Figure 1.7) were initially developed for wastewater treatment and then they have been used for commercial production of microalgae and cyanobacteria (Chisti, 2016). Raceway ponds are shallow, rectangular or oval-shaped ponds where the water flow is guided around bends by baffles placed in the flow channel. They require some form of turbulence, most commonly in the form of a paddle wheel, to distribute nutrients, maintain uniform temperature, and prevent the settling of microalgae cells (Christenson & Sims, 2011).

Raceway ponds are shallow, typically ranging from 15 to 30 centimetres in depth. This shallowness maximizes light penetration throughout the pond, ensuring optimal photosynthesis for microalgae growth (Shen *et al*., 2009). Paddlewheels and surface agitation aerate the water, ensuring that microalgae receive the oxygen they need for respiration and preventing carbon dioxide from accumulating near the surface. Once the microalgae biomass reaches the desired density, it can be harvested using a variety of methods, such as sedimentation, flocculation, or centrifugation.

In sedimentation, the microalgae cells are allowed to settle to the bottom of the pond. In flocculation, chemicals are added to the water to cause the microalgae cells to clump together. In centrifugation, the water is spun in a centrifuge to separate the microalgae cells from the culture medium. Raceway ponds are a relatively inexpensive way to cultivate microalgae, but they can be difficult to control and are susceptible to contamination.

Circular ponds (Figure 1.8) are a type of open cultivation system for microalgae that is similar to RP. They are designed to provide an environment conducive to efficient photosynthesis and biomass production. Circular ponds are named after their circular or oval shape, which promotes uniform light exposure and circulation within the pond. As RP, they are typically shallow, with depths of about 30 to 70 cm and diameters of 40 to 50 m (Ekin, 2020).

The movement and mixing of the culture in circular ponds are assisted by a central pivot agitator, but this design is only suitable for ponds up to 10,000 square meters in area. Circular ponds are also more expensive to build and require more land space than raceway ponds, as they cannot be as long and narrow (Ahmad *et al*., 2021).

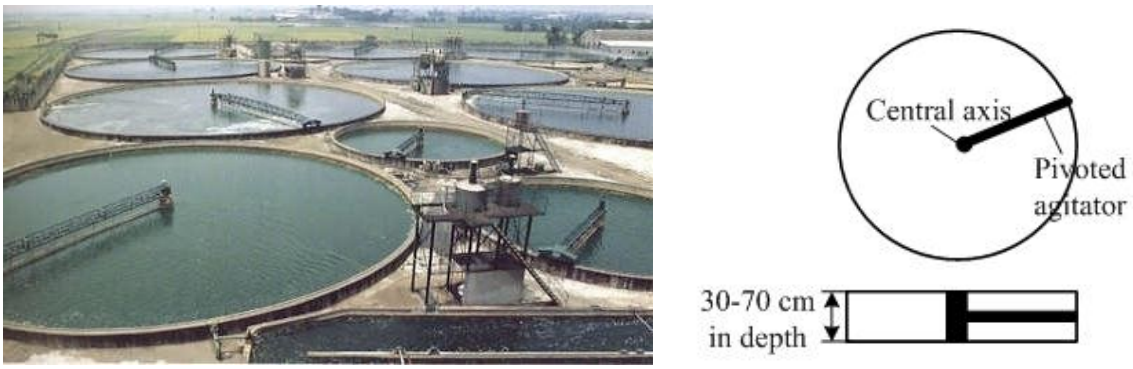

Figure 1.8. *Circular ponds with a schematic view (Shen et al., 2009).*

The highest growth rate and productivity have been achieved in cultivation systems with microalgae layer thickness lower than 50 mm (Masojídek *et al*., 2015). Thin-layer cascades (Figure 1.9) are inclined-surface platforms usually characterized by low depth (<10 mm) and fast flow (0.4–0.5 m/s) of culture (Grivalský *et al*., 2019). High frequency (10-100 Hz) of light/dark cycles of cells are needed to match the turnover of the photosynthetic apparatus for optimizing light utilization and maximizing biomass productivity (Qiang *et al*,. 1998).

With respect to the other open systems, thin-layer cascade can be operated at much higher cell concentrations, which can lead to higher biomass productivity due to their high surface-to-volume ratio. Moreover, they can store cultures in a retention tank during night-time or

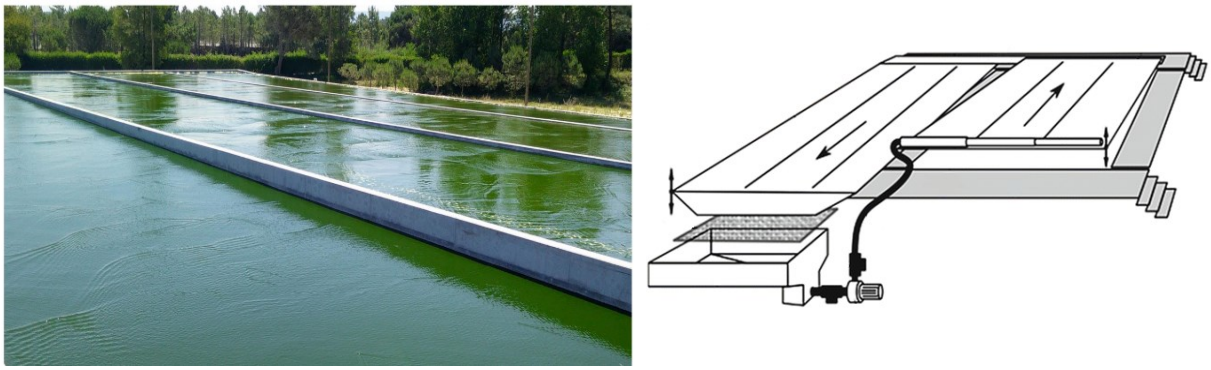

Figure 1.9. *Thin-layer cascades (Grivalský et al., 2019) with a schematic view (Masojídek et al., 2015).*

adverse weather conditions which can help to protect the culture and prevent contamination (Grivalský *et al*., 2019). Indeed, as all the open systems, contamination by other microalgae strains is one of the limitations of these systems: this vulnerability can result in the preferential growth of fast-growing strains or those that have been cultivated in specific environment (Egbo & Okoani, 2018).

Open cultivation systems are cost-effective and easy to maintain. They are also easy to scale-up and have low operation costs, as they use sunlight as the primary energy input and require little energy to mix the culture. Additionally, they have good gas exchange with the atmosphere (e.g., release of O_2), which is essential for microalgae growth (Jerney & Spilling, 2018).

Although open pond systems are the most commonly used for commercial microalgae cultivation, they have several drawbacks. They are susceptible to contamination by other algae strains and predators, making it difficult to maintain a monoculture of a desired algal strain and also susceptible to seasonal variations in temperature and sunlight intensity, which can negatively affect biomass productivity. Additionally, open pond systems have low productivity, due to poor mixing and water-gas transfer and their exposure to evaporation can lead to water loss and decreasing productivity. Moreover, growth parameters such as pH, temperature, mixing, and light availability are more difficult to monitor and control than closed systems, as well as a less efficiency utilizing carbon dioxide (Qin. *et al*., 2019).

1.4.2 Closed systems

Closed cultivation systems, also known as photobioreactors (PBRs) are enclosed and illuminated vessels for cultivating organisms which are shielded from direct atmospheric exposure and encompass a transparent enclosure or are confined within transparent tubing (Shen *et al*., 2009). These enclosures are typically made of materials such as glass, PVC, or polyethylene, which play a crucial role in determining the system's durability and significantly influence the initial investment required (Egbo & Okoani, 2018). Gas exchange necessary for the culture's well-being is facilitated through a sterilized gas filter, ensuring contamination-free conditions within the culture system (Zhang, 2015).

A well-optimized photobioreactor (PBR) design should allow for practical adjustment and maintenance of operational parameters and should minimize the non-illuminated portion of the reactor which is crucial to enhance light exposure. Furthermore, an ideal PBR design should strive for reduced initial investment and operational costs, along with lower energy consumption (Xiaogang *et al*., 2020). Various types of photobioreactors have emerged, categorized based on reactor geometry, including vertical column, tubular, and flat panel PBRs (Qin *et al*., 2019). Furthermore, additional reactor designs such as membrane, hybrid, and biofilm PBRs have also been developed, demonstrating the evolving nature of these innovative systems.

Vertical column photobioreactors (Figure 1.10 A) are typically constructed from vertical cylinders made of transparent materials and are equipped with a gas sparger system at the bottom as agitation setup. They provide an efficient mass transfer, gentle mixing and low energy consumption, but on the other hand they need have restricted illuminated surface area upon scaling-up.

Tubular photobioreactors (Figure 1.10 B) are widely used in commercial algae cultivation for their simple assembly, efficient gas transfer, high surface area-to-volume ratio, and high biomass productivity (Pulz, 2001). They can be configured in straight, spiral, or bent patterns with a small tube diameter and agitation are maintained by an air pump (Xiaogang *et al*., 2020; Zhang, 2015). Tubular PBRs can use artificial or natural light, but face challenges like microalgae growth on tube surfaces, high oxygen concentrations, and limited tubing length (Zhang, 2015).

Another cultivation system for microalgae are flat-panel PBRs (Figure 1.10 C) which have a design made of a planar arrangement of transparent panels or sheets which improves light penetration, simplifies operation, and reduces self-shading. However, scaling-up flat-panel PBRs can be challenging due to increasing hydrostatic pressure with rising volume (Zhang, 2015).

Considering the expansive surface areas of membranes, membrane PBRs excel in improving efficient gas-to-liquid mass transfer (Lehr and Posten, 2009) facilitating prolonged and

consistent production periods (Qin *et al*., 2019). However, a drawback linked to the porous configuration of these PBR setups is their cost and pronounced water vapor permeability (Johnson *et al*., 2018). Membrane PBRs are usually used in combination with other PBRs, obtaining the so-called hybrid photobioreactors, which exploits the individual advantages of each one.

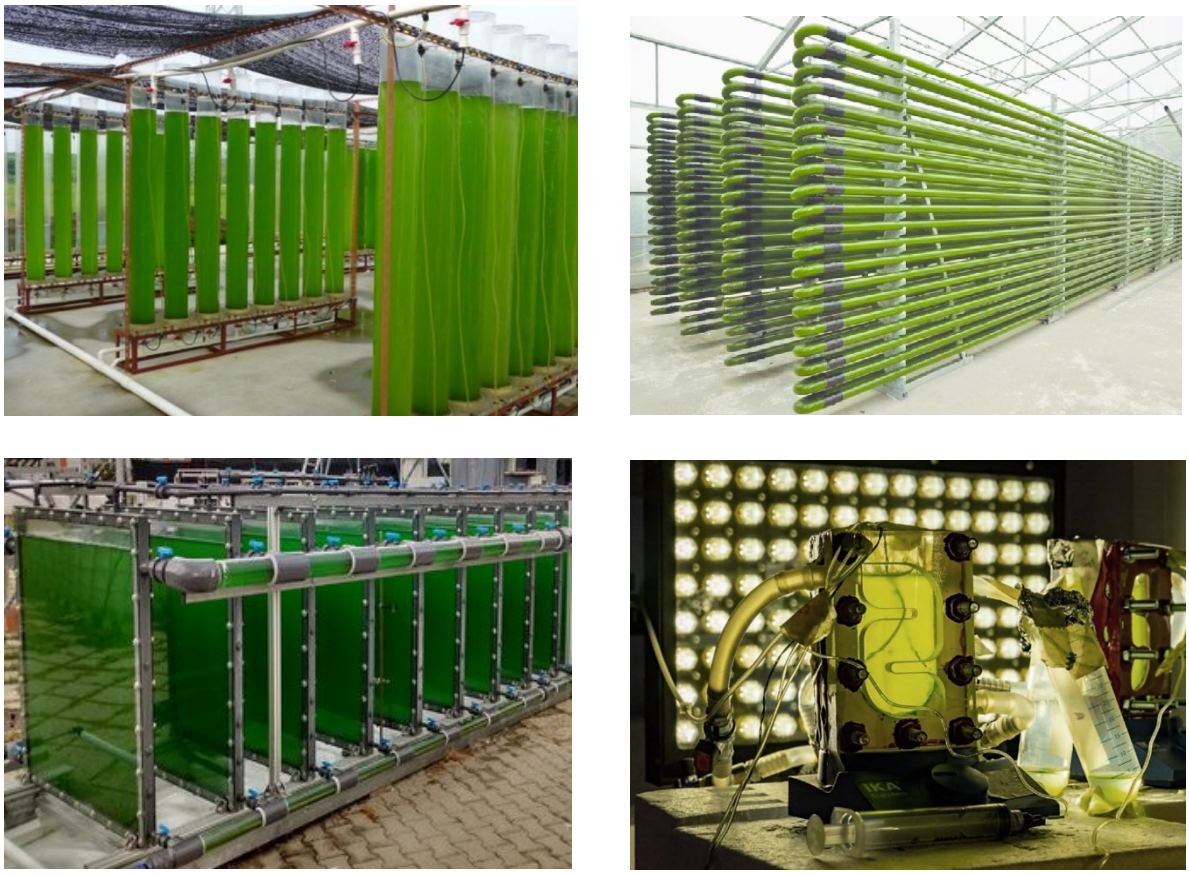

Figure 1.10. *Examples of photobioreactor systems. Vertical PBR (A) (Huo et al., 2018); Tubular PBR (B)(Alaswad et al., 2015); Flat panel (C) (Lindblad et al., 2019); Milli-PBR (D) (current research).*

1.4.2.1 Milli-photobioreactors

A millilitre-photobioreactor (milli-PBR) (Figure 1.10 D) is a compact and controlled cultivation system whose small-scale design provides a controlled environment that enables precise manipulation of growth conditions. This includes regulation of factors such as light intensity, temperature, nutrient concentrations, and gas exchange, all of which are crucial for optimal microorganism cultivation. These miniaturized bioreactors are well-suited for high-throughput screening of different strains and conditions, making them valuable tools in identifying ideal growth parameters, nutrient requirements, and strain performances. Their space-efficient nature is advantageous for laboratories or facilities with limited room and their

controlled environment and the suitability for rapid screening make milli-PBRs integral to advancing research and development in fields such as biotechnology, biofuels, and environmental sciences. Over the past few decades, there has been a gradual reduction in cultivation volumes to micro and millilitre scales. This shift underscores the necessity for non-invasive sensor systems capable of real-time monitoring of bioprocesses at these smaller scales (Krujatz *et al*., 2016).

In summary, photobioreactors offer multiple advantages, including enhanced parameter control to optimize biomass for subsequent biofuel production, mitigation of evaporation and contamination risks and attainment of high biomass productivity. They also contribute to the reduction of water and carbon dioxide losses and enable more efficient regulation of cultivation conditions like temperature and pH (Fernández, *et al*., 2012).
However, as previously mentioned, these benefits come with higher construction and maintenance costs compared to open systems. As a result, PBRs are not commonly employed for large-scale production purposes (Egbo & Okoani, 2018), except for specialized applications like high-value products such as cosmetics and nutraceuticals (Jerney & Spilling, 2018).

1.4.3 Batch and continuous mode

Microalgae cultivation can be carried out through two main modes: batch and continuous systems.
In a batch cultivation system, microalgae are grown in a closed container or bioreactor with a fixed volume of nutrient-rich medium. The growth process begins with inoculating the culture medium with microalgae, allowing them to multiply and grow under controlled conditions. As the cultivation progresses, the microorganisms utilize the available nutrients until they are depleted, and the growth slows down. This mode is characterized by four distinct growth phases, represented in Figure 1.11. The initial phase is the *lag* phase which follows the inoculation of a known concentration of biomass: the cells in this phase adapt to the new environment and do not increase in number. Then, in the *exponential growth* phase, an abundant supply of nutrients and light is maintained, cell division follows an exponential pattern over time and the growth rate is influenced by environmental factors such as nutrient availability, light intensity, and temperature. This state allows for the highest achievable cell growth rate. However, when one or more nutrients or light availability becomes limited, an equilibrium is established between active cell proliferation and mortality, resulting in the onset of the *stationary* phase (or *steady-state* condition). In this situation, microalgae population remains relatively constant over time with stable properties and once the nutrients are exhausted, the culture is harvested, and a new batch can be started. If it is not harvested,

the lack of nutrients and the accumulation of toxic metabolites leads to the death of microalgae. The *decline and cell death* phase is followed by the end of the culture, which results in the cleaning and sterilization of the reactor, in order to make it ready for a subsequent inoculation.

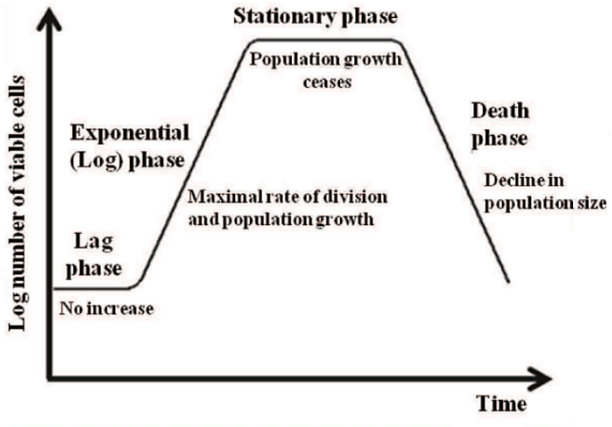

Figure 1.11. *Microbial growth curve (Cruz et al., 2018a).*

Batch cultivation is relatively simple, easy of use and flexible, so very popular on a commercial level (Lee and Shen, 2004). However, it may result in lower overall productivity due to downtime during nutrient exhaustion and harvesting and in higher costs.

In continuous cultivation, also known as chemostat cultivation, a constant flow of fresh medium is added to the culture while an equal volume of culture is removed at the same rate (Coelho *et al*., 2014): this maintains a steady-state condition and prevents nutrient depletion. Thus, as microalgae grow, they are harvested at a constant rate, maintaining a stable population, overcoming the high costs for each new batch process. In this condition, all variables remain constant (such as pH, CO_2 concentration, lipid and protein content, substrate and biomass concentration) and so they can be easily monitored and controlled. This condition allows for the production of a high quality product with stable characteristics over time and for the optimization of operating conditions (Egloff *et al*., 2018).

The time it takes to fill the reactor volume with a constant medium flow rate through the reactor once, is called the residence time (τ) (Equation 2.1) and is a critical operating variable for biomass growth. It is strictly connected to the volumetric productivity which is the biomass concentration produced per unit of time and volume as in Equation 1.3.

$$P_x = \frac{C_{x_{out}}}{\tau} \tag{1.3}$$

Setting an optimal residence time is essential for maximizing productivity. As residence time increases, biomass concentration asymptotically rises toward a maximum point, while

productivity declines. This phenomenon arises from the *self-shading* effect (§1.3.1) resulting from heightened culture density, which blocks the light from reaching deeper cells and limits their growth. Conversely, if the residence time is too low, biomass concentration and productivity abruptly decrease due to the *washout* phenomenon: cells are diluted out of the reactor more rapidly than they can proliferate and exit the reactor. This approach of controlling the biomass productivity through setting a defined residence time, has been shown to achieve productivity up to 2.3-5 times higher than what can be obtained in a batch cultivation (Lee *et al*., 2013).

In addition to the aforementioned benefits, there is also the near-complete elimination of dead times for biomass harvesting and the *lag* phase of growth, allowing for greater and more consistent production over time.

However, continuous cultivation systems are more complex to set up and require careful control of flow rates and nutrient concentrations. Moreover, the probability of contamination is higher due to the longer operating time and special equipment is required with respect to batch reactors, such as peristaltic pumps to ensure the continuous supply of fresh soil and the removal of exhausted medium, sensors for monitoring, controllers and other downstream processing equipment (Zhu, 2015).

The choice between batch and continuous cultivation depends on the specific goals of the microalgae production process. Each method carries its own benefits and drawbacks, with the choice influenced by factors like desired output, available resources, and the level of control needed over growth. Batch systems are often suitable for small-scale operations, research, or when specific growth phases or metabolite production are of interest. Continuous systems are favoured for larger-scale production, where consistent biomass or metabolite yields are essential.

1.4.4 Industrial scale-up

When transitioning microalgae cultivation from laboratory settings to larger scales, a series of algal culture transfers is employed, involving the stepwise transfer of cultures from smaller to larger systems along with the addition of culture media (Seidl *et al*., 2018). This scale-up process typically entails augmenting reactor volume, mixing speed, and light intensity in three main stages: progressing from discontinuous cultivation at a lab-scale, such as 500 mL Beckers, to semi-continuous (with a volume of 2500 mL) or continuous cultivation at lab-scale as exemplified by Bertucco *et al.* (2014), and ultimately culminating in continuous cultivation at a pilot-scale with volumes up to 100 L (Paladino & Neviani, 2020). Among the closed photobioreactors, only tubular and flat plate designs have found utility in large-scale microalgal cultivation due to their ability to maintain geometric similarities within the scale-up and so, substantial surface-volume ratios across various sizes (Posten, 2009). In contrast,

the bubble column design finds wider use in aquaculture settings. Consequently, a significant hurdle involves developing successful strategies for scaling-up, ensuring that photobioreactors at a larger industrial level exhibit the same level of efficiency as their smaller laboratory-scale counterparts. This challenge emerges due to the emergence of the limiting factors that become more pronounced at larger scales (Xu *et al*., 2009); some of them are presented below.

- Ensuring consistent light distribution and thorough mixing within larger culture volumes becomes increasingly complex as size grows, critical for optimizing productivity.
- Facilitating adequate gas exchange becomes a concern with system enlargement, as sufficient CO_2 supply for photosynthesis and efficient removal of generated O_2 become essential.
- The issue of minimizing shear stress, which escalates proportionally with culture medium volume, demands a delicate equilibrium to balance mixing and aeration without compromising cell integrity (Benner *et al*., 2022).
- The stringent oxygen control, the battle against biofouling, and the frequent necessity of material replacement contribute to elevated construction and operational costs compared to ponds. This comes in addition with the sterilizing of the PBR for specific high-value pharmaceuticals products (Da Silva & Reis, 2015).
- Temperature control can be a challenging task, particularly in large-scale outdoor cultivation systems. Fluctuations in temperature, whether on a daily basis or throughout different seasons, can have a significant negative impact on productivity. Cooling becomes especially crucial in closed PBRs and various strategies have been suggested to address this issue. One approach involves blocking a portion of the incoming radiation that reaches the reactor by covering the reactor with an opaque material affecting also the amount of light received by the system. Another method involves spraying the surface of the reactor with cool water or a cascade system where cool water is distributed over the reactor's surface. Alternatively, submerging the reactor in a pool of cool water can serve as a heat dissipator (Da Silva & Reis, 2015). On the other hand, when heating is necessary, for example during winters, a common solution is incorporating a heat exchanger within the air degasser. Another approach, as proposed by Albarello *et al.* (2019), involves air conditioning the greenhouse itself. This strategy helps avoid extreme temperature fluctuations and ensures a more stable environment for cultivation.
- Contamination prevention is another key consideration, with larger systems being more susceptible than their smaller counterparts, risking productivity loss or system failure.
- Biomass harvesting becomes challenging, due to the expensive and energy-intensive nature of biomass separation from the culture medium.
- Furthermore, the intricacies of sterilizing the photoreception unit within any closed photobioreactor have hindered their applicability for specific end-products like high-value

pharmaceuticals, underscoring technical obstacles in closed systems (Da Silva & Reis, 2015).

When considering the transition to large-scale production, optimizing the utilization of photosynthetically active radiation (PAR) emerges as a pivotal parameter for achieving substantial yields in terms of biomass and lipid content per unit area, while concurrently minimizing initial investment costs. Computational fluid dynamics (CFD) can be used to refine the structural design of photobioreactors to address the challenges of the industrial scaling-up (Xu *et al*., 2009). Additionally, predicting the behaviour of PBRs through kinetic models is fundamental for the feasibility of large-scale production units (Lee *et al*., 2015) and the most common ones are explained in the following section.

1.5 Mathematical models for microalgae growth

Integrating growth kinetic models into the scale-up of PBRs is pivotal for enhancing the production process. This integration facilitates the optimization of production by enabling more precise control over growth conditions and preventing critical regimes that could lead to a drop in productivity. Consequently, multiple studies have examined a variety of kinetic models, investigating the individual or combined impacts of forecasting the biomass growth rate, while maintaining the remaining parameters at saturation levels. The following sections will be focused on light intensity and temperature. It is important to notice that parameters of the model are adjusted for each case, so they might not really capture the actual physical, chemical, or biological actions taking place (Legrand *et al*., 2021).

1.5.1 Models considering light as a single factor

The growth kinetic models that focus on the singular influence of light intensity resemble Monod-like functions (Monod, 1949). In these models, the growth rate exhibits an exponential rise with increasing substrate concentration until it reaches a saturation point (μ_{max}), as illustrated in Figure 1.12.

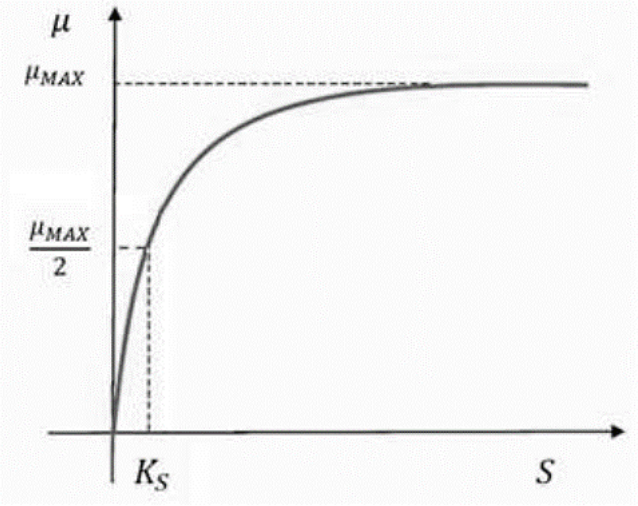

Figure 1.12. *Graphical representation of the Monod model.*

For instance, in the work of Tamiya *et al*. (1953), they replaced substrate concentration with light intensity, leading to the Equation 1.4.

$$\mu = \mu_{max} \frac{I}{I + K_I} \tag{1.4}$$

In this model, the growth rate is related to the incident light intensity with two parameters: μ_{max} is the maximum specific growth rate (d^{-1}) which indicates the maximum achievable specific growth rate when culture is in light saturated condition and K_I (µmol m^{-2} $s^{-1)}$ which is the light half-saturation constant at which the specific growth rate is half its maximum value.

It is important to consider that the Monod model is limited in its ability to explain growth in the absence of nutrients in the growth medium: an excess of nutrients must be present for the model to be valid. The Droop model (Droop, 1983), on the other hand, provides a method for modelling microalgal growth based on the cells' internal nutrient stores, as well as nutrient uptake and storage from the medium. Thus, when nutrients are abundant in the bulk medium, as in the current research, algal growth becomes independent of nutrient availability (Bernard, 2011).

These Monod-like models describing the effect of light are valid for low and moderate algae concentrations under laboratory conditions, assuming that each cell receives the same amount of incident light, meaning that there is minimal self-shading by the microalgae cells. However, in reality, light attenuation is commonly observed in microalgae cultivation systems. So, to account for light attenuation, the distribution of light according to Lambert-Beer (Equation 2.19) was introduced in the models instead of the incident or average light intensity (Béchet *et al*., 2013).

In addition, the equations described above do not take into account photoinhibition since the Monod-like behaviour implies that, as the light intensity increases, the growth rate increases until it reaches a maximum value. However, if the light intensity is too high, photoinhibition can occur, which will cause the growth rate to decrease.

The impact of light, when accounting for photoinhibition can be described by the Steele model (1962) which is based on an exponential function that represents both the activation of growth by light and the photoinhibition that occurs after a certain threshold and is expressed in Equation 1.5:

$$\mu = \mu_{max} \frac{I}{I_{opt}} e^{1-\frac{I}{I_{opt}}} \tag{1.5}$$

where I_{opt} (µmol m^{-2} s^{-1}) is the optimum light intensity that achieves the maximum growth rate, beyond which any increase in light intensity results in a lower growth rate.

Moreover, the Haldane kinetics model, which is derived from the model of Eilers and Peeters (1988), is also often used to describe the growth of microalgae. However, the reparametrized Haldane model, as suggested by Bernard and Rémond (2012), is more convenient to calibrate. This model is described in more detail in Section §2.4.

1.5.2 Models considering light and temperature

In non-limiting nutrient condition, temperature is the second most important parameter affecting microalgal growth, so finding an appropriate model which introduces the temperature influence on the growth is crucial.

A first approach to model the effect of temperature on photosynthesis is to consider light and temperature as two independent factors. These are called 'uncoupled' models since they express the rate of photosynthesis as the product of two distinct functions of light intensity and temperature. One example is the model by Bordel *et al*. (2009) in Equation 1.6 which multiplies a Monod function for light intensity with the Arrhenius term (Béchet *et al*., 2013):

$$\mu = \mu_{m,0} \frac{I_{av}}{K + I_{av}} e^{-\frac{E_a}{kT}} \tag{1.6}$$

where $\mu_{m,0}$ is the maximum specific growth rate (h^{-1}), E_a is the activation energy for photosynthesis (J), k is the Boltzmann constant (J/K), I_{av} is the average light intensity (µmol m^{-2} s^{-1}), and K is a light constant (µmol m^{-2} s^{-1}).

Alternatively, Bernard and Rémond (2012) expressed the maximum specific growth rate as a function of the minimum, maximum and optimum temperatures for photosynthesis (T_{min}, T_{max}, and T_{opt}). This model is explained in detail in §2.4 since is the one adopted in the current research.

However, also 'coupled' models were developed in order to account for the potential interdependence of light and temperature on the rate of photosynthesis.

In fact, under light-limited conditions, the rate of photosynthesis is limited by the rate of photon supply (Davison, 1991) and the rate of photon capture can be considered quite independent from temperature, while in condition of light-saturation, temperature may impact the threshold at which the dark reactions of photosynthesis can occur and with it, the maximum growth at light saturation (Béchet *et al*., 2013).

For example, in the model developed by Dermoun *et al*. (1992), the parameters of the 'light-inhibition model' were all made functions of temperature and the specific growth rate and is shown in Equation 1.7.

$$\mu = 2\mu_m(T)(1 + \beta_I) \frac{\frac{I}{I_{opt}(T)}}{1 + 2\beta_I \frac{I}{I_{opt}(T)} + \left(\frac{I}{I_{opt}(T)}\right)^2} \tag{1.7}$$

Where $\mu_m(T)$ is the maximum specific growth rate (d^{-1}) at the temperature T (°C), β_I is a constant and $I_{opt}(T)$ is the optimum light intensity µmol m^{-2} s^{-1} for photosynthesis at temperature T.

Another model that has been developed is the Hinshelwood model (Hinshelwood, 1945). This model is more mechanistic than the Monod model and has the advantage of explicitly

including a deactivation term making a significant difference for growth modelling (López Muñoz & Bernard, 2021).

While coupled models theoretically offer a more accurate portrayal of temperature impact compared to uncoupled models, it is important to note that the limiting step of photosynthesis is not always temperature-dependent. Furthermore, coupled models demand the empirical fitting of a substantial number of parameters (for instance, 9 in the model illustrated by Equation (1.7)). As a result, 'overfitting' could occur: apparent good fitting during validation may only be due to a good adjustment of the set of parameters (Béchet *et al*., 2013). Consequently, the reliability of such models in predictive applications becomes questionable, with few of authentic predictive models available that can be applied across diverse conditions without necessitating parameter fitting (Lee *et al*., 2015).

1.6 Constraints to microalgae applications

Despite all the advantages and potentialities of microalgae commercialization, there are still many challenges that need to be addressed in the field which come in addition to the already treated problems of industrial scale-up (§1.4.4).

Some of the most critical problems are the low biomass productivity, the difficult in providing nutrients and water to grow, the availability of carbon dioxide and its cost of capturing and transporting which can be prohibitive. To address these issues, methods such as mixotrophic cultivation, the use of cheap low-carbon sources, industrial and municipal wastewater as cultivation media can be used to increase biomass production. With the development of efficient large-scale cultivation systems, microalgal biotechnology can meet the demanding requirements of food, feed, nutraceuticals, pharmaceuticals, and biofertilizers (Udayan *et al*., 2021). However, the availability of advanced technologies for large-scale biomass production and lipid conversion into biodiesel, microalgal biodiesel is still too expensive. This limitation is caused by costs related to the careful control of temperature and other growth-limiting conditions that the cultivation system design requires. Thus, the commercially viable production of algal biofuel remains a challenge. Although an increase in productivity has been observed at the lab-scale and pilot-scale using photobioreactor systems (PBRs), their large-scale implementation is limited by the challenges of scaling-up and the high costs involved. As a result, about 95% of commercial microalgae biomass cultivation is still done in open raceway ponds (Veeramuthu & Ngamcharussrivichai, 2021).

The economically successful cultivation of microalgae biomass is contingent on overcoming several production cost-influencing barriers. The severity of these production cost barriers depends on the market value of the final product and includes: the cost of water and limitations on its recycling, the cost and recycling of nutrients, CO_2 utilization, the energy

costs associated with harvesting and biomass loss due, for instance, to biocontamination (Lane, 2022).

1.7 Aim of the thesis

In the context of the development of the microalgae industry, it is essential to improve the scaling-up from lab-scale to large-scale cultivation in order to address the technical and economic challenges related to microalgae commercialization.

The aim of this thesis is to characterize the parameters for a suitable mathematical model of microalgal growth based on laboratory experimental results. This will allow to find the best conditions of light and temperature for large-scale cultivation.

The analysis of the combined effect of light and temperature is performed in a small-scale photobioreactor of 45 mL. The microalgae strain under analysis is the microalga *A. obliquus* and the biomass concentration is monitored for each condition. A parallel study is also conducted to analyse the pigment content as a function of light and temperature, as well as an image analysis to evaluate the effect of both variables on cell diameter.

Chapter 2

Materials and methods

This chapter will focus on the cultivation conditions of the microalga *Acutodesmus obliquus* and on the setup built for the experiments. Moreover, the monitoring analysis and protocols to follow the growth of the biomass will be discussed, as well as the laboratory equipment. In the end the equations used to build a mathematical model for the scale-up are reported.

2.1 Microalgae strain and culture medium

Acutodesmus obliquus 276-7 from the SAG collection of the University of Goettingen was cultivated in sterile BG11 medium (Stanier *et al*., 1979). The concentration of the nutrients (Table 2.1) was duplicated with respect to the original medium, with the exception of K_2HPO_4 which was 4x concentrated to guarantee non-limiting nutrient condition.

Table 2.1. *Composition of culture medium.*

Nutrient	Concentration (2x) [mg L^{-1}]
Na_2Mg EDTA	2
(NH4)5[Fe(C6H4O7)2]	12
Citric Acid · H_2O	12
$CaCl_2 \cdot 2H_2O$	72
$MgSO_4 \cdot 7H_2O$	150
K_2HPO_4	122
H_3BO_3	5.72
$MnCl_2 \cdot 4H_2O$	3.62
$ZnSO_4 \cdot 7H_2O$	0.44
$CuSO_4 \cdot 5H_2O$	0.16
$CoCl_2 \cdot 6H_2O$	0.1
$Na_2MoO_4 \cdot 2H_2O$	0.78
Na_2CO_3	40
$NaNO_3$	3000

The medium was buffered with HEPES 10 mM, pH 8, to avoid acidification due to CO_2 excess and to maintain the pH in the range of algal viability, i.e., between 7 and 8 (Gris *et al*., 2014). The value of pH was monitored using a Hanna portable pH-meter (code HI9124), in 250 mL Erlenmeyer flasks placed in an orbital shaker. The media and the setup materials were sterilized by autoclaving for 20 min at 121 °C to avoid possible contaminations.

2.2 Cultivation system

The pre-cultured microalgae were initially grown in a sterile 1L Erlenmeyer flask which was maintained at ambient temperature. From the pre-inoculum some biomass was taken and diluted in a reactor which was kept in batch mode inside a refrigerated incubator (Frigomeccanica Andreaus, Padova) at a constant temperature of 24 ±1°C. It was periodically renewed with fresh medium under a laminar flow hood and was stirred by a magnet, bubbled with air and illuminated to speed up the acclimation of the biomass. There cultures were used to inoculate the reactors of the study.

Experiments were carried out in two milli-photobioreactors in parallel. The reactors were equipped with a thermal jacket and thanks to a thermostat were maintained at a constant temperature. They were also connected to a pumping system which fed fresh medium according to a set volumetric flowrate, as Figure 2.1 shows.

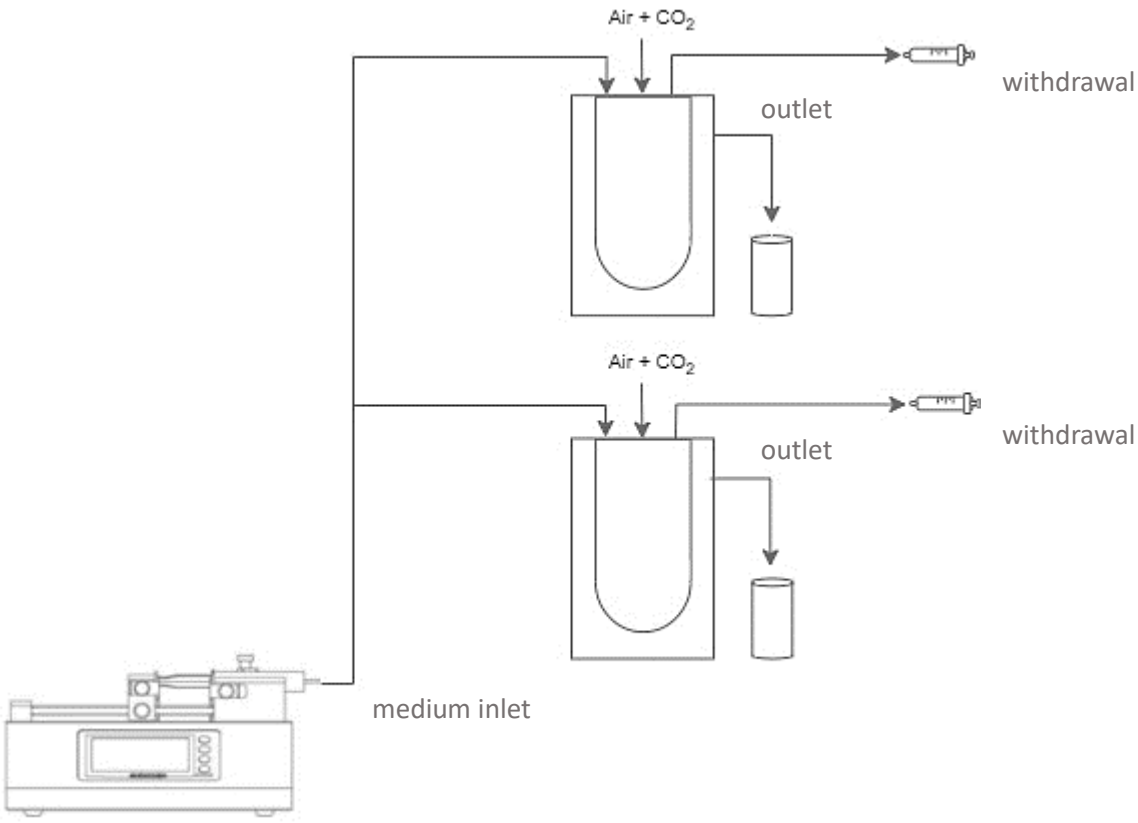

Figure 2.1. *Scheme of the continuous cultivation system. Temperature control is not reported here.*

This configuration is equivalent to a CSTR (Continuous Stirred Tank Reactor) where the volume is kept constant overtime thanks to a liquid outlet stream placed on the top of the reactor. The biomass and exhausted medium are then collected and kept aside for the analysis. The ideal perfect mixing is ensured by the combined effect of the gas bubbling and the mechanical mixing.

The fresh medium was fed constantly by a two-way PHD ULTRA syringe pump (Harvard apparatus, USA), as in Figure 2.2, with 60 mL syringes, connected to a tube of small diameter without contacting the liquid medium inside the reactor to avoid clogging phenomena due to biomass aggregation.

Figure 2.2. *Two-way PHD ULTRA syringe pump*

The flow rate of the pump is programmed depending on the wanted residence time. The residence time τ (d) is inversely proportional to the flow rate ($\dot{V}$) according to the following relation:

$$\tau = \frac{1}{D} = \frac{V_{PBR}}{\dot{V}} \tag{2.1}$$

Since the dilution rate D is equal to the specific growth rate μ (d^{-1}), by changing the residence time, a different growth rate can be imposed on the culture (Gons and Mur, 1980).

Figure 2.3 *LED lamp and LED controller*

Reactors are maintained at a constant temperature thanks to the cooling thermostat ECO RE420 S (Lauda, Germany) which uses cryogenic decalcified water (Aqua 90) that flows

inside the reactor's jacket. Temperature is monitored through a thermocouple that transmits data on a software (PicoLog) which draws a graph of temperature trend over time.
Reactors were illuminated by a continuous light provided by a white LED lamp (SL 3500, Photon Systems Instruments), connected to a controller to modulate the incident light intensity, as in Figure 2.3. Light intensity was measured by a photoradiometer (HD 2101.1 from Delta OHM), which quantifies the photosynthetically active radiation (PAR).

2.2.1 Milli-photobioreactors

The two milli-PBRs of 45 mL of volume are built in the same way, by three main parts. All the details about the dimensions are shown in Figure 2.4. They are composed of a polycarbonate central flat plate with a bottom U shape (15 mm of thickness) with a hole for the outlet stream and an irradiation surface of 9 cm^2. The particular shape is useful to ensure a good mixing and reducing the deposition phenomena to the minimum. The choice of polycarbonate is due to the good balance of its performance and cost. It is used for its transparency which allows a good transmission of the incident light providing the necessary energy for the microalgae's photosynthetic process. Moreover, its durability makes it able to withstand corrosion and mechanical damage; its light weight is an advantage in the installation, but most of all, the chemical inertness ensure that it does not react or release harmful substances for the microalgae.

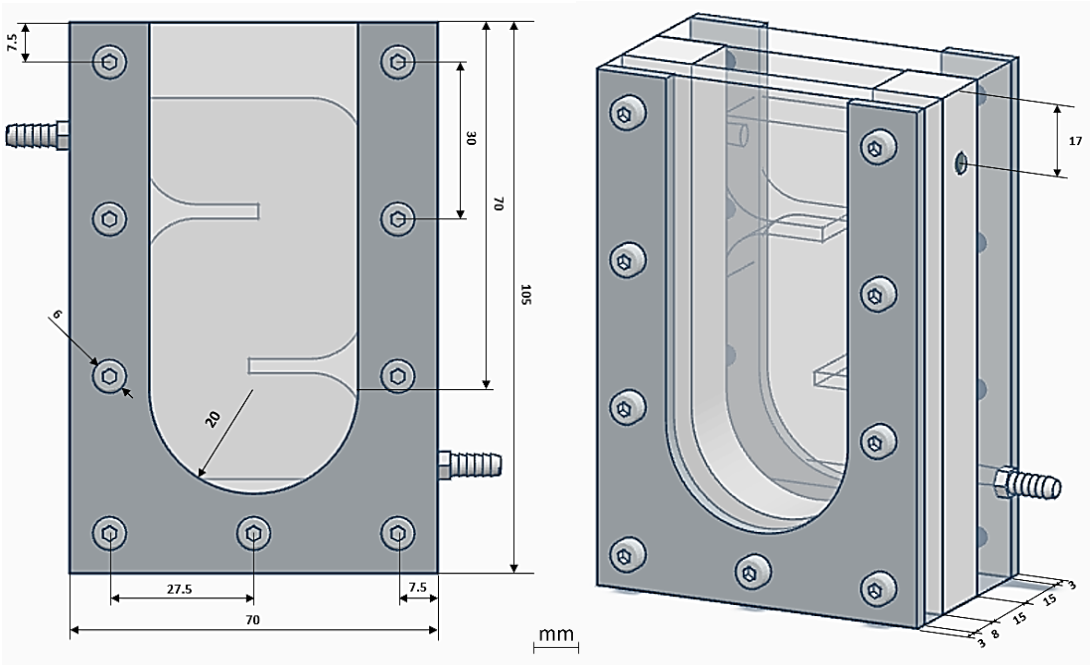

Figure 2.4. *Details and dimensions of the reactor.*

The frontal face, made in polycarbonate as well, guarantees, thanks to its transparency, the maximum utilization of the light energy. The third part is represented by the thermal jacket.

All the plates have holes to insert INOX screws and bolts and between them two silicone sheets are set.
The strength with which it is assembled is of paramount importance: a particular attention is needed to tighten the screws as much as possible to avoid leaks in the reactor but not so much to cause ruptures in the plates. To ensure a homogeneous distribution of the strength along the reactor and to prevent cracks, an INOX plate with the same bottom U shape was inserted later in the front.
The two thermal jackets were specifically printed for the reactors with a 3D printer and provided by Leibniz University Hannover.
It was ensured thanks to a micro stirring magnet placed at the bottom of the reactors (reactors are placed on a magnetic agitator) and through an air flow from a sparger placed at the bottom of the panel. Mixing velocity of the magnet was set at minimum possible because excessive mixing may produce cell damage and result in culture collapse, if the microalgae are susceptible to the shear force (Acién Fernández *et al*., 2013). The bubbling system was performed by air pump connected with 0.2µm PTFE in line air filter (Sartorius Midisart 2000, USA). The line passes previously through a humidification system with deionized water to saturate all gases and avoiding an excessive evaporation of the liquid inside the reactor. Thanks to a system of valves, the air sparger reaches the reactor and it is placed at the bottom, above the stirrer, and, preferentially, far away from the outlet.
The daily biomass sample needed for the analysis was withdrawn thanks to a small tube placed inside the reactors and connected to a 10 mL syringe.
The reactors were not closed completely in order to guarantee the gas exchange with the atmosphere, but at the same time so that the risk of contamination was reduced much as possible. Due to the position of the inlet and the outlet, both on the upper part of the reactor, an additional plastic piece was introduced. In this way, the medium path is forced to prevent a "short-circuiting" situation: creation of a preferential flow path and the exit of the medium before microalgae have absorbed the nutrients.

2.3 Monitoring protocols

2.3.1 Optical density

To track stability of the growth of the microorganisms, the value of the optical density at 750 nm (OD_{750}) and at 680 nm (OD_{680}) was checked daily. The measurement was performed using a double beam spectrophotometer (UV1900, by Shimadzu, Japan) with a 1 cm optical path length at a wavelength of 750 nm, which is outside the absorption range of chlorophyll and other photosynthetic pigments, therefore accounting for scattering effects only (Trentin *et al*., 2022). The optical density at wavelength of 680 nm, associated with chlorophyll absorption,

was useful for monitoring the change in in the ratio of OD_{680}/OD_{750}, used as a proxy for chlorophyll content per cell (Sivakaminathan *et al*., 2018).

The biomass sample was taken from the 10 mL syringe, after having resuspended properly the liquid inside the reactor. The instrument was loaded with two cuvettes, each containing 2 mL of volume: one with the biomass sample and the other, the blank, composed of BG11 medium (described in Table 2.1) to subtract in absorbance measurements the contribution of its components. The beam coming out from the instrument's monochromator is split into two beams, one sent to the sample and one to the blank. After crossing the samples, the signals arrive at the detectors.

The measure of the optical density is important to indirectly have a measure of the concentration of the biomass in the reactor, using the linear correlation between the two variables described by Lambert-Beer's law:

$$A = -log\ \frac{I}{I_0} = \varepsilon \cdot C \cdot l \tag{2.2}$$

where I_0 is the incident intensity of light, I is the intensity of light transmitted through the sample and measured by the photo sensor, A represents the absorbance measured by the instrument, ε the attenuation coefficient at a given wavelength, C is cell concentration and l the optical path. The attenuation coefficient (extinction cross-section) characterizes how strongly a suspension attenuates light (Myers at al., 2013). In a range of A comprised between 0.1 and 1, the attenuation coefficient and the pathlength can be considered constant and so, the Beer-Lambert law can be used to proportionately correlate biomass concentration (g/L) with optical density.

2.3.2 Dry weight

Dry weight (DW) represents the weight of biomass within a given volume of culture. By knowing the dry weight, it is possible to trace the concentration of the culture in terms of grams per litre. The protocol for measuring dry weight involves taking a sample of 10 mL and placing it on a nitrocellulose filter with a pore diameter of 0.45 μm (Whatman ®). The filter was previously dried in a ventilated oven at 110°C for 10 min to allow the moisture evaporation and weighed through a precision balance (Atilon Acculab Sartorius Group®) which has a sensitivity up to 10^{-4} g, obtaining the tare. Then, activating a vacuum pump, the supernatant was separated leaving only biomass on the filter. The filter was then dried at 110°C for about 2 hours before weighing it again. The cell concentration was calculated as follows (Pastore, 2016):

$$DW\ [gL^{-1}] = \frac{gross\ weight - tare}{V_{sample}} \tag{2.3}$$

2.3.3 Front and back irradiance measurements

In order to assess the density of the photon flux absorbed by the culture (PFDabs) at steady state, the irradiance was measured at the level of the liquid inside the milli-PBRs both in the front and behind the reactor (*back irradiance*). Nevertheless, since the photoradiometer's probe is highly sensitive, the measurement of light intensity is suggestive.

2.3.4 Cell counting

The cellular concentration of the cultures was also evaluated by means of the manual cellular counting using an optical microscope (OPTIKA®). This analysis was performed in a Bürker counting Chamber (Optik Labor, Germany). It is a slide 7.5x3.5 cm in size and 4 mm thick on which there are two chambers of 10 µL volume each covered by a coverslip stuck to the sides. Each of these two square chambers is distinguished by a particular lattice: it is partitioned into 9 quadrants with a triple line as a separator (3x3 lattice), measuring 1 mm on each side. Each of these, in turn, consists of 16 small squares (4x4 lattice), separated by a double line, expanded by 0.20 mm. The two primary squares are divided among themselves and enclosed by small drains to gather surplus sample.

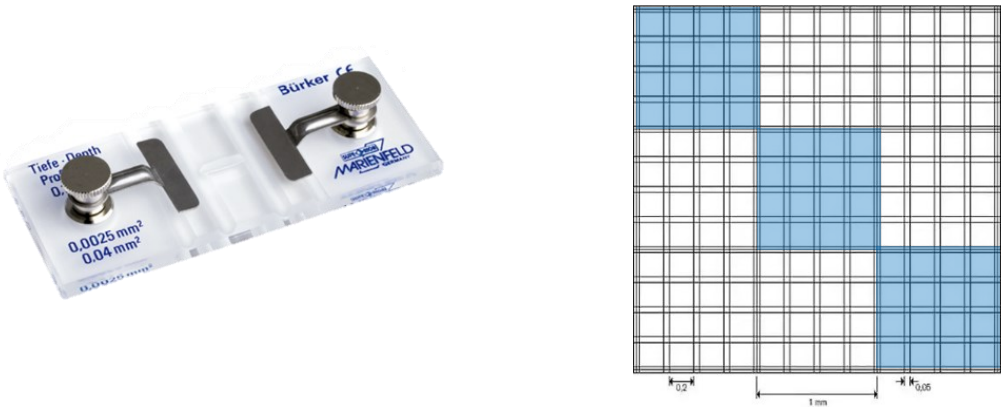

Figure 2.5 *Bürker chamber and the counting grid of one quadrant*

The sample was appropriately diluted, between 20 and 500, depending on the estimated concentration, with deionized water and loaded with slightly excess volume (20 µL) inside each of the 2 chambers by exploiting the phenomenon of capillarity.
Since the cellular count is characterized by an inherent discrepancy of approximately 1 to 10%, it is recommended to work with no more than 100 cells per row. This can be achieved by diluting the original sample with deionized water to a sufficient extent (typically using dilutions of 1:100 or 1:500), in order to increase the accuracy of the counting results. Counting is done for 3 squares only, following the diagonal of the 3x3 grid, for each of the

two chambers, as shown in Figure 2.5, which each of these has a volume of 0.1 mm^3(10^{-4} mL). The number of cells per unit volume is calculated as follows.

$$Cell\ concentration\ [cell\ mL^{-1}] = \frac{\sum cells}{6} \cdot 10^4 \cdot dilution\ factor \quad (2.4)$$

Where the ratio stands for the average of the cells counted in the 6 quadrants and the term 10^4 represents the volumetric factor of the Bürker chamber, which depends on the volume of the square, which is 0.1 μL (1/.0001 mL).

2.3.5 Image analysis

In order to evaluate the joint effect of light and temperature on the cell diameter, image analysis was performed. According to the protocol, a camera (CANON EOS 4000D) equipped with an 18-megapixel high-sensitivity MOS sensor, was placed in the designated tube of the microscope. Pictures were taken in steady state condition, for 3 days, both for diameter analysis and for the automatic cell counting. The Bürker Chamber was filled with 1:1 dilution of the sample and one picture was taken for each of the 3x3 diagonal quadrants of the two main squares, for a total of 6 photos for each T-I combination.

A MatLaB® script was developed to analyse the photos. Each image was first rotated and cropped to obtain the desired analysis area. Next, the images were converted from RGB to grayscale, and then into binary images, where background noise were removed. Once the cells were correctly selected through a watershed segmentation, some statistical measurements were performed to compare diameter, volume and shape of the cells of each experiment. This results with the evaluation of the following average values of the 6 images for each day:

- Average Feret diameter (μm), calculated from the mean between minimum and maximum diameters (d and D, respectively).
- Cell volume (μm^3), calculated as reported in Sun & Liu (2003) :

$$Volume\ = \frac{\pi}{6} d^2 D \quad (2.5)$$

- Circularity (-), calculated as (internal MatLaB® function):

$$Circularity = \frac{4 \cdot\ area\ \cdot \pi}{perimeter^2} \quad (2.6)$$

- Elongation (-), calculated as:

$$Elongation\ = \frac{D}{d} \quad (2.7)$$

Thus, 3 sets of average values were obtained, one for each stationary day. In conclusion, the mean and standard deviation of each average value between the 3 days, were plotted as function of light and temperature.

2.3.6 Pigments

According to the protocol of the extraction and the analysis of chlorophyll and carotenoids from the biomass, developed by Moran and colleagues (Moran *et al*., 1980), a solvent was used for the lysing of the cell wall and membrane which solubilized and stabilized the extracted pigments with a very fast reaction. In this protocol, N-Ndimethyl-formamide (DMF) was used. After centrifuging 1 mL of sample for 10 minutes at 13500 rpm, the supernatant was removed and then the pellet was resuspended in 1 mL of DMF under a chemical fume hood. It was essential to operate in the dark after the DMF addition, to avoid the degradation of the photosensitive pigments. The samples were then frozen in the dark at -20°C for at least 24 hours.

In order to perform the pigment analysis, the samples were thawed and centrifuged for 10 minutes at 13500 rpm to separate the pellet from the supernatant which was recovered, loaded into quartz cuvettes, and analysed with the spectrophotometer (Shimadzu UV-1900). Absorption spectra in the 350-750 nm range were acquired, where absorbance at 480, 647 and 664 nm was used to calculate concentrations of the pigments. An important notice was that, if the spectrum profile exceeded the absorbance value of 1, the sample had to be diluted properly. The following equations were used for quantification of chlorophyll *a* (Chl *a*), chlorophyll *b* (Chl *b*) and carotenoids (Car) (Wellburn, 1994):

$$Chl\ a\ [\mu g\ mL^{-1}] = (11.65\ \cdot\ A_{664} - 2.69\ \cdot\ A_{647}) \cdot dilution\ \cdot\ \frac{V_{DMF}}{V_{sample}} \quad (2.8)$$

$$Chl\ b\ [\mu g\ mL^{-1}] = (20.81\ \cdot\ A_{647} - 4.53\ \cdot\ A_{664}) \cdot dilution\ \cdot\ \frac{V_{DMF}}{V_{sample}} \quad (2.9)$$

$$Car\ [\mu g\ mL^{-1}] = \frac{1000\ \cdot\ A_{480} - 0.89\ \cdot\ Chl\ a - 52.02 \cdot\ Chl\ b}{245} \cdot dilution\ \cdot\ \frac{V_{DMF}}{V_{sample}} \quad (2.10)$$

where V_{DMF} was for the overall DMF volume of the blank reference (1 mL), while V_{sample} stands for the initial sample volume (1 mL).

2.3.7 Orthophosphates

The analysis of orthophosphate content (PO_4^{3-}) is a colorimetric assay (Innamorati *et al*, 1990) whose reaction was based on the use of a pre-prepared reagent composed of 5N sulfuric acid (H_2SO_4, 2.5 M), potassium antimony tartrate (1.36 g L^{-1}), ammonium molybdate tetrahydrate (30 g L^{-1}) and ascorbic acid (54 g L^{-1}).

For the reaction, 400µL of reagent and 2 mL of sample were needed to form of a blue complex of molybdate, revealing the presence of phosphate ions in the sample. Then, a spectrophotometer (Shimadzu UV-1900) measured the concentration of the sample at a

wavelength of 705 nm, which is the one absorbed by the phosphomolybdate complex. If the absorbance value exceeded 1, a dilution was needed. The concentration of the sample was determined by interpolation using a calibration line obtained with a solution of known phosphate concentration, with the following equation:

$$PO_4^{3-}(mg\ L^{-1}) = 7.5905\ \cdot abs - 0.012 \quad R^2 = 0.997 \tag{2.11}$$

where *abs* is the absorbance.

2.3.8 Respirometry

Respirometry is a test that is based on the measurement of dissolved oxygen concentration during light-dark cycles. Indeed, during the light period there is an increase in the concentration of dissolved oxygen (Oxygen Production Rate, OPR) due to the photosynthetic activity of the microalgae, while during the dark period, oxygen is consumed due to endogenous respiration/organic carbon consumption. The oxygen production/consumption depends mainly on temperature, nutrients and incident light intensity, but is monitored as a function of one single variable at a time, keeping the other ones, constant. For the purpose of this thesis, the respirometry was executed varying only temperature in order to calculate the kinetic parameters for the mathematical model. In order to cover the vital range of *A. obliquus*, from 12 to 40°C, the analysis was performed examining 5 steps of temperatures: 12, 19, 26, 33, 40 °C within 10 hours.

The sample of microalgae to be tested was taken from a steady-state condition, where the microalga was perfectly acclimated to light and temperature, in order to be sure of the value of the concentration in the reactor. The latter must be between 0.2 and 0.4 g L^{-1} for a correct monitoring of the oxygen and due to limitations of the equipment, so the sample withdrawn from the reactor should be diluted appropriately to have the right concentration and reaching 90 mL of total volume. The sample was inserted in a glass flask of 100 mL and square section (4.2 cm x 4.2 cm x 8 cm) and the biomass was constantly stirred from below with a magnetic stirrer. Inside the flask also the oximeter probe was inserted as well as the nitrogen tube, used for the oxygen stripping. All the components were placed such that a minimum gas headspace was left to avoid gas losses in the gas phases and closed perfectly with PARAFILM. The flask was inserted into a thermostatic water bath for temperature monitoring and control and then, exposed to a constant light provided by a LED lamp which was measured by the photoradiometer. This setup was located inside of a dark box, isolated from external light sources, both for the light cycle to have an illumination as precise as possible and for ensuring total darkness during the dark phase. The concentration of dissolved oxygen in the medium was measured every 15 seconds using an oximeter (Delta OHM HD 2109.1) and monitored

using *DeltaLog9* software. The oxygen concentration shall remain in the range of 4-8 ppm to prevent microalgae being under stress condition. Each test consisted in alternating cycles of light and dark obtained by means of a digital controller connected to a LED lamp. At the point when the oxygen concentration value approaches the value of 8 ppm, the sample was bubbled with nitrogen gas to bring it down again. The evolution of oxygen over time was observed for at least four replicates per condition, obtaining a profile resulting in a "sawtooth" profile with positive and negative slopes, corresponding to light and dark conditions, respectively.
Starting a new run meant setting the new set-point temperature in the dark phase, waiting for transmission in the bath and so, the first 10 min of data acquisition were discarded to allow the acclimation of the microorganisms to the environmental conditions applied.
The angular coefficient of the obtained curves represents the rate of production and consumption of Oxygen and allows obtaining the Oxygen Production Rate (OPR) and the Oxygen Consumption Rate (OCR). These values can be related to the biomass growth rate via a yield term Y_{X/O_2}.
The variation of the dissolved oxygen, DO, (mg L^{-1}) in time can be expressed as:

$$\frac{d(DO)}{dt} = OTR + OPR \tag{2.12}$$

where the Oxygen Transfer Rate, OTR (mg L^{-1} min^{-1}) refers to the rate at which oxygen is transferred from the gas phase to the liquid phase and is:

$$OTR = k_L a\ (DO_{sat} - DO) \tag{2.13}$$

The term DO_{sat} is the saturation concentration oxygen which refers to the maximum amount of dissolved oxygen that can be held by water at a given temperature and pressure, under equilibrium conditions. Obtaining OPR from the Equation 2.12, OPR measured (apparent) can be calculated:

$$OPR_{app} = OPR - OCR \tag{2.14}$$

In order to compute the overall oxygen transfer coefficient ($k_L a$), the differential equation (2.12) can be integrated from DO to DO_{sat} and the (2.16) is found.

$$\frac{d(DO)}{dt} = k_L a\ (DO_{sat} - DO) \tag{2.15}$$

$$ln\ (DO_{sat} - DO)\ = -k_L a\ \ (DO_{sat} - DO) \tag{2.16}$$

Experimentally, starting from an oxygen-saturated solution, the decreasing concentration of oxygen is measured and plotting $ln\ (DO_{sat} - DO)$ in time, the slope obtained is -$k_L a$.

2.4 Mathematical model

In order to assess a possible correlation between light and temperature, they were first assumed as two independent functions. So, the specific growth rate, μ (d^{-1}) namely, the rate of increase of cell population per unit of biomass concentration, was expressed as in the model described by Bernard and Rémond (2012). It is presented as the result of the multiplication between a function depending only on light, $\mu_{opt}(I)$ which is the optimal specific growth rate reachable (d^{-1}) corresponding to a temperature T_{opt}, and another depending only on temperature, $\phi(T)$:

$$\mu(T,I) = \mu_{opt}(I) \cdot \phi(T) \tag{2.17}$$

Then, a parametric estimation with the experimental data was done to validate the model and depending on the goodness-of-fit, that assumption could be accepted or not.
The optimum specific biomass growth rate can be defined according to the Haldane function:

$$\mu_{opt}(I) = \mu_{max} \cdot \frac{I(z)}{I(z) + K_I\left(\frac{I(z)}{I_{opt}} - 1\right)^2} \tag{2.18}$$

where K_I and I_{opt} (μmol m^{-2} s^{-1}) are the half-saturation constant of the light response curve and the light intensity for maximal growth rate, respectively.
Considering a rectangular geometry of the reactor, light extinction profile along the culture depth, W (m) can be calculated according to the Lambert–Beer law:

$$I(z) = I_0 \cdot e^{-k_a \cdot C_{x_{out}} \cdot z} \tag{2.19}$$

where I_0 is the incident light intensity (μmol m^{-2} s^{-1}), k_a is the biomass light absorption coefficient (m^2 g^{-1}), $C_{x_{out}}$ is the biomass concentration inside the reactor (g m^{-3}) and z is the axial coordinate of the reactor depth (m).
According to the Bernard model (2012) which is, in turn, based on the so-called cardinal temperature model with inflexion (CTMI) proposed by Rosso *et al.* (1993), the dependency on temperature in Equation 2.17 can be expressed as:

$$\phi(T) = \frac{(T - T_{max})(T - T_{min})^2}{(T_{opt} - T_{min})[(T_{opt} - T_{min})(T - T_{opt}) - (T_{opt} - T_{max})(T_{opt} + T_{min} - 2T)]} \tag{2.20}$$

This is a four-parameter model: T_{min} (°C) and T_{max} (°C) that are the limiting temperatures outside which there is not growth and the optimal temperature T_{opt} (°C).
Consequentially, considering that the dependency of the growth rate on nutrients concentration is neglected since they were provided in excess (as well as CO_2), the net growth rate of the cell population r_x (g $m^{-3}d^{-1}$), can be expressed as follows:

$$r_x(z) = \mu(T, I) \cdot C_{x_{out}} - k_d \cdot C_{x_{out}} \tag{2.21}$$

where k_d (d^{-1}) is a specific decay rate that accounts for cell respiration and maintenance (Barbera *et al*., 2020).

Thus, substituting the 2.17 (combined with the 2.18, 2.19, 2.20) in the 2.21, it is obtained the following:

$$r_x(z) = \mu_{max} \cdot \phi(T) \cdot \frac{I(z)}{I(z) + K_I \left(\frac{I(z)}{I_{opt}} - 1\right)^2} \cdot C_{x_{out}} - k_d \cdot C_{x_{out}} \tag{2.22}$$

Averaging the biomass growth rate along the axial coordinate of the milli-PBR due to its dependency on the varying light intensity along the reactor thickness, W (m) (Saccardo *et al*., 2022), the average biomass growth rate $\bar{r_x}$ (g $m^{-3}d^{-1}$), is obtained as:

$$\bar{r_x} = \frac{1}{W} \int_0^W r_x(z) dz \tag{2.23}$$

As previously said, each PBR can be modelled as a CSTR where the biomass concentration inside the reactor can be considered constant along the culture depth. So, the mass balance can be defined as below:

$$\frac{dC_{x_{out}}}{dt} = \bar{r_x} - \frac{1}{\tau} C_{x_{out}} \tag{2.24}$$

where τ (d) is the biomass residence time, already defined in Equation 2.1.

$$\bar{r_x} - \frac{1}{\tau} C_{x_{out}} = 0 \tag{2.25}$$

Once the model had been established, some experimental data were used for the estimation of the 8 parameters: $T_{opt}, T_{min}, T_{max}, I_{opt}, \mu_{max}, k_a, k_d, K_I$, then, model validation was performed using other experimental data.

Chapter 3

Results and discussion

This chapter will present and discuss the experimental results of the continuous cultivation of *A. obliquus* in milli-photobioreactors. The study specifically investigates the combined effect of light intensity and temperature on various aspects of the microalgae, including biomass concentration (dry weight), pigment content, cell morphology, and dimensions. Additionally, the outcomes of modelling simulation and its parametric estimation will be shown and analysed.

3.1 Biomass concentration and productivity at steady state

After the microalgae were inoculated, the biomass growth was monitored daily by measuring OD_{750} and when the values stabilized, as shown in Figure 3.1, the steady state was considered to be reached and the value of the dry weight, together with the appropriate biochemical analyses were then carried out according to the protocols reported in Chapter 2. These measurements were executed at least for 3 days of steady state, in order to obtain more precise results. The time required to reach the stationary condition depended on the microalgae acclimation time to a new environment: could vary due to the temperature and irradiance step change or to the initial inoculum concentration. In all experiments, the steady state was always reached, except in cases of contamination, when reactor required to be re-inoculated.

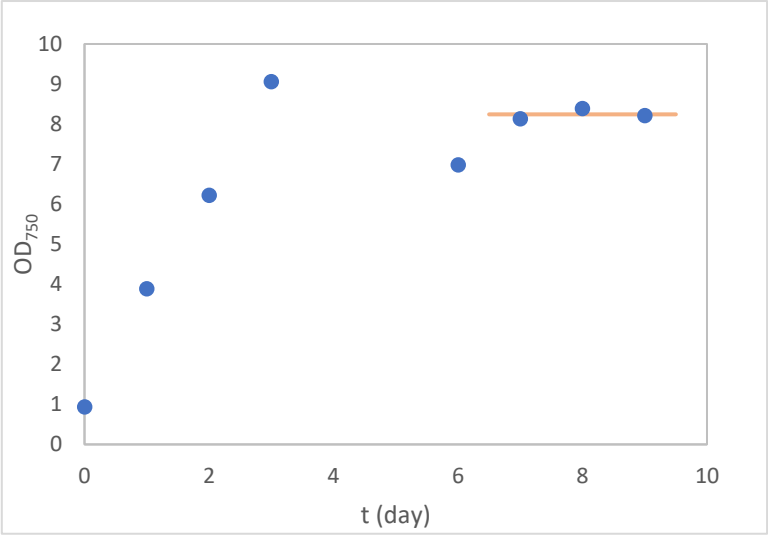

Figure 3.1. *Optical density (OD) variation in time and reaching of a steady state at 600 µmol $m^{-2}s^{-1}$ and 30°C.*

Experiments were conducted at 5 light intensities (150, 300, 600, 900, and 1200 µmol m^{-2} s^{-1}) and 4 temperature levels (18, 24, 30, and 36 °C), with a volumetric flow rate of 30 mL day^{-1} to achieve a constant residence time of τ = 1.3 days.

3.1.1 Dry weight results

Figures 3.2 and 3.3 present the outcomes concerning biomass concentration at steady state, expressed as dry weight (g L^{-1}) as a function of light intensity and temperature, respectively. The specific numerical findings are outlined in Table 3.1.

As described upon in the light effects discussion (§1.3.1), the pattern of biomass concentration aligns with the light-response curve. At lower light intensities, the rate of photosynthesis is limited by the rate of photon supply, which is considered to be independent from temperature, resulting in an almost linear increase in biomass concentration with irradiance (Béchet *et al*., 2013). Subsequently, the rate of photosynthesis attains a saturation threshold (maximum light), beyond which it declines due to the deactivation of crucial proteins within the photosynthetic units (Rubio *et al*., 2002). The plot effectively highlights that highest biomass concentration at steady state is obtained at 600 µmol m^{-2} s^{-1}, regardless of temperature.

Likewise, the impact of temperature on biomass concentration (Figure 3.3) reveals an optimal temperature of 30°C for all light levels. Below and above this optimal temperature, the growth and concentration of microalgae can decline: at significantly lower temperatures, an overproduction of energy supply can occur, due to the reduction in the carboxylase activity, reducing the rate of photosynthesis (§1.3.3). Conversely, elevated temperatures can subject microalgae to thermal stress, which can affect the functionalities of enzymes (inactivation, denaturation) which are involved in photosynthetic processes, thereby inhibiting growth (Ras *et al*., 2013).

It can be observed how the impact of temperature on microalgal growth varies upon light conditions. Even though the peak growth remains steady at 600 µmol m^{-2} s^{-1}, it is worth noting that at lower light levels, the effect of temperature on concentration is less marked compared to more intense light conditions (in Figure 3.2, data points at 150 µmol m^{-2} s^{-1} are closer to each other in comparison to 600 or 1200 µmol m^{-2} s^{-1}). Indeed, under higher light intensities, temperature can potentially impact the rate of photosynthesis's dark reactions, possibly unsettling the equilibrium between energy supply and consumption and consequently affecting the threshold.

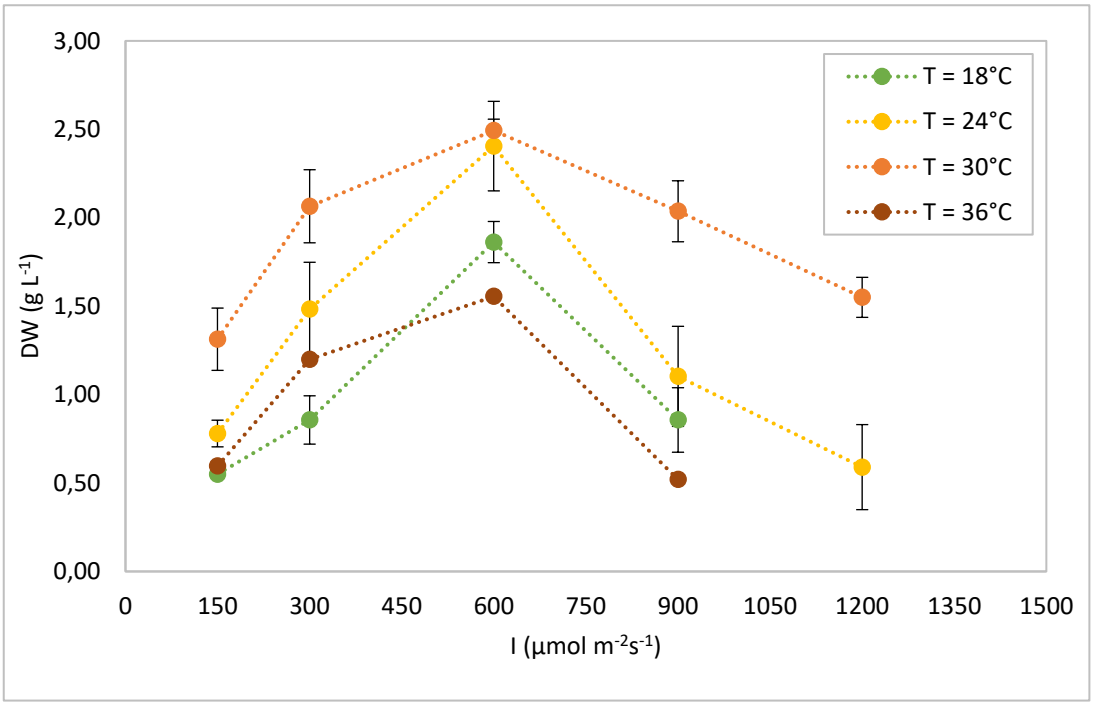

Figure 3.2. *Experimental data of the dry weight (DW) against incident light intensity obtained at steady state. Plot parametric in temperature.*

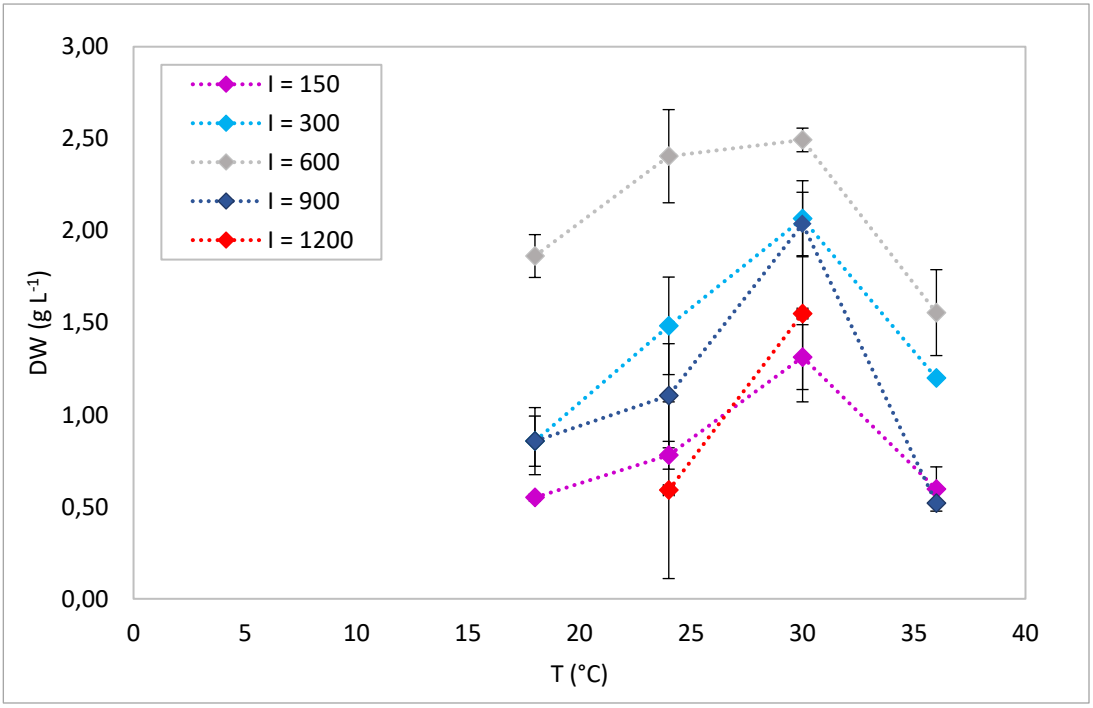

Figure 3.3. *Experimental data of the dry weight (DW) against temperature obtained at steady state. Plot parametric in incident light intensity.*

It is also interesting to notice how the phenomenon of photosaturation and photoinhibition seems to manifest at significantly elevated irradiance levels in contrast to those typically documented in literature (typically ranging between 100 and 150 µmol m^{-2} s^{-1}). For instance, in the study by Gris *et al*., 2014, the reported value of light saturation corresponds to 150 µmol m^{-2} s^{-1}. This disparity might find its explanation in the fact that such values are often derived from batch experiments, where algal cells have less time to fully acclimate to high light conditions (Barbera *et al*., 2017). Conversely, within a continuous culture, following a transient period that affords cells the opportunity to adjust to the new environment, a steady-state is achieved in which microalgae are fully acclimated. In this context, the outcomes align with the findings of Barbera *et al*. (2017), who conducted their investigations in continuous mode, where the optimal light intensity was identified as 500 µmol m^{-2} s^{-1}.

Another potential factor contributing to discrepancies in the literature is reactor thickness. For instance, the study conducted by Fagnol (2021) resulted in photosaturation at 90-100 µmol m^{-2} s^{-1} using a reactor with a thickness of 0.2 cm. This disparity can be attributed to the self-shading effect, which becomes more pronounced in thicker reactors, enhancing their ability to withstand photoinhibition and tolerate higher light intensities.

The highest biomass concentration (2.49 g L^{-1}) was found at an irradiance of 600 µmol m^{-2} s^{-1} and at a temperature of 30°C. However, it is preferable to compare the values of productivity with literature ones, as the residence time would influence the comparison.

Furthermore, it is crucial to notice that the data at 36°C require further analysis: at these temperatures, competition with other algae is more intense, potentially leading to contamination phenomena, and as a result, only a limited amount of data for each steady state has been collected.

Table 3.1. *Mean and standard deviation values of dry weight obtained at various temperatures and incident light intensities.*

	Dry weight (g L^{-1})									
Light intensity	**150 µmol m^{-2} s^{-1}**		**300 µmol m^{-2} s^{-1}**		**600 µmol m^{-2} s^{-1}**		**900 µmol m^{-2} s^{-1}**		**1200 µmol m^{-2} s^{-1}**	
Temperature	Mean	SD	Mean	SD	Mean	SD	Mean	SD	Mean	SD
18 °C	0.55	0.02	0.86	0.14	1.86	0.12	0.86	0.18	-	-
24 °C	0.78	0.08	1.48	0.27	2.41	0.25	1.10	0.28	0.59	0.24
30 °C	1.31	0.18	2.07	0.21	2.49	0.06	2.04	0.17	1.55	0.11
36 °C	0.60	0.12	1.20	-	1.56	0.23	0.52	-	-	-

3.1.2 Washout condition

In the experiment conducted at 24°C with an illumination intensity of 1200 µmol m^{-2} s^{-1}, an intriguing phenomenon transpires. The culture appears to initially attain an apparent steady state. However, after several days of apparent stability, the concentration diminishes, and if the experiment were to continue, it would lead to a washout state (as depicted in Figure 3.4).

This particular scenario is not straightforward and induced to carry out experiments at an intensity of 900 µmol m^{-2} s^{-1}, specifically to check whether the steady state at an intermediate light intensity between 600 and 1200 µmol m^{-2} s^{-1} would be in line between those two values or present a descending trend, which is what, indeed, occurred. Consequently, this pattern of an initial quasi-equilibrium is uncommon and challenging in terms of explanation.

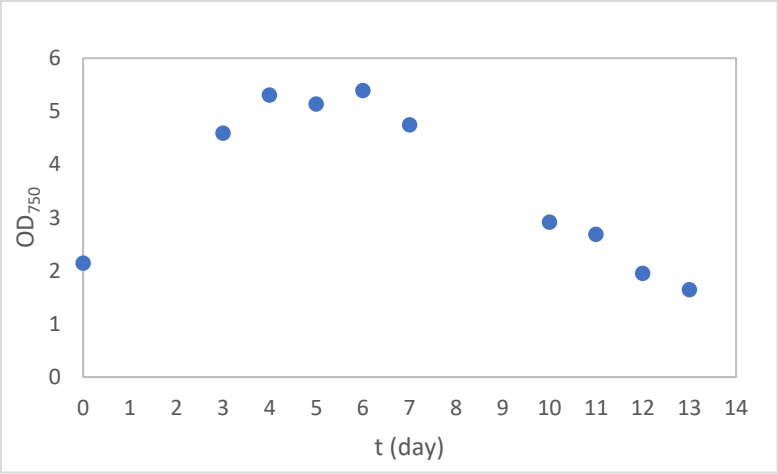

Figure 3.4. *Optical density (OD) variation in time for I=1200 µmol $m^{-2}s^{-1}$ and T=24°C.*

One possible hypothesis could be linked to the oxidative metabolism of chlorophyll during the growth of *A. obliquus*. In microalgae cultures, high light intensity might result in heightened light energy absorption, which, in turn, could trigger a cascade of intracellular reactions leading to the generation of reactive oxygen species (ROS) which serve as secondary messengers or are part of the cellular defence response against pathogens in various cellular processes. Nonetheless, an excessive buildup of ROS can give rise to a state known as "oxidative stress", culminating in damage to various cellular components and compelling cells to produce more lipids as a protective measure (Rezayian *et al*., 2019). In this context, the investigation carried out by Maroneze *et al*. (2019) revealed that *A. obliquus* employs a controlled strategy involving the conversion between chlorophyll *a* and *b* to mitigate the formation of ROS at elevated irradiances, along with carotenoid-based photoacclimation. This research observed that the presented strategy might be effective for a certain duration; however, with prolonged exposure to high irradiance, the accumulation of ROS could escalate beyond a manageable threshold, which, was observed after 72 hours in batch mode with a continuous illumination of 150 µmol m^{-2} s^{-1}. Thus, one plausible hypothesis for the unusual

behaviour at 1200 μmol m^{-2} s^{-1} is that the higher light intensity and the continuous mode might potentially extend this timeframe since the culture is fully acclimated and more stable: the culture initially attains a state of stability, only to succumb to oxidative stress thereafter. Nonetheless, further analyses are warranted, particularly under the 1200 μmol m^{-2} s^{-1} illumination, across varying temperatures, maintaining the culture for at least 15 days.

3.1.3 Assessment of the self-shading effect

It is also of interest to determine whether the cells actually receive the light intensity that is incident to the PBR. For this purpose, the dry weight was plotted against the average light intensity (I_{av}). Although the incident light intensity represents the total light that reaches the surface, the average light intensity takes into account the interactions between light and microalgae within the cultivation system, providing a more accurate measure of the actual amount of light used by the microalgae. In particular, it denotes the photons available to each microalgal cell in the culture. The assessment of the average light intensity is useful for identifying the self-shading phenomenon: the average light intensity may be lower if the amount of light actually used by the microalgae is reduced due to the shadows created by the same cells (Fallahi *et al*., 2020).
The average irradiance within the entire thickness of the reactor (W) is estimated by integrating the Lambert-Beer law (Equation 2.19) over the entire culture depth:

$$I_{av} = \frac{1}{W}\int_0^W I(z)\, dz \tag{3.1}$$

Assuming the biomass is uniformly distributed over the whole reactor volume, the average light intensity within the reactor can be described by:

$$I_{av} = \frac{I_0}{k_a \cdot C_{x_{out}} \cdot z}\left(1 - e^{-k_a \cdot C_{x_{out}} \cdot z}\right) \tag{3.2}$$

In Figure 3.5 the representation of the DW as a function of the average light intensity is shown. It was observed that the actual amount of light reaching microalgae is significantly less than the one measured on the surface of the mPBRs and this phenomenon becomes more pronounced as irradiance increases. This observation aligns with the fact that densely concentrated cultures are achieved within a confined volume with a depth of 15 mm. Consequently, the denser cell distribution intensifies the self-shading phenomenon as cells farther from the PBR surface receive reduced light. Hence, this is consistent with the findings of Saccardo *et al*. (2022), where small-scale reactors detect the self-shading phenomenon starting from 15 mm, making them effective for simulating large-scale growth.

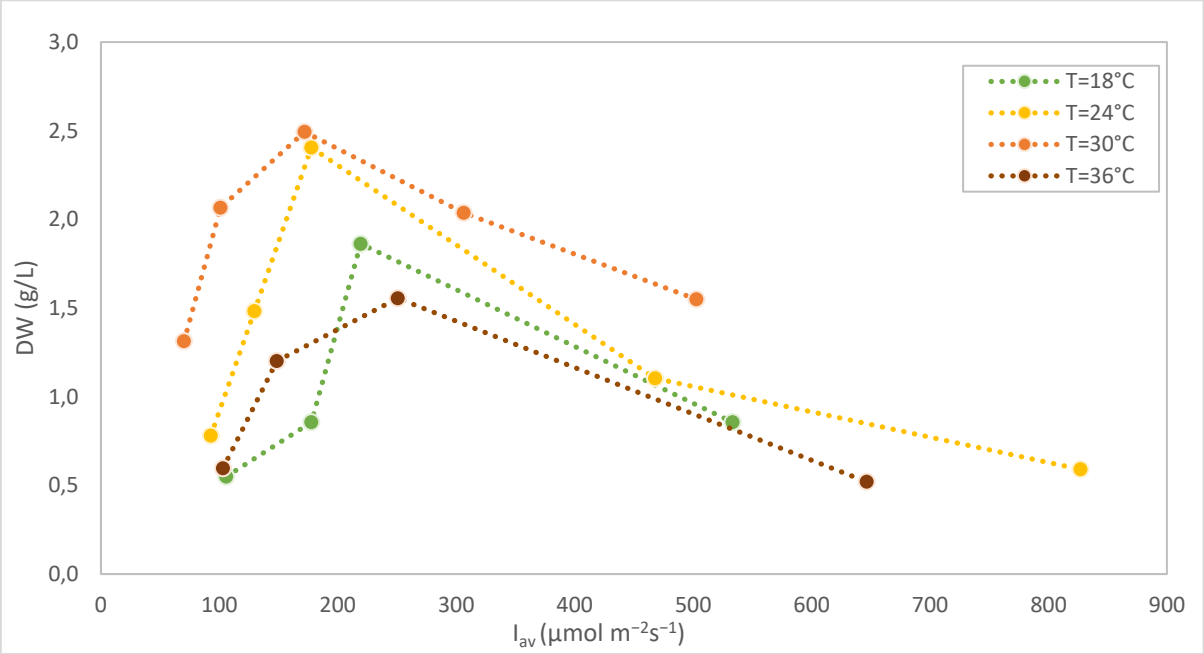

Figure 3.5. *Experimental data of the dry weight (DW) against averaged light intensity. Plot parametric in temperature.*

3.1.4 Biomass productivity

Figure 3.6 displays the productivity patterns for each steady state in relation to different light intensities for each temperature and numerical results are shown in Table 3.2. These productivity curves, determined by the ratio of concentration over residence time (§1.4.3), reflect a similar trend as the growth curves, since the τ remains constant.

Thus, the conclusions previously drawn about the interactions between concentrations and light intensities remain consistent in this context. Notably, productivity rises as irradiance increases, reaching a peak value before photoinhibition sets in, leading to a subsequent decrease. The highest productivity value occurs at 600 µmol m^{-2} s^{-1} and 30°C, resulting in a biomass productivity of 1.66 g L^{-1} day^{-1}. It is interesting to compare these outcomes with relevant findings in the existing literature.

In the study conducted by Borella *et al*., 2021, a continuous-flow PBR was employed for the cultivation of *A. obliquus*, with a reactor thickness of 3.5 cm. The maximum productivity values obtained were 1.24 g L^{-1} day^{-1}, corresponding to a temperature of 30°C and a light intensity of 800 µmol m^{-2} s^{-1}. So, the results in productivity are aligned with what found in literature and the observation that the peak productivity occurs at higher light intensities confirms that an increase in thickness leads to a maximal productivity at generally elevated light intensities (Fagnol, 2021).

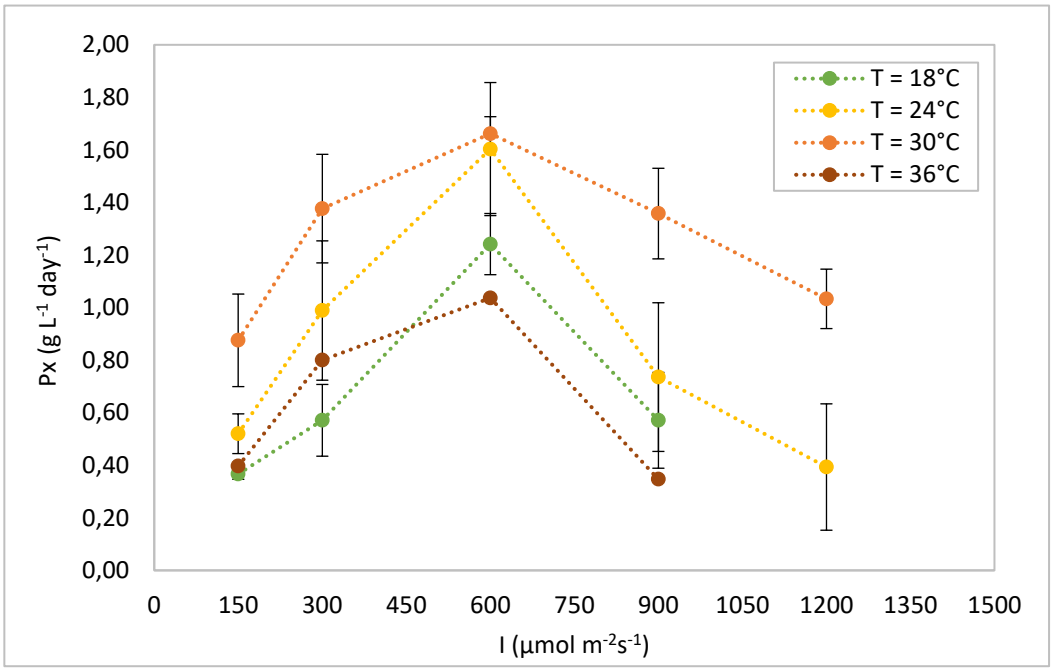

Figure 3.6. *Experimental data of biomass productivity against incident light intensity obtained at steady state. Plot parametric in temperature.*

Table 3.2. *Mean values of biomass productivity obtained at various temperatures and incident light intensities.*

	Productivity (g L^{-1} day^{-1})				
Light intensity	**150 µmol m^{-2} s^{-1}**	**300 µmol m^{-2} s^{-1}**	**600 µmol m^{-2} s^{-1}**	**900 µmol m^{-2} s^{-1}**	**1200 µmol m^{-2} s^{-1}**
Temperature					
18 °C	0.37	0.57	1.24	0.57	-
24 °C	0.52	0.99	1.60	0.74	0.39
30 °C	0.88	1.38	1.66	1.36	1.03
36 °C	0.40	0.80	1.04	0.35	-

3.2 Pigment content

The variation of the pigment content in mg per g biomass with respect to the different light conditions was analysed, according to the protocol reported in paragraph §2.3.6 and results are reported in Figure 3.7 and 3.9.

The pigment composition within algae cells can exhibit substantial variation during outdoor cultivation (Béchet *et al*., 2013). This variability is due to the phenomenon of light acclimation: under low light conditions, cells often augment their pigment content to optimize light absorption. Conversely, in high light conditions, cells typically reduce their pigment content to mitigate the potential for light-induced inhibition (Geider *et al*., 1997). The decline in chlorophyll *a* and *b* levels as light intensity increases is supported by the findings in the investigation conducted by Gris *et al*. in 2014 (Figure 3.10). Furthermore, the outcomes exhibit numerical consistency with the research undertaken by Barbera *et al*. (2017), who employed continuous-flow PBR at 24°C, yielding chlorophyll content of 0.7 pg cell^{-1}. In comparison, the current study, conducted under the same operational conditions, results with chlorophyll content of 0.2 pg cell^{-1}, thus demonstrating alignment in values (Figure 3.8).

Furthermore, it is evident that chlorophyll content decreases with increasing temperatures. The impact of temperature is particularly pronounced at low light intensities, while it appears to be less significant at higher light intensities. This observation is quite interesting, and this aspect has been further explored in the subsequent section.

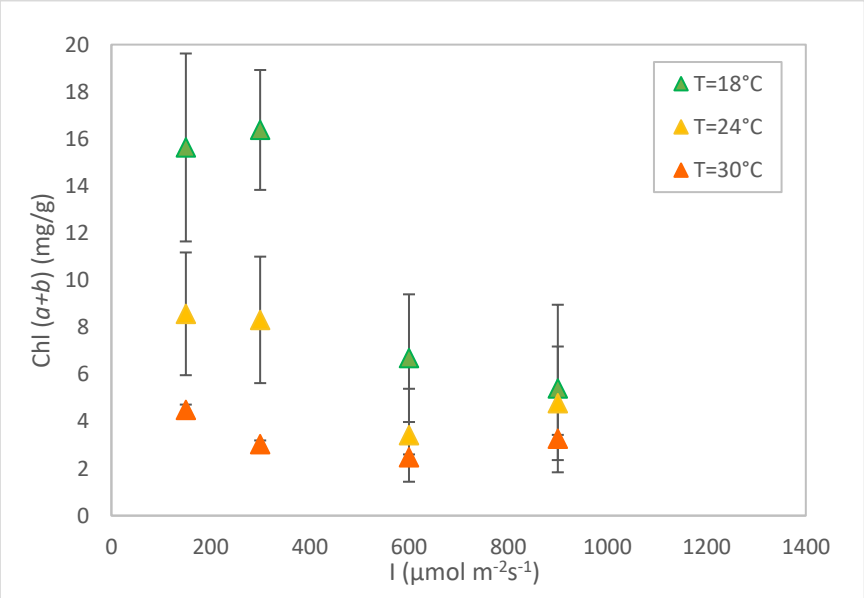

Figure 3.7. *Summation of chlorophyll a and b content (Chl (a+b)) against incident light intensity. Plot parametric in temperature,*

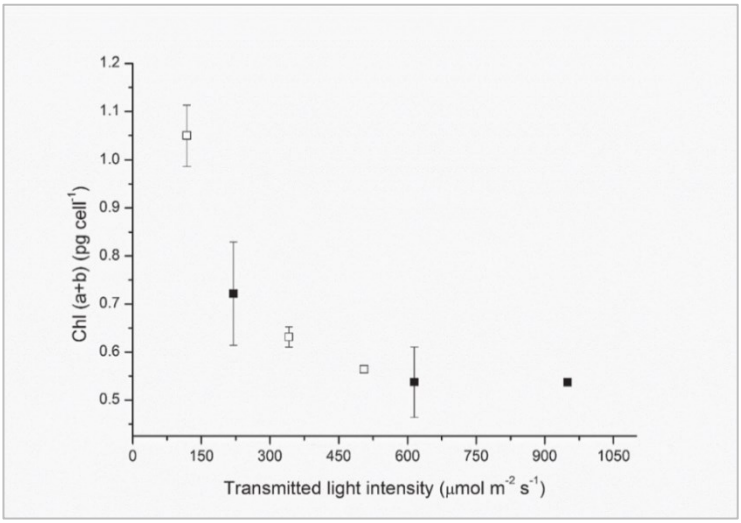

Figure 3.8. *Chlorophyll content per cell as a function of transmitted light intensity (full dots) from Barbera et al., 2017.*

In terms of the carotenoids over chlorophyll ratio (Car/Chl a), the results reported in Figure 3.9 are consistent with those reported by Gris *et al*. (2014) in Figure 3.10, indicating an increasing trend with higher irradiance, as also noted by Andersen (2013). The adaptation mechanisms of microalgae to varying light intensities exhibit a specific pattern in pigment molecules: under low light intensities, chlorophyll *a* increases, whereas with increased irradiance, a relatively higher concentration of carotenoids is observed. Furthermore, comparable values are found in Sforza *et al.* (2014), with a Car/Chl a ratio of 0.19 at 150 µmol m^{-2} s^{-1} and 24°C, whereas from the current study it is obtained 0.14 under the same conditions, indicating similarity.

However, due to the significant variability in carotenoid content, only approximate considerations can be made regarding their alignment with existing literature.

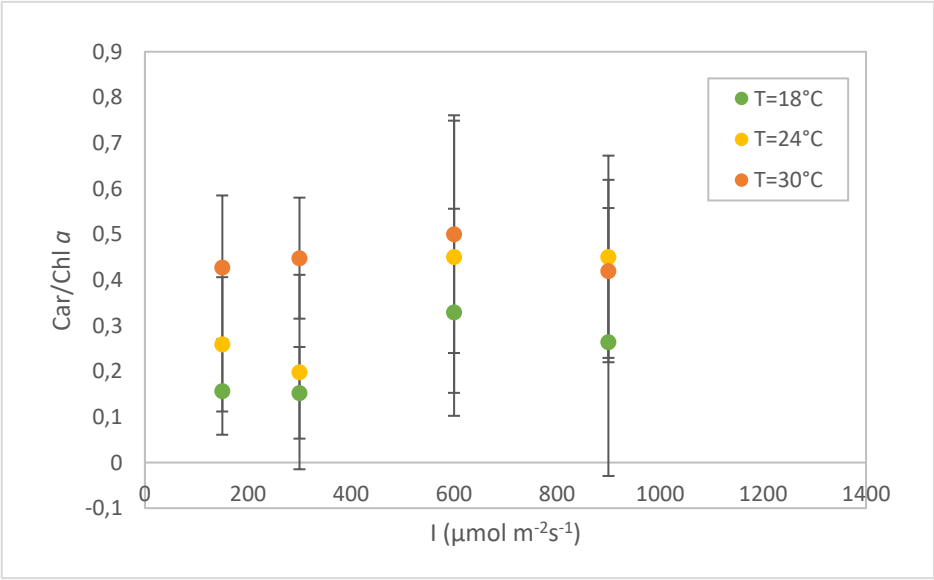

Figure 3.9. *Ratio of carotenoids and chlorophyll a content (Car/Chl a) against incident light intensity. Plot parametric in temperature.*

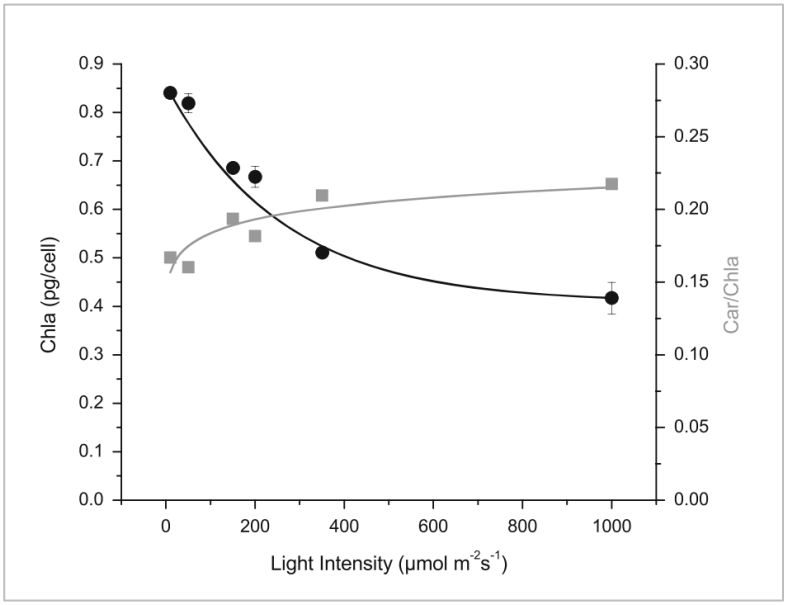

Figure 3.10. *Chlorophyll content per cell against light intensity (circles) and Car/Chla ratio (squares) from Gris et al., 2014.*

For the sake of comprehensiveness in the results, Figure 3.11 displays the graph of chlorophyll content along with dry weight over time for the specific condition at 1200 µmol m^{-2} s^{-1} and 24°C. It becomes evident that the pigment content reflects the changes in biomass concentration over time. The anomaly observed on the 7th day might be attributed to measurement variability.

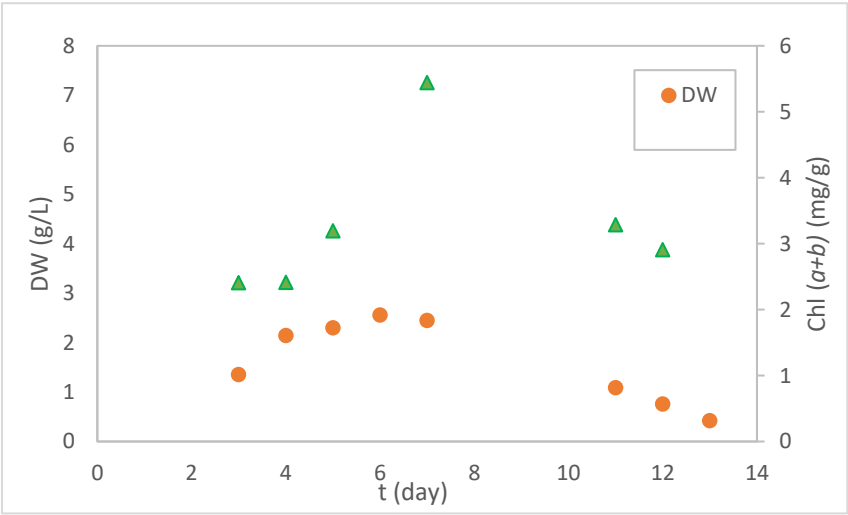

Figure 3.11. *Dry weight (in circles) in circles and chlorophyll content (in triangles) variation in time for I=1200 µmol $m^{-2}s^{-1}$ and T=24°C.*

3.2.1 Temperature dependency on pigment content

A dynamic experiment was conducted to gain a deeper insight into the impact of temperature on pigment variations. The same initial culture was used and a consistent light intensity of 150 µmol m^{-2} s^{-1} was maintained. The experiment was initiated at 30°C and the culture was allowed to reach a steady state; then the same procedure was repeated, gradually decreasing the temperature to 24°C, and then further down to 18°C, spanning across several days.

The results are shown in Figure 3.12: both optical density and dry weight exhibit a reduction corresponding to the decrease in temperature while the overall content of chlorophyll displays an increase.

This finding appears to contrast with the study conducted by Carvalho *et al*. (2009), which investigated the simultaneous effects of irradiance and temperature on the biochemical composition of the microalga *Pavlova lutheri*. Their conclusion revealed that both chlorophyll *a* and carotenoid contents consistently increased with temperature, regardless the irradiance level. However, it is worth noting that their study was performed using batch cultivation and a different microalga, prompting the need for a more specific literature comparison.

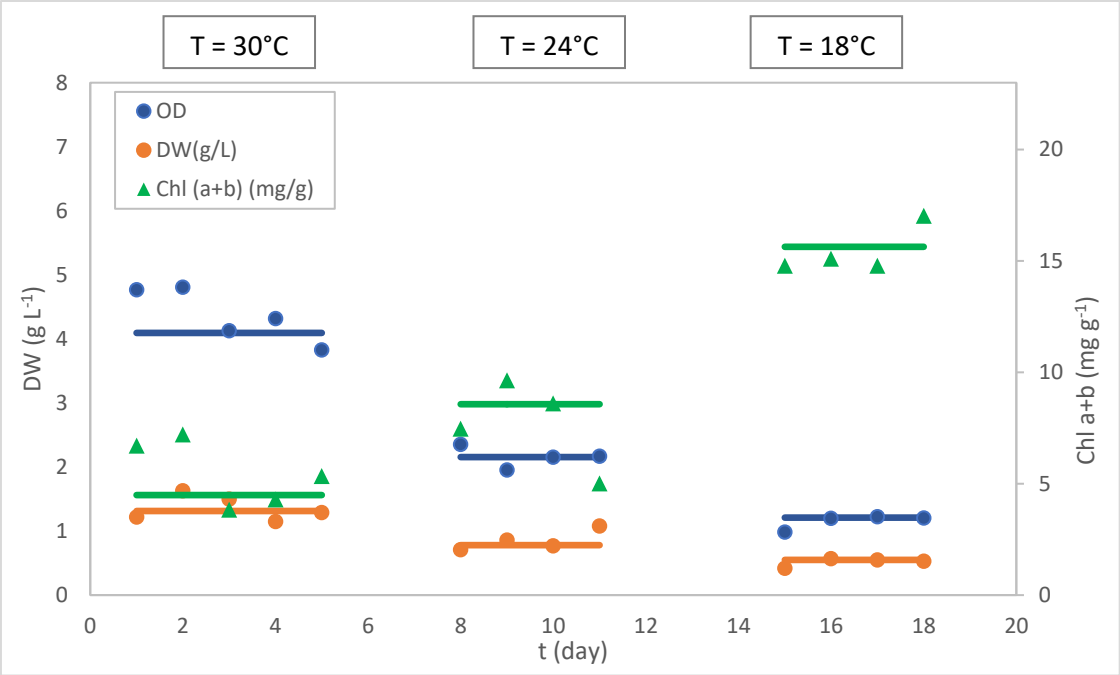

Figure 3.12. *Variation of optical density (OD), dry weight (DW) in circles and chlorophyll content (Chl a+b) in triangles, for 18 days of culture at 150 µmol $m^{-2}s^{-1}$. Temperature decreases from 30°C to 24 °C to 18°C without interrupting the experiment.*

For instance, Chalifour & Juneau (2011) examined the temperature-dependent sensitivity of growth and photosynthesis in various microalgal strains, including *A. obliquus*, in semi-continuous cultures with a light intensity of 100 µmol m^{-2} s^{-1}. Thus, their experimental conditions closely align with the situation of the current study. In their research, the cultures

were acclimated to different temperatures (10, 15, and 25 °C) and was observed that for *A. obliquus*, decreasing the acclimation temperature led to an increase in chlorophyll and Car/Chl *a* ratio. However, the trend differed from the one observed in some other microalgae. Specifically, their findings indicated that when temperature decreased from 25°C to 10°C, the growth rate of *A. obliquus* became 3.4 times lower and that the overall photosynthesis decreased by about 10%. Consequentially to a lower photosynthesis rate, the inhibition in electron transport would lead to increased chlorophyll accumulation. In addition, the Car/Chl a ratio was found to be 1.5 times higher at 10 °C compared to 25 °C, marking a distinct difference from the ratio observed in the current study. However, due to the variability present in the dataset, further validation of the results would be appropriate.

In another study, conducted by Ras *et al*. (2013) the same trend of rising chlorophyll with the decreasing temperature was found and explained with an enhancement in carboxylase activity, which effectively facilitates the dissipation of excess energy that is produced.

Thus, although there is a discrepancy with certain findings in the existing literature (Carvalho *et al*., 2009; Maxwell *et al*., 1995) demonstrating that algal cultures grown at low temperature (2-5 °C) had lower amounts of chlorophylls and carotenoids, some other authors (Rhee and Gotham, 1981) have shown an increase in Chl *a* with decreasing temperature in green algae indicating that the effect of temperature on Chl content may vary depending on factors such as species, growth temperature, or light intensity.

Nonetheless, this aspect calls for more in-depth exploration through additional experiments. For instance, it would be intriguing to observe the same dynamic experiment at higher light intensities to verify the conclusion drawn from Figure 3.7, which indicates that at high light levels, the influence of temperature is nearly negligible.

3.3 Respirometry results

A respirometry test was conducted following the protocol outlined in §2.3.8 to assess photosynthetic activity in response to short-term temperature changes. This approach aimed to identify potential temperature acclimation effects, particularly if variations in photosynthesis rates distinct from those observed in long-term steady-state cultivation were detected. The analysed sample was acclimated to a light intensity of 1200 μmol m^{-2} s^{-1} and 30°C, and subjected to the analysis, with dissolved oxygen measurements (DO) serving as an indicator of photosynthetic activity.

It is intriguing to observe the results of separated contributions of OPR and OCR at each temperature, as depicted in Figure 3.13. At 12°C, OCR slightly prevails while at 19°C their contribute is the same and at higher temperatures, OPR becomes notably more dominant.

As discussed earlier, a reduction in temperature was found to correspond to a decrease in the photosynthesis rate. This explains the predominance of OCR over OPR at lower temperatures, while OPR becomes more prominent at elevated temperatures: the enhanced metabolic activity of microalgae at higher temperatures, resulting in increased oxygen production through photosynthesis.

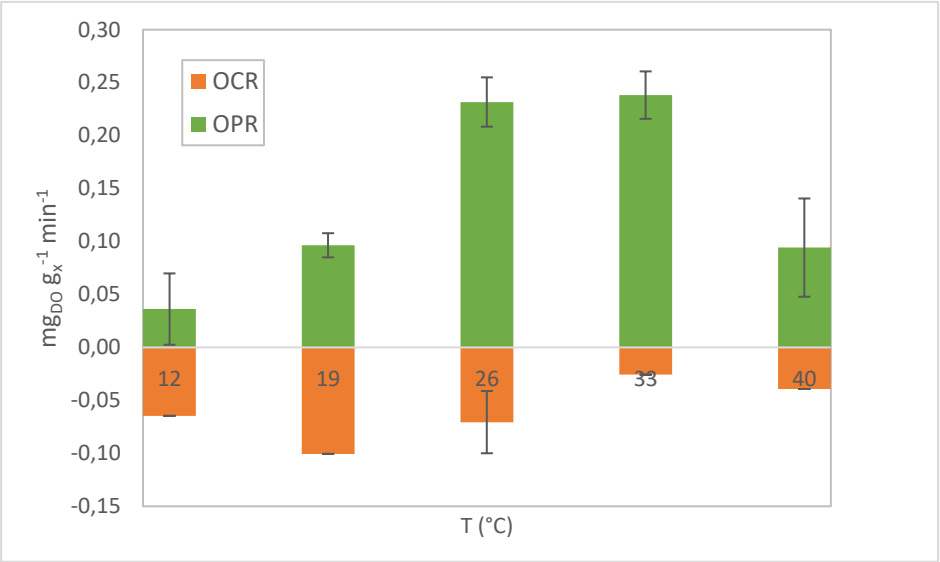

Figure 3.13. *Bar chart of the oxygen produced and consumed in terms of oxygen production rate (OPR) and oxygen consumption rate (OCR) per grams of biomass.*

Then, the experimental data of the dissolved oxygen concentration were fitted according to the model developed by Bernard and Rémond (2012) described in §2.4. Since light is maintained constant, μ_{opt} was considered a constant parameter. So, the estimated temperature parameters of the model (T_{opt}, T_{min} and T_{max}) will be then used a guess for the parameters estimation when temperature and light will consider varying simultaneously. It can be observed that the model (represented in Figure 3.14 as a solid line) fits well the experimental points and follows the trend as expected by Bernard and Rémond (2012): the biomass growth rate becomes null below the T_{min} and above the T_{max} thresholds, while attaining its peak when the temperature aligns with T_{opt}. Specifically, when T exceeds T_{opt}, the growth rate experiences a rapid decline attributed to thermal stress (Barbera *et al.*, 2019). This stress can potentially impact enzyme activities (such as denaturation and inactivation) or induce alterations in proteins engaged in the process of photosynthesis (Ras *et al.*, 2013). The resulting parameter values are reported in Table 3.3.

Table 3.3. *Estimated values of temperature parameter from respirometry analysis.*

T_{min} (°C)	T_{max} (°C)	T_{opt} (°C)
7.2	42.0	31.2

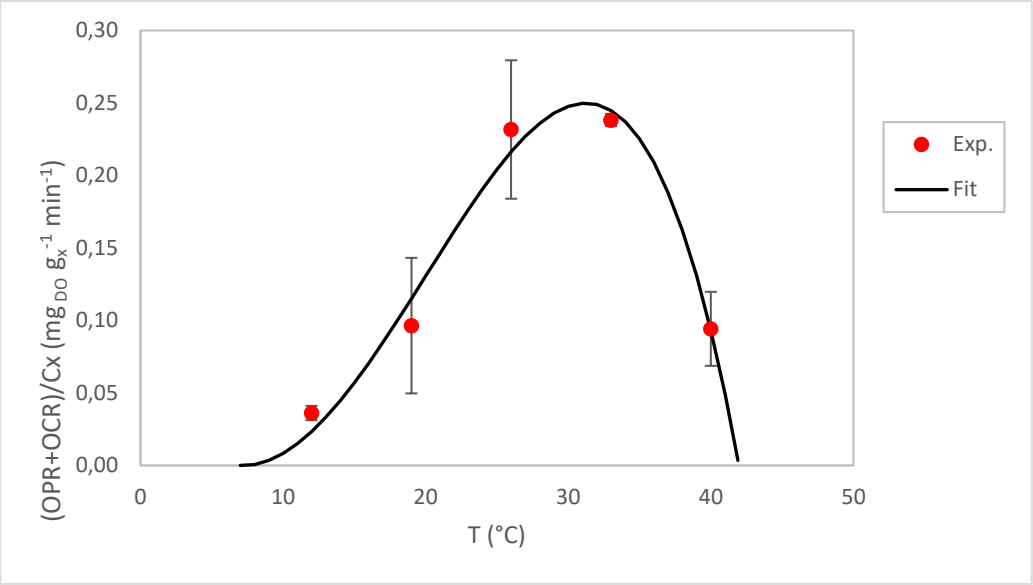

Figure 3.14. *Behaviour of the specific dissolved oxygen concentration (DO) changing over temperature. Experimental data at 29, 26, 33, 40 °C as a result of the respirometry analysis and fitting curve.*

Thus, the most substantial growth rates were achieved at temperatures approximately around 30°C, confirming the outcomes obtained from the long-term cultures. Nevertheless, it is worth noting that these findings might vary if a sample acclimated to a different temperature is tested, an investigation that holds intriguing potential for further exploration.

3.4 Image analysis results

The results of the image analysis are reported below, as indicated in the procedure at §2.3.5.
Figure 3.15 shows the influence of temperature on the Feret diameter foe each light intensities. At light intensity of 150 and 600 µmol m^{-2} s^{-1}, a clear pattern emerges: temperature significantly influences cell diameter, displaying a distinct negative correlation. Specifically, as temperatures range from 18 to 36°C, cells exhibit a larger diameter at lower temperatures and progressively decreasing in size as the temperature rises (decreasing up to 1 µm). Cell size peaks at 300 µmol m^{-2} s^{-1} and 24°C , while at 900 µmol m^{-2} s^{-1}, temperature does not seem to have a very strong effect.
Although the impact of temperature is evident, the influence of light intensity on the diameter exhibits more variability, contingent upon temperature conditions (Figure 3.16).
At a temperature of 24°C, the maximum size is evident when light intensity is set at 300 µmol m^{-2} s^{-1}. Meanwhile, the trends at 30°C and 18°C demonstrate consistency: sizes decrease from 150 to 300 µmol m^{-2} s^{-1}, then increase at 600 µmol m^{-2} s^{-1}, followed by another decrease. Conversely, at 36°C, the effect of light intensity is quite subtle, resulting in an almost flat line.

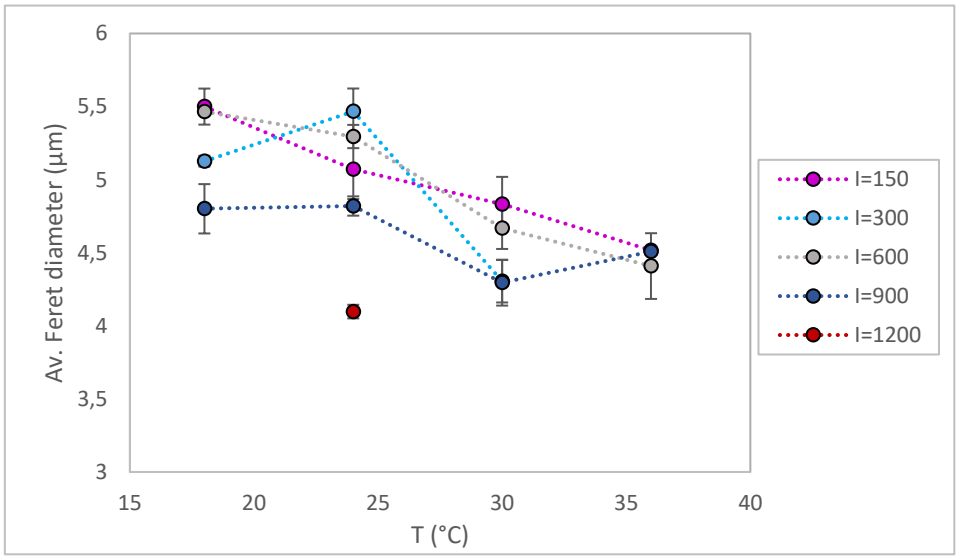

Figure 3.15. *Average Feret diameter against temperature for each light intensity*

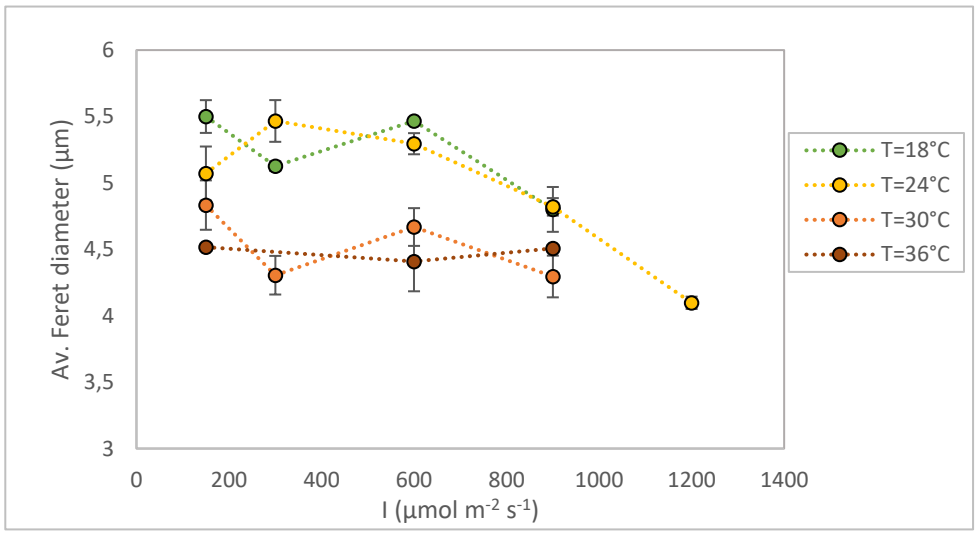

Figure 3.16. *Average Feret diameter against light intensity for each light temperature.*

Concerning cell volume, an analysis of Figure 3.17 indicates a prevailing negative correlation with temperature, except for the case at 900 µmol m^{-2} s^{-1}, where a somewhat conflicting trend emerges (although not distinctly defined).

In Figure 3.18, a parallel observation can be made: the overall trend aligns with the outcomes derived from cell diameter measurements, as the impact of light exhibits temperature-dependent variations. Specifically, a convex pattern manifests at lower temperatures, while a concave pattern emerges at higher temperatures.

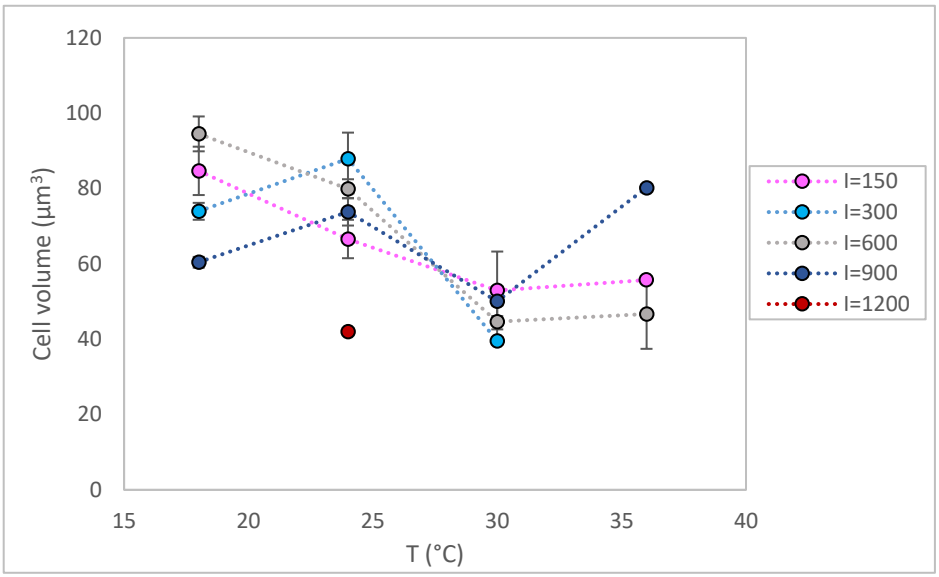

Figure 3.17. *Cell volume against temperature for different light intensities. *: only one replicate.*

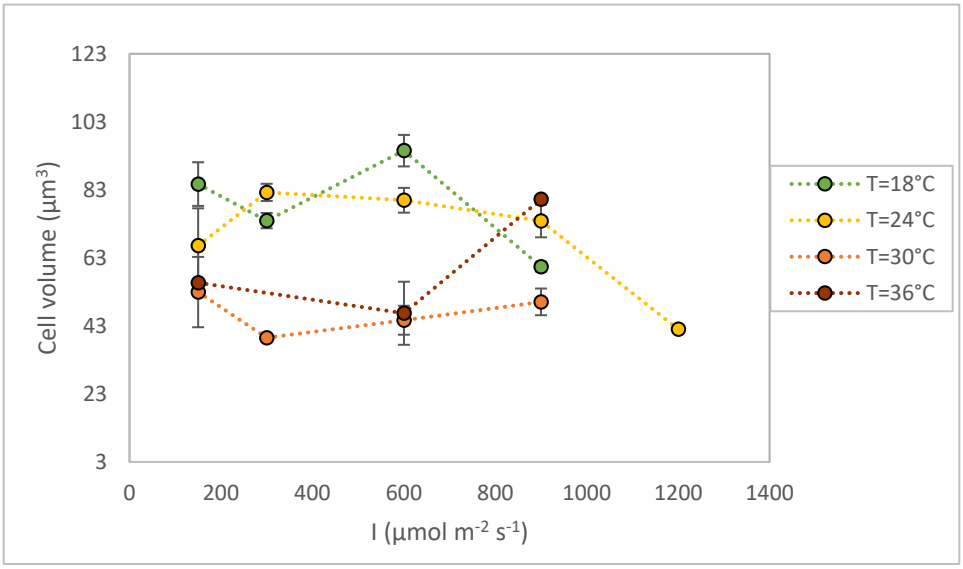

Figure 3.18. *Cell volume against light intensity for different temperatures.*

The circularity aspect is also noteworthy. Examining Figure 3.19, there is a clear interaction between light and temperature: the lowest light intensity takes on a pronounced convex shape, while the highest intensity exhibits a concave shape.

In Figure 3.20, a general trend becomes apparent: higher light intensity tends to have a negative effect on circularity. It is important to note that the data point at 1200 µmol m^{-2} s^{-1} might raise doubts about its reliability; nonetheless, it has been included in the discussion for transparency.

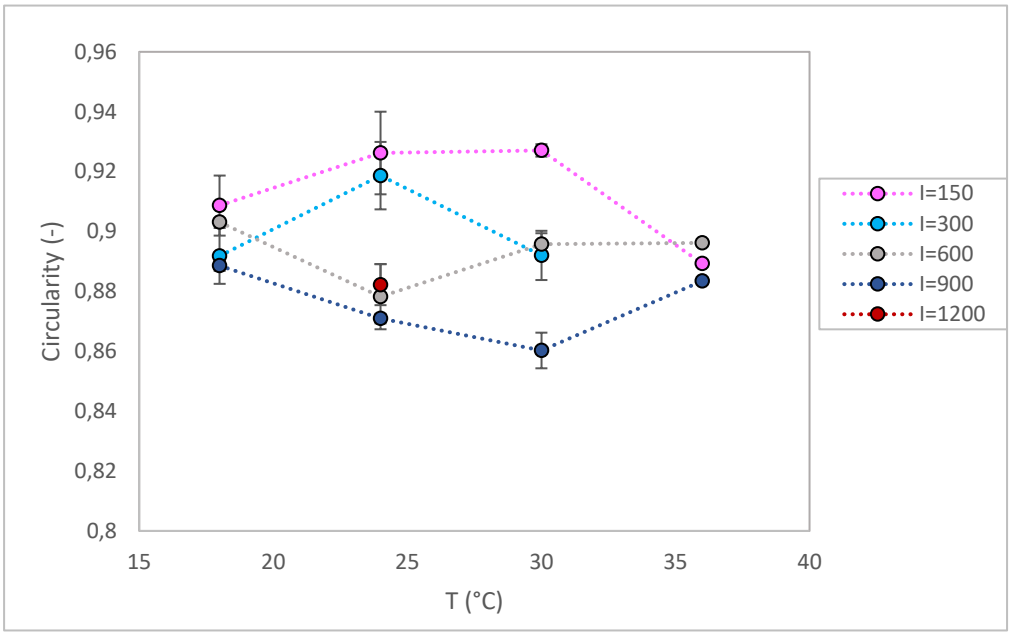

Figure 3.19. *Circularity against temperature for each light intensity.*

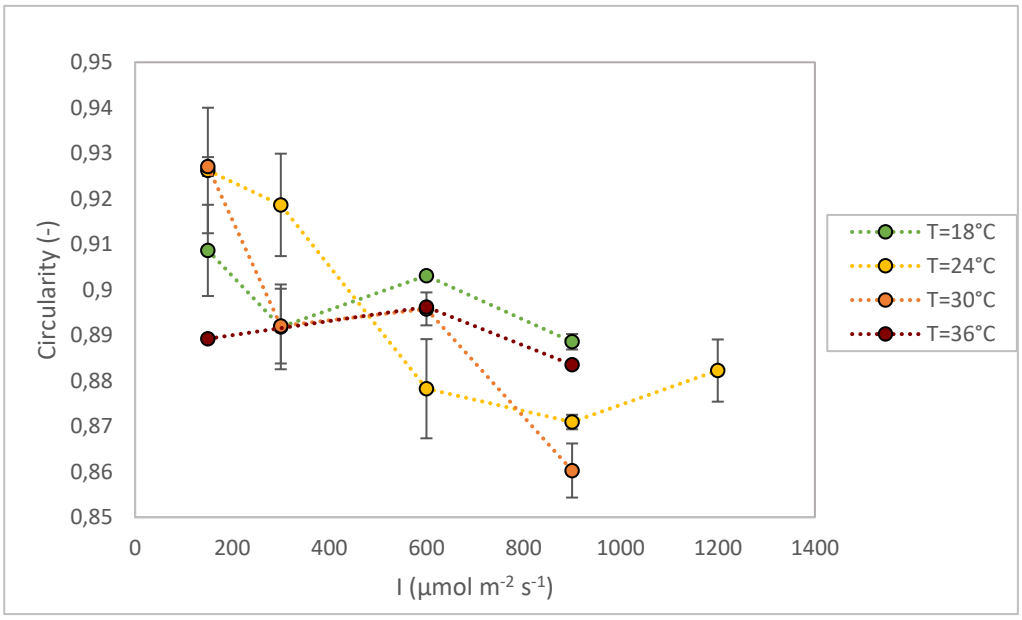

Figure 3.20. *Circularity against light intensity for each light temperature.*

The trend of elongation observed in Figure 3.21 and 3.22 corresponds to the one in Figure 3.19 and 3.20: the conditions reflecting the highest circularity also exhibit the lowest elongation. Overall, a comparable form of interaction between light and temperature becomes evident.

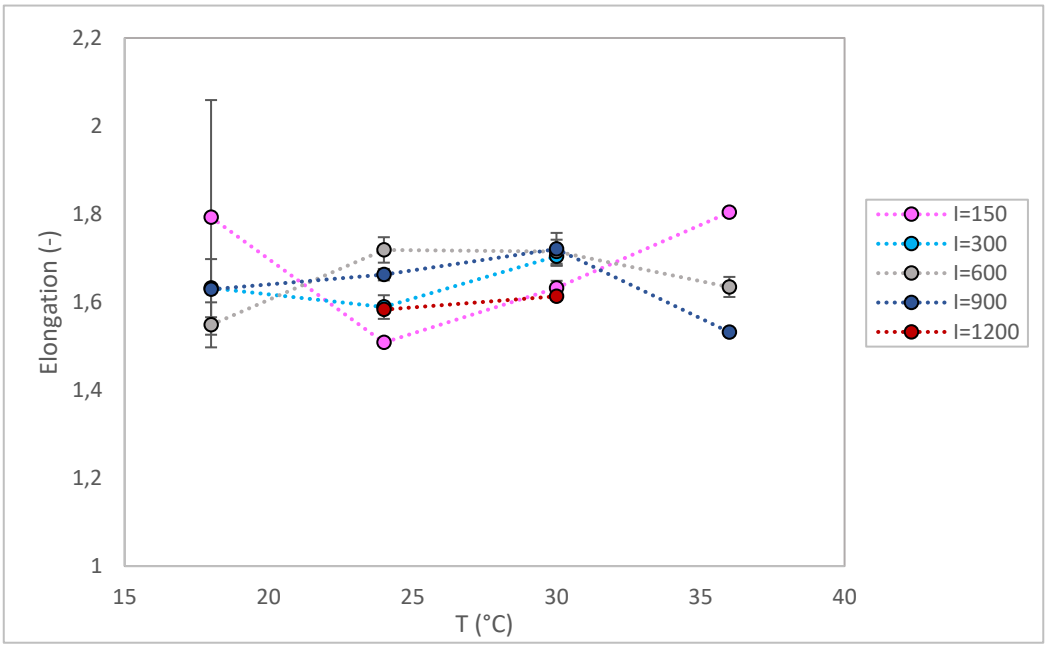

Figure 3.21. *Elongation against temperature for each light intensity.*

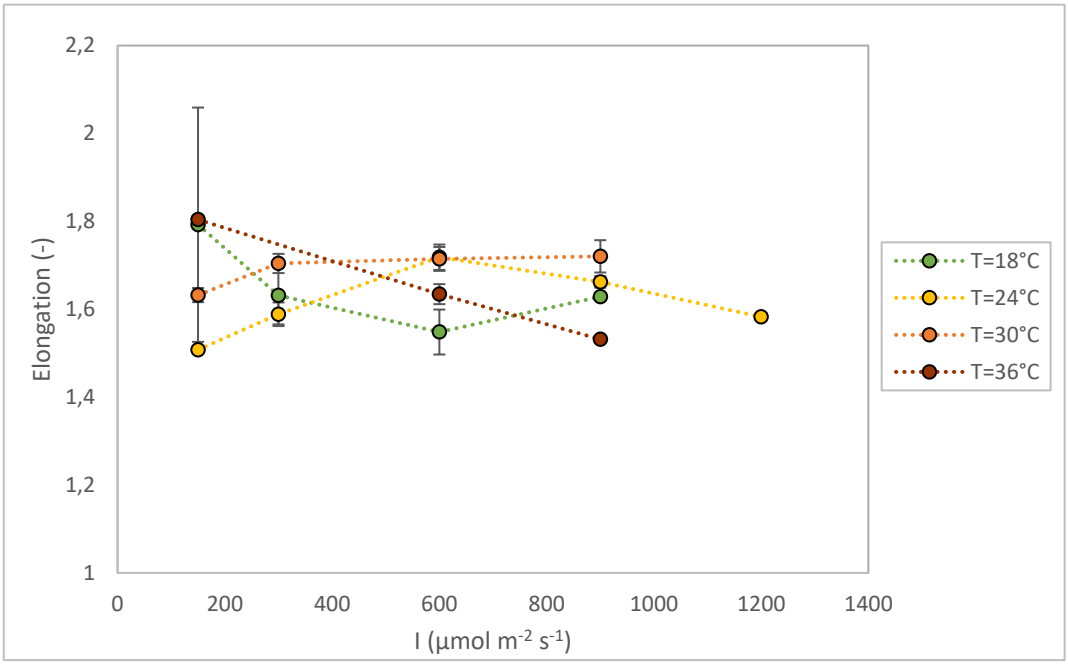

Figure 3.22. *Elongation against light intensity for each temperature.*

In conclusion, this study demonstrates the synergistic effect of temperature and light intensity on cellular characteristics. Results indicate that, at each light intensity level, increasing temperatures prompt cellular shrinkage. This observation aligns with the hypothesis that cells tend to decrease in size under higher temperatures to reinforce nutrient uptake rates and

alleviate metabolic expenses, considering the heightened resource demands at elevated temperatures.

In addition, mid-light intensities produce a maximum cell volume at low temperatures and a minimum volume at high temperatures as evident in Figure 3.23 which compares cell size at 18°C and 30°C, under the light intensity of 600 µmol m^{-2} s^{-1}.

Furthermore, the study identifies a relationship between cell shape and the interaction of temperature and light: in moderate temperatures and low light intensity, cells tend to be rounded, while extreme temperatures lead to elongated shapes, as evident in Figure 3.24. This pattern reverses under stronger light conditions. Overall, lower light levels tend to favour rounder cell shapes.

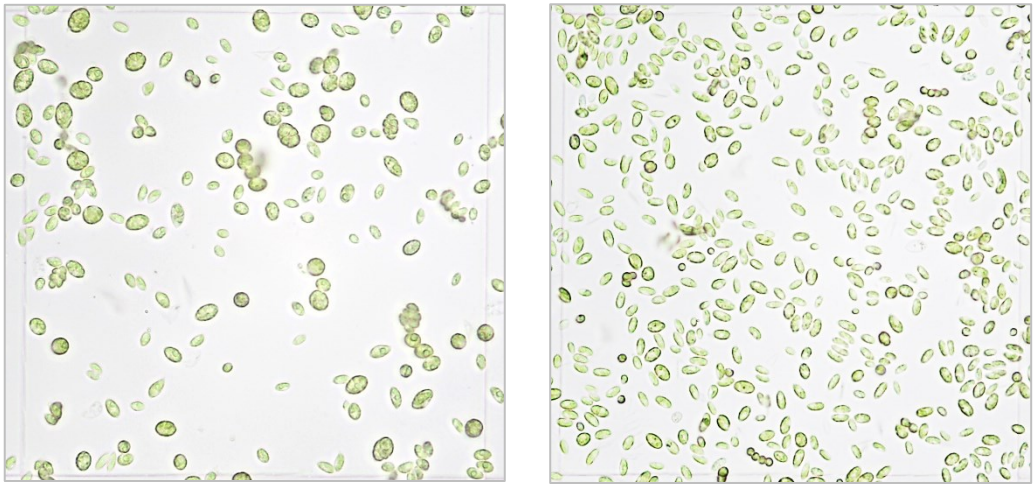

Figure 3.23. *Effect of temperature at 600 µmol m^{-2} s^{-1} . Cells at 18°C (left) are bigger than at 30°C (right).*

.

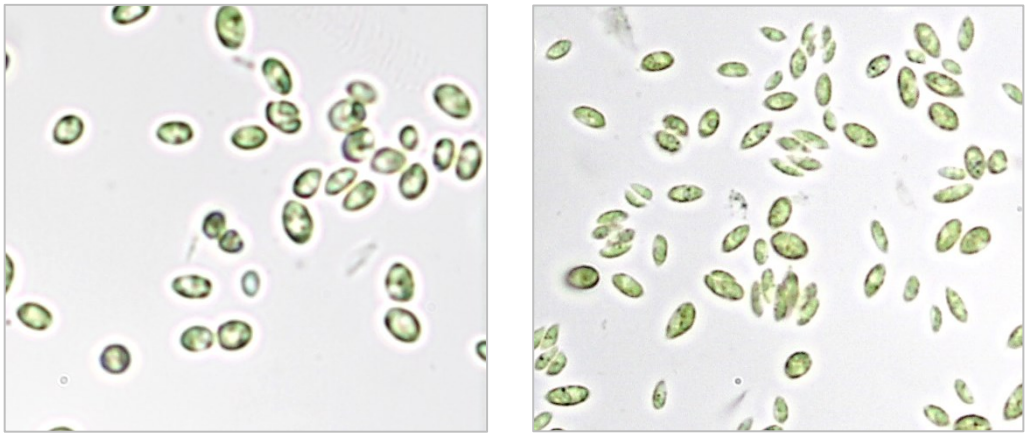

Figure 3.24. *Effect of light intensity at mid temperature (24°C). Cells at 150 µmol m^{-2} s^{-1} (left) are more round shaped than at 600 µmol m^{-2} s^{-1} (right) which are more elongated.*

3.5 Model simulation

The objective of the model simulation is to derive estimates for a set of model parameters ($T_{opt}, T_{min}, T_{max}$, I_{opt}, μ_{max}, k_a, k_d, K_I) that enable accurate prediction of biomass concentration behavior across varying light intensities and temperatures, utilizing the acquired experimental data. The experimental data were collected under steady-state conditions, implying that the balance equation (Equation 2.24) required a null dC_{xout}/dt value. For a correct MatLaB ® implementation, a dynamic simulation was conducted for all conditions to observe the point at which concentration attains a stable value (an example is depicted in Figure 3.25). A pragmatic approach of assuming the 10th day as an approximate representation of steady-state conditions for all scenarios.

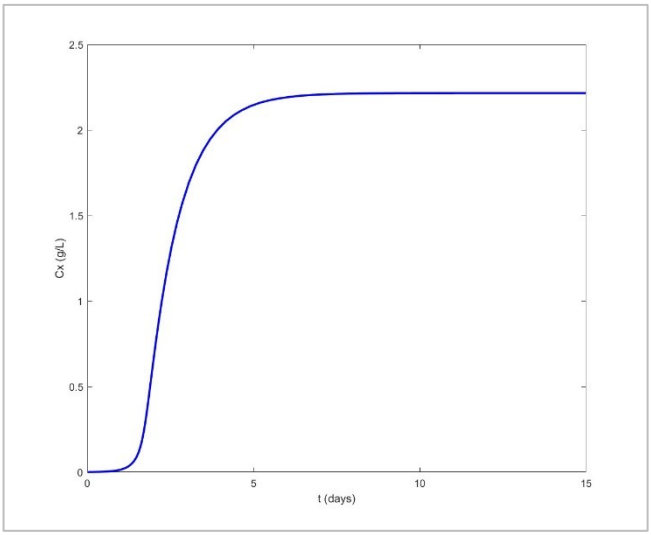

Figure 3.25. *Calculated concentration of biomass in time at 600 µmol m^{-2} s^{-1} and 24°C. Steady state assumed to be reached on the 10th day.*

The estimation of the 8 model parameters involved a comparison between experimental data taken at 5 different light intensities (150, 300, 600, 900) and the calculated concentration values at the 10th day for each light intensity. Notably, data points from an intensity of 1200 were excluded due to their uncertainty.

Initially, the parameter estimation procedure was carried out by comparing experimental and calculated data points at the same light intensity. Subsequently, the estimated parameters were employed to generate a concentration curve that could effectively fit the entire light intensity range of 100 to 1300.

To validate the proper implementation of the model, a preliminary step was taken by conducting the simulation at a constant temperature. This resulted in 4 distinct sets of 8 parameters and 4 corresponding fitting curves (Figure 3.26). Following this, the procedure was repeated with data spanning 4 different temperatures (18°C, 24°C, 30°C, 36°C), yielding

a single set of 8 estimated parameters. The results of this comprehensive analysis are presented in Figure 3.27 and numerical results in Table 3.5.

Given that the model, as outlined in §2.4, assumes light intensity and temperature effects on growth as two independent functions, a successful fitting of the model to the complete dataset would imply the absence of interactions between light intensity and temperature. Conversely, if the fit results unsatisfactory, it indicates a joint influence necessitating a distinct model for explanation.

The initial values of 5 of the parameters derived from the study by Saccardo *et al*. (2022), that shared similarities in terms of biomass culture and reactor depth with the present research. Conversely, the temperature parameter guesses were taken from the respirometry essay (Table 3.4). Based on these considerations, lower and upper parameter bounds were subsequently established.

Table 3.4. *Parameter initial values.*

I_{opt} (µmol m^{-2} s^{-1})	K_I (µmol m^{-2} s^{-1})	μ_{max} (day^{-1})	k_a (m^2 g^{-1})	k_d (day^{-1})	T_{max} (°C)	T_{min} (°C)	T_{opt} (°C)
405	110	2	0.14	0.45	42	7.2	31.2

The optimization function “fmincon” was used to estimate the model parameters that best fit the experimental data. The objective function was defined as the squared difference between the predicted concentrations using the model and the actual experimental concentrations and the optimization process minimized the squared differences across all data points.

The results show that by applying the model to each dataset at a constant temperature, it manages to fit the data very well. However, when the model has to fit the data at all temperatures, the fitting isn't as good. Indeed, the R^2 values (Table 3.6) and the residual plots (Figure 3.28) suggest a good fit at the temperature of 30°C (R^2=0.96), temperature which is close to the optimal temperature found (29.53°C), while the fit is worse for other temperatures as they deviate from the optimal one. It can be noted that data points at low intensity tend to be fitted better (residuals closer to 0) than those at high intensity. This aligns with the observations made by López Muñoz & Bernard (2021), suggesting that this model is suitable for moderate ranges of light and temperature, where the interaction is not as intense. However, at low temperatures and high light levels, the poor fit seems to indicate an interaction between light and temperature, likely due to photosaturation and photoinhibition effects, which could be better captured by 'coupled' models.

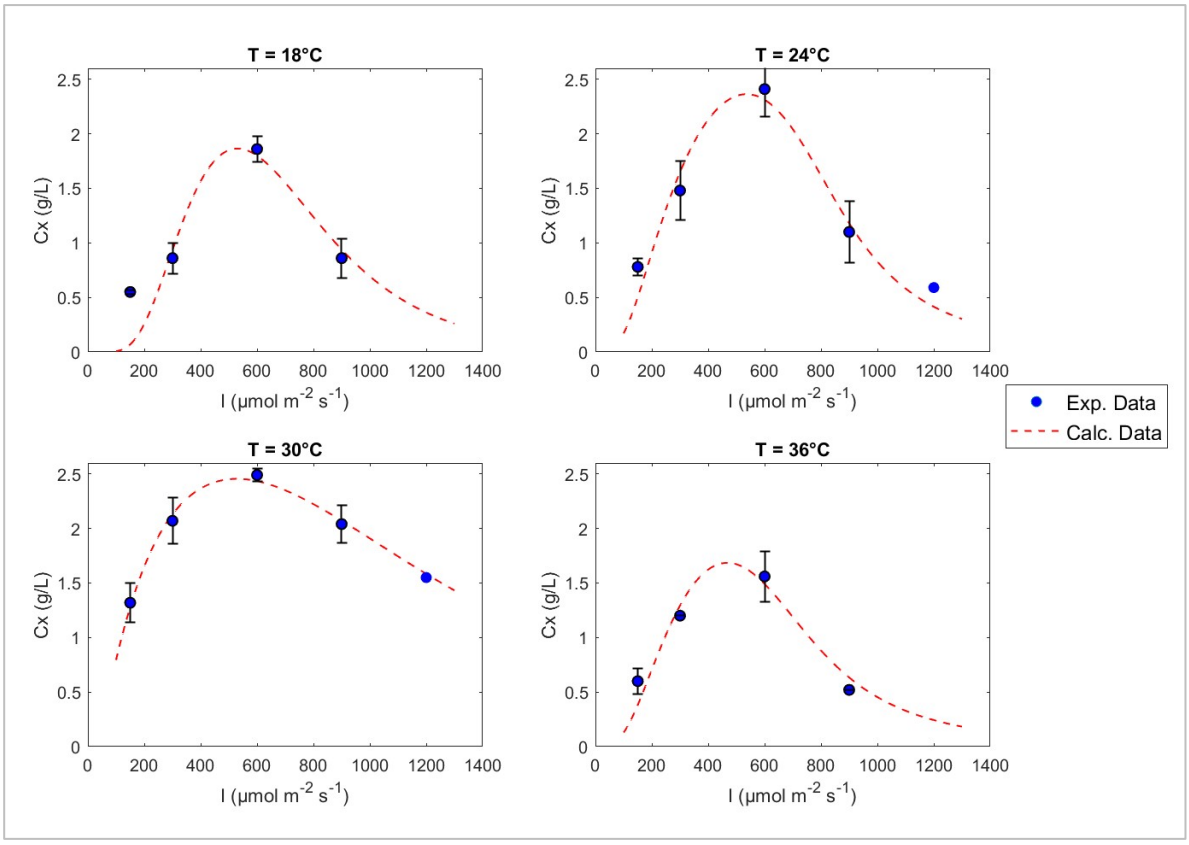

Figure 3.26. *Calculated vs experimental biomass concentration at steady-state for each temperature, separately.*

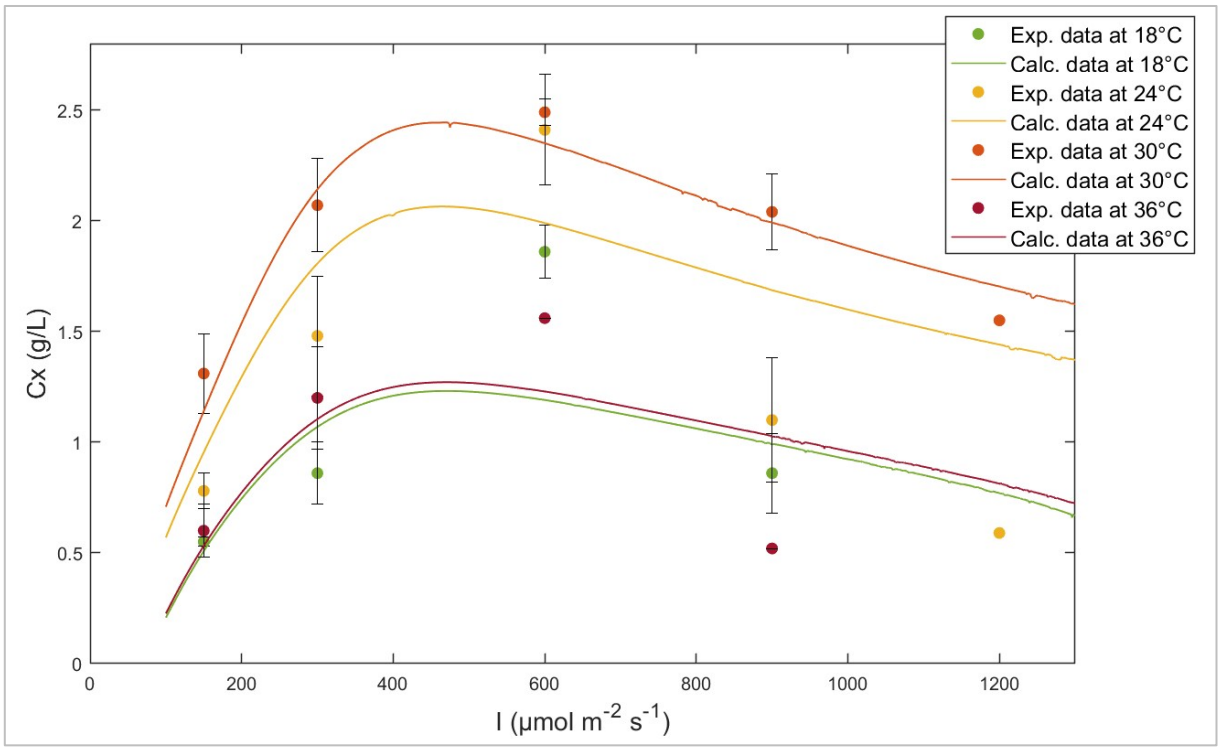

Figure 3.27. *Calculated vs experimental biomass concentration at steady-state for all temperatures fitted together.*

Table 3.5. *Estimated parameter values considering the overall data.*

I_{opt} ($\mu mol\ m^{-2}\ s^{-1}$)	K_I ($\mu mol\ m^{-2}\ s^{-1}$)	μ_{max} (day^{-1})	k_a ($m^2\ g^{-1}$)	k_d (day^{-1})	T_{max} (°C)	T_{min} (°C)	T_{opt} (°C)
331.55	400	4.93	$6 \cdot 10^{-4}$	0.37	37.98	5.00	29.53

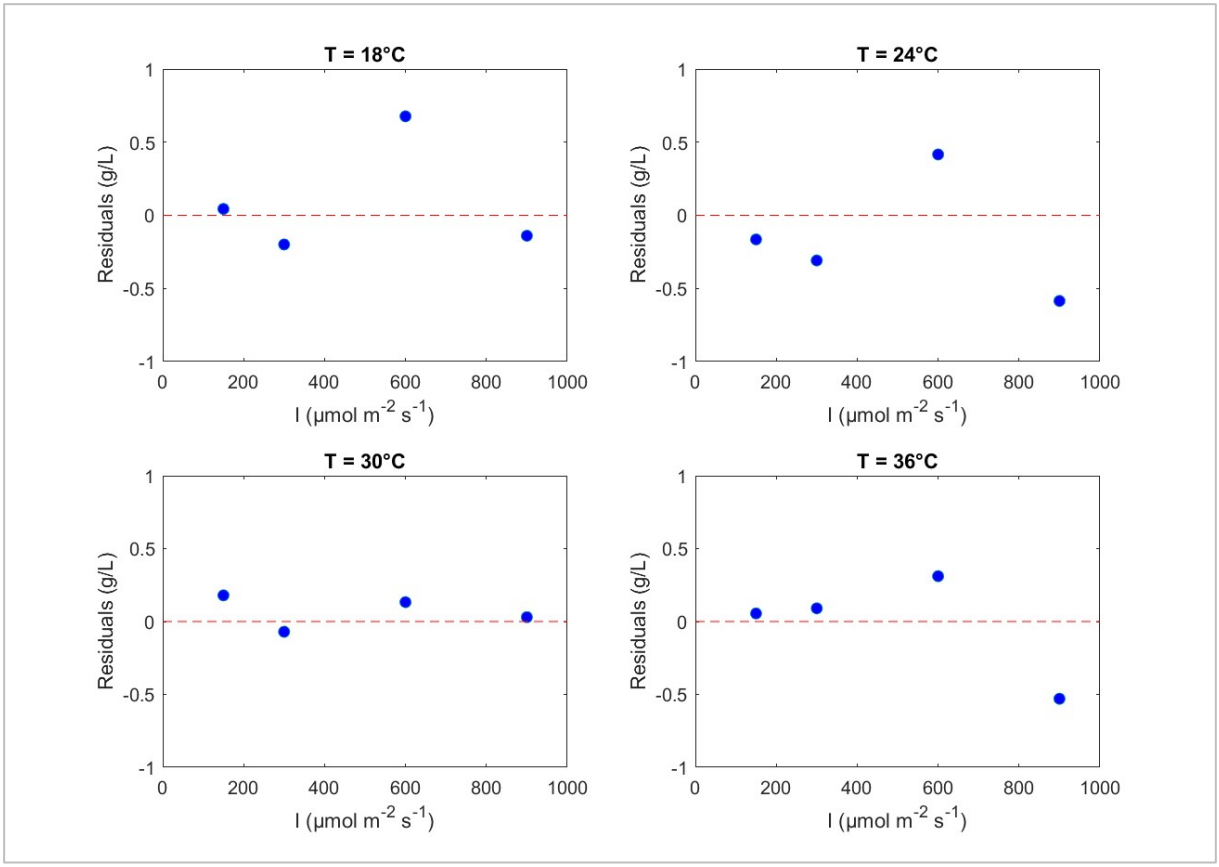

Figure 3.28. *Residuals plot at each temperature.*

Table 3.6. *R^2 values of fitting the overall data at each temperature.*

Temperature (°C)	18	24	30	36
R^2	0.56	0.67	0.96	0.48

Conclusions

The objective of this thesis was to investigate the combined impact of temperature and light intensity on the growth of the microalga *Acutodesmus obliquus*. The experiments were conducted using a 45 mL small-scale photobioreactor operated in continuous mode. The primary aim is to enhance the scaling up process, addressing the technical and economic challenges associated with microalgae industry. Consequently, analysis in concentration, measured in terms of dry weight, as well as morphological features (size and shape), and the biomass composition (pigment content) were conducted varying together light and temperature. These analyses enabled the collection of experimental data required for developing a model that could effectively describe and potentially predict the growth of the microalga under various light and temperature conditions, tailored for extrapolation to larger scales. It resulted that the designed milli-photobioreactor was effective both for a dependable small-scale depiction of larger-scale dynamics (such as the presence of the self-shading effect), and allowing for a more precise manipulation of growth conditions, resulting in resource savings, cost efficiency, and accelerated data acquisition. Growing microalgae in continuous mode facilitated the monitoring of variables that, once steady state is attained, remain constant, allowing for growth optimization based on these attributes and production of high-quality products. Experiments were conducted at different light intensities (150, 300, 600, 900, and 1200 μmol m^{-2} s^{-1}) and temperature levels (18, 24, 30, and 36 °C), with a volumetric flow rate of 30 mL day^{-1} to achieve a constant residence time of 1.3 days.

Results showed that the highest productivity at steady state was achieved at 600 μmol m^{-2} s^{-1} and 30°C, corresponding to a value of 1.66 g L^{-1} day^{-1}, which is consistent with the findings of Borella *et al*. (2021) and that combined impact of light and temperature on biomass concentration was more pronounced at higher light intensities compared to lower ones. The optimal temperature was also being confirmed by the respirometry analysis run on a culture acclimated at 30°C and 1200 μmol m^{-2} s^{-1}. Furthermore, more frequent episodes of contamination occur at high temperature, as 36°C, limiting data acquisition. Regarding biomass composition, specifically in terms of pigments, it was observed that chlorophyll content decreases as light intensity increases, and that reducing temperature made the chlorophyll content increase, especially at low light intensities. Moreover, the findings from the image analysis reveal the joined effect of light and temperature, resulting in cellular shrinkage, particularly noticeable under moderate light intensities. Conversely, the effect of temperature on cell shape (cell elongation) becomes more pronounced under conditions of either low or high irradiance. Thus, the interplay of light and temperature exhibits distinct ways contingent upon the specific aspect under consideration. This assertion was further

validated by the inadequate fitting of data using the model proposed by Bernard and Rémond (2012), especially under conditions of low temperatures and high irradiance.

Looking ahead, it would be useful to try implementing models that take into account the interactions between light and temperature, as the one by Dermoun *et al*. (1992). Moreover, investigating the effects of extreme temperatures (18°C and 36°C) under high light conditions (e.g., 1200 μmol m^{-2} s^{-1}) and studying the dynamic impact of temperature on pigments at elevated light intensities (e.g., 900 μmol m^{-2} s^{-1}) would be intriguing. Furthermore, exploring experiments involving pulsed light could offer new perspectives on how it alters the self-shading effect. Another interesting direction involves incorporating nutrient availability, the third factor influencing microalgal growth, into the existing model.

Considering all that has been explored, the insights and recommendations offered in this study provide a solid starting point for future research on the progress and sustainability of microalgae-based production methods.

References

Acién Fernández, F. G., Fernández Sevilla, J. M., & Molina Grima, E. (2013). Photobioreactors for the production of microalgae. *Reviews in Environmental Science and Bio/Technology*, **12,** 131–151. doi:10.1007/s11157-012-9307-6.

Ahmad, I., Abdullah, N., Koji, I., Yuzir, A., & Eva Muhammad, S. (2021). Evolution of Photobioreactors: A Review based on Microalgal Perspective. IOP Conference Series: *Materials Science and Engineering*, **1142**, 012004. doi:10.1088/1757-899X/1142/1/012004.

Alaswad, A., Dassisti, M., Prescott, T., & Olabi, A. G. (2015). Technologies and developments of third generation biofuel production. *Renewable and Sustainable Energy Reviews*, **51**, 1446–1460. doi:10.1016/j.rser.2015.07.058.

Albarello, A., Simionato, D., Morosinotto, T., & Bezzo, F. (2019). Model-based optimization of microalgae growth in a batch plant. *Industrial & Engineering Chemistry Research*, **58**, 5121–5130. doi:10.1021/acs.iecr.9b00270.

Andersen, R. A. (2013). The Microalgal Cell. *Handbook of Microalgal Culture*, **148**, 1–20.

Anjos, M., Fernandes, B. D., Vicente, A. A., Teixeira, J. A., & Dragone, G. (2013). Optimization of CO2 bio-mitigation by chlorella vulgaris. *Bioresource Technology*, **139,** 149–154. doi:10.1016/j.biortech.2013.04.032.

Barbera, E., E. Sforza, and A. Bertucco (2015). Maximizing the Production of Scenedesmus Obliquus in Photobioreactors under Different Irradiation Regimes: Experiments and Modeling. *Bioprocess and Biosystems Engineering*, **38**, 2177–88. doi: 10.1007/s00449-015-1457-9.

Barbera, E., Grandi, A., Borella, L., Bertucco, A., & Sforza, E. (2019). Continuous cultivation as a method to assess the maximum specific growth rate of photosynthetic organisms. *Frontiers in Bioengineering and Biotechnology*, **7**. doi:10.3389/fbioe.2019.00274.

Barbera, E., Sforza, E., Guidobaldi, A., Di Carlo, A., & Bertucco, A. (2017). Integration of dye-sensitized solar cells (DSC) on photobioreactors for improved photoconversion efficiency in microalgal cultivation. *Renewable Energy*, **109**, 13–21. doi:10.1016/j.renene.2017.03.013

Bartley, M. L., Boeing, W. J., Dungan, B. N., Holguin, F. O., & Schaub, T. (2013). Ph effects on growth and lipid accumulation of the biofuel microalgae Nannochloropsis Salina and

invading organisms. *Journal of Applied Phycology*, **26**, 1431–1437. doi:10.1007/s10811-013-0177-2.

Béchet, Q., Shilton, A., & Guieysse, B. (2013a). Modeling the effects of light and temperature on algae growth: State of the art and critical assessment for productivity prediction during outdoor cultivation. *Biotechnology Advances*, **31**, 1648–1663. doi:10.1016/j.biotechadv.2013.08.014.

Becker, E. W. (1994). *Microalgae - Biotechnology and Microbiology. Cambridge Studies in Microbiology*, **10**.

Becker, E.W. (2013). Microalgae for human and animal nutrition. *Handbook of microalgal culture: applied phycology and biotechnology*. **2**. 461–503. doi: 10.1002/9781118567166.ch25.

Benner, P., Meier, L., Pfeffer, A., Krüger, K., Oropeza Vargas, J. E., & Weuster-Botz, D. (2022). Lab-scale photobioreactor systems: Principles, applications, and scalability. *Bioprocess and Biosystems Engineering*, **45**, 791–813. doi:10.1007/s00449-022-02711-1.

Bernard, O. (2011). Hurdles and challenges for modelling and control of microalgae for CO2 mitigation and biofuel production. *Journal of Process Control*, **21**, 1378–1389. doi: 10.1016/j.jprocont.2011.07.012.

Bernard, O., & Rémond, B. (2012). Validation of a simple model accounting for light and temperature effect on microalgal growth. *Bioresource Technology*, **123**, 520–527. doi:10.1016/j.biortech.2012.07.022.

Bertucco, A., Beraldi, M., & Sforza, E. (2014). Continuous microalgal cultivation in a laboratory-scale photobioreactor under Seasonal Day–night irradiation: Experiments and simulation. *Bioprocess and Biosystems Engineering*, **37**, 1535–1542. doi:10.1007/s00449-014-1125-5.

Bordel, S., Guieysse, B., & Muñoz, R. (2009). Mechanistic model for the reclamation of industrial wastewaters using algal−bacterial photobioreactors. *Environmental Science & Technology*, **43**, 3200–3207. doi:10.1021/es802156e.

Borella, L., Sforza, E., & Bertucco, A. (2021). Effect of residence time in continuous photobioreactor on mass and energy balance of microalgal protein production. *New Biotechnology*, **64**, 46–53. doi:10.1016/j.nbt.2021.05.006.

Borella, L., Sforza, E., & Bertucco, A. (2022). An internally LED illuminated photobioreactor to increase energy conversion efficiency: Design and operation. *Energy Conversion and Management*, **270**, 116224. doi: 10.1016/j.enconman.2022.116224.

Borowitzka, M. A. (2016). Algal physiology and large-scale outdoor cultures of microalgae. *The Physiology of Microalgae*, **6**, 601–652. doi:10.1007/978-3-319-24945-2_23.

Brown, N., Shilton, A. (2014). Luxury uptake of phosphorus by microalgae in waste stabilisation ponds: current understanding and future direction. *Rev Environ Sci Biotechnol,* **13**, 321–328. doi:10.1007/s11157-014-9337-3.

Carvalho, A. P., Meireles, L. A., & Malcata, F. X. (2006). Microalgal reactors: A review of enclosed system designs and performances. *Biotechnology Progress*, **22,** 1490–1506. doi:10.1002/bp060065r.

Carvalho, A. P., Monteiro, C. M., & Malcata, F. X. (2009). Simultaneous effect of irradiance and temperature on biochemical composition of the microalga Pavlova Lutheri. *Journal of Applied Phycology*, **21**, 543–552. doi:10.1007/s10811-009-9415-z.

Chalifour, A., & Juneau, P. (2011). Temperature-dependent sensitivity of growth and photosynthesis of scenedesmus obliquus, Navicula pelliculosa and two strains of Microcystis aeruginosa to the herbicide atrazine. *Aquatic Toxicology*, **103**, 9–17. doi:10.1016/j.aquatox.2011.01.016.

Chisti, Y. (2007). Biodiesel from microalgae. *Biotechnology Advances*, **25**, 294–306. doi:10.1016/j.biotechadv.2007.02.001.

Chisti, Y. (2016). Large-scale production of algal biomass: Raceway Ponds. *Algae Biotechnology*, 21–40. doi:10.1007/978-3-319-12334-9_2.

Christenson, L., Sims, R. (2011). Production and harvesting of microalgae for wastewater treatment, biofuels, and bioproducts. *Biotechnol Adv* **29**, 686–702. doi:10.1016/j.biotechadv.2011.05.015.

Coelho, R. S., Vidotti, A. D. S., Reis, É. M., & Franco, T. T. (2014). High cell density cultures of microalgae under fed-batch and continuous growth. *Chemical Engineering Transactions*, **38**, 313–318. doi:10.3303/CET1438053.

Cruz, Y. R., Aranda, D. A. G., Seidl, P. R., Diaz, G. C., Carliz, R. G., Fortes, M. M., … Paula, R. C. V. (2018a). Cultivation Systems of microalgae for the production of biofuels. *Biofuels - State of Development*. doi:10.5772/intechopen.74957.

Da Silva, T. L., & Reis, A. (2015). Scale-up problems for the large scale production of algae. *Algal Biorefinery: An Integrated Approach*, 125–149. doi:10.1007/978-3-319-22813-6_6.

Davison, I. R. (1991). Environmental effects on algal photosynthesis: Temperature. *Journal of Phycology*, **27**, 2–8. doi:10.1111/j.0022-3646.1991.00002.x

Debnath, C., Bandyopadhyay, T. K. , Bhunia, B., Mishra, U., Narayanasamy S., & Muthuraj, M. (2021). Microalgae: Sustainable Resource of Carbohydrates in Third-Generation Biofuel Production. *Renewable and Sustainable Energy Reviews*, **150**, 111464. doi: 10.1016/j.rser.2021.111464.

Dermoun, D., Chaumont, D., Thebault, J.-M., & Dauta, A. (1992). Modelling of growth of porphyridium cruentum in connection with two interdependent factors: Light and temperature. *Bioresource Technology*, **42**, 113–117. doi:10.1016/0960-8524(92)90069-a.

Difusa, A., Talukdar, J., Kalita, M. C., Mohanty, K., & Goud, V. V. (2015). Effect of light intensity and ph condition on the growth, biomass and lipid content of microalgae scenedesmus species. *Biofuels*, **6**, 37–44. doi:10.1080/17597269.2015.1045274.

Droop, M. R. (1983). 25 Years of Algal Growth Kinetics: A Personal View. *Botanica Marina* **26**, 99–112. doi: 10.1515/botm.1983.26.3.99.

Egbo, M., Okoani, A., & Okoh, I. (2018). Photobioreactors for microalgae cultivation-An Overview. *Int J Sci Eng Res.*, ***9***, 65–74.

Egloff, S., Tschudi, F., Schmautz, Z., & Refardt, D. (2018). High-density cultivation of microalgae continuously fed with unfiltered water from a recirculating aquaculture system. *Algal Research*, **34**, 68–74. doi:10.1016/J.ALGAL.2018.07.004.

Eilers, P. H. C., Peeters, J.C.H. (1988). A model for the relationship between light intensity and the rate of photosynthesis in phytoplankton. *Ecol. Model*., **42**, 199–215. doi:10.1016/0304-3800(88)90057-9

El-Kassas, H. Y. (2013). Growth and fatty acid profile of the marine microalga picochlorum sp. grown under nutrient stress conditions. *The Egyptian Journal of Aquatic Research,* **39**, 233–239. doi:10.1016/j.ejar.2013.12.007.

Fagnol, A. (2021). Experimental analysis of the effect of different light conditions on microalgal growth in small-scale continuous photobioreactors. *Tesi magistrale in Ingegneria Chimica e dei Processi Industriali.* Dipartimento di Ingegneria Industriale, Università di Padova.

Fallahi, A., & Tavakoli, O. (2020). *Effect of Light Irradiance on Growth and Lipid Content of Microalgae Chlorella Vulgaris Grown in a Flat Panel Photobioreactor Biohydrogen production from microalgae.* The 11th International Chemical Engineering Congress & Exhibition, Fouman, Iran.

Fernández, I., Acién, F. G., Fernández, J. M., Guzmán, J. L., Magán, J. J., & Berenguel, M. (2012). Dynamic model of microalgal production in tubular photobioreactors. *Bioresource Technology*, **126**, 172–181. doi:10.1016/j.biortech.2012.08.087.

Ferro, Lorenza. (2019). Wastewater treatment and biomass generation by Nordic microalgae Growth in subarctic climate and microbial interactions. *PhD dissertation*, Umeå University.

Geider, R., MacIntyre, H., & Kana, T. (1997). Dynamic model of phytoplankton growth and acclimation: responses of the balanced growth rate and the chlorophyll a:carbon ratio to light, nutrient-limitation and temperature. *Marine Ecology Progress Series*, **148**, 187–200. doi:10.3354/meps148187.

Goldman, J. C., Azov, Y., Riley, C. B., & Dennett, M. R. (1982). The effect of pH in intensive microalgal cultures. I. Biomass Regulation. *Journal of Experimental Marine Biology and Ecology*, **57**, 1–13. doi:10.1016/0022-0981(82)90140-x.

Gonçalves, A. L., Simões, M., & Pires, J. C. M. (2014). The effect of light supply on Microalgal Growth, CO2 uptake and nutrient removal from wastewater. *Energy Conversion and Management*, **85**, 530–536. doi:10.1016/j.enconman.2014.05.085.

Gonçalves, G. C., Nazari, M. T., Magro, F. G. G., Margarites, A. C. F., & Colla, L. M. (2022). Effects of culture medium recycling in the chemical composition of Spirulina platensis biomass cultivated in semi-continuous mode. *Ciência e Natura*, **44**, 52. doi:10.5902/2179460X69474.

Gons, H. J., & Mur, L. R. (1980). Energy requirements for growth and maintenance of Scenedesmus protuberans Fritsch in light-limited continuous cultures. *Archives of Microbiology*, **125**, 9–17. doi:10.1007/bf00403192.

Gris, B., Morosinotto, T., Giacometti, G. M., Bertucco, A., & Sforza, E. (2014). Cultivation of Scenedesmus obliquus in photobioreactors: Effects of light intensities and light-dark cycles on growth, productivity, and biochemical composition. *Applied Biochemistry and Biotechnology*, **172**, 2377–2389. doi:10.1007/s12010-013-0679-z

Grivalský, T., Ranglová, K., da Câmara Manoel, J. A., Lakatos, G. E., Lhotský, R., & Masojídek, J. (2019). Development of thin-layer cascades for microalgae cultivation: Milestones (review). *Folia Microbiologica*, **64**, 603–614. doi:10.1007/s12223-019-00739-7.

Grobbelaar, J. U. (2007). Algal Nutrition - Mineral Nutrition. *Handbook of Microalgal Culture*, 95–115. doi:10.1002/9780470995280.ch6.

Guiry, M. D. (2012). How many species of algae are there? *Journal of Phycology*, **48**, 1057–1063. doi: 10.1111/j.1529-8817.2012.01222.x.

Haase, M., Osch, C. R., & Ketzer, D. (2016). GIS-based assessment of sustainable crop residue potentials in European regions, *Biomass & Bioenergy,* **86**, 156. doi:10.1016/j.biombioe.2016.01.020.

Habibi, G., & Sibi, G. (2019). Light Emitting Diode (LED) Illumination For Enhanced Growth And Cellular Composition In Three Microalgae. *Advances in Microbiology Research*, **3**, 1–6. doi: 10.24966/amr-694x/100007.

Hannon, M., Gimpel, J., Tran, M., Rasala, B., & Mayfield, S. (2010). Biofuels from algae: Challenges and potential. *Biofuels*, **1**, 763–784. doi:10.4155/bfs.10.44.

Hinshelwood, C. N. (1952). *The chemical kinetics of the bacterial cell*. Oxford: Clarendon.

Qiang, H., Richmond, A., & Zarmi, Y. (1998). Combined effects of light intensity, light-path and culture density on output rate of spirulina platensis (cyanobacteria). *European Journal of Phycology*, ***33***, 165–171. doi:10.1080/09670269810001736663

Huang, Q., Jiang, F., Wang, L., & Yang, C. (2017). Design of photobioreactors for mass cultivation of photosynthetic organisms. *Engineering*, **3,** 318–329. doi:10.1016/j.eng.2017.03.020.

Huo, S., Wang, Z., Zhu, S., Shu, Q., Zhu, L., Qin, L., Zhou, W., Feng, P., Zhu, F., Yuan, Z., & Dong, R. (2018). Biomass accumulation of Chlorella zofingiensis G1 cultures grown outdoors in photobioreactors. *Frontiers in Energy Research*, **6**. doi:10.3389/fenrg.2018.00049.

Innamorati M., Ferrari I., Marino D., Ribera D'Alcalà M. (1990). Metodi nell'ecologia del plancton marino. *Nova Thalassia*, **11**, 372.

Janssen, M. (2016). Microalgal Photosynthesis and Growth in Mass Culture. *Advances in Chemical Engineering*, **48**, 185–256. Doi:10.1016/BS.ACHE.2015.11.001.

Jeanfils, J., Canisius, M. F., & Burlion, N. (1993). Effect of high nitrate concentrations on growth and nitrate uptake by free-living and immobilized Chlorella vulgaris cells. *Journal of Applied Phycology*, **5**, 369–374. doi:10.1007/BF02186240.

Jerney, J., & Spilling, K. (2018a). Large scale cultivation of microalgae: Open and closed systems. *Methods in Molecular Biology*, 1–8. doi:10.1007/7651_2018_130.

Jin, H., Zhang, H., Zhou, Z., Li, K., Hou, G., Xu, Q., Chuai, W., Zhang, C., Han, D., & Hu, Q. (2020). Ultrahigh-cell-density heterotrophic cultivation of the unicellular green microalga Scenedesmus acuminatus and application of the cells to photoautotrophic

culture enhance biomass and lipid production. *Biotechnology and Bioengineering*, **117**, 96–108. doi.:10.1002/bit.27190

Johnson, T. J., Katuwal, S., Anderson, G. A., Gu, L., Zhou, R., & Gibbons, W. R. (2018). Photobioreactor cultivation strategies for microalgae and cyanobacteria. *Biotechnology Progress*, **34**, 811–827. doi:10.1002/btpr.2628.

Kanamarlapudi, S., Chintalpudi, V., & Muddada, S. (2018). Application of biosorption for removal of heavy metals from wastewater. *Biosorption*, **69**. doi:10.5772/intechopen.77315.

Khan, M. I., Shin, J. H., & Kim, J. D. (2018). The promising future of microalgae: Current status, challenges, and optimization of a sustainable and renewable industry for biofuels, Feed, and other products. *Microbial Cell Factories*, **17**. doi:10.1186/s12934-018-0879-x.

Khan, S., Das, P., Abdul Quadir, M., Thaher, M. I., Mahata, C., Sayadi, S., & Al-Jabri, H. (2023). Microalgal Feedstock for Biofuel Production: Recent Advances, Challenges, and Future Perspective. *Fermentation,* **9**. doi:10.3390/fermentation9030281.

Kholssi, R., P. Vogelei Ramos, E. A. N. Marks, O. Montero, and C. Rad (2021). 2 Biotechnological Uses of Microalgae: A Review on the State of the Art and Challenges for the Circular Economy. *Biocatalysis and Agricultural Biotechnology*, **36**, 102114. doi: 10.1016/j.bcab.2021.102114.

Krujatz, F., Fehse, K., Jahnel, M., Gommel, C., Schurig, C., Lindner, F., … Steingroewer, J. (2016). MicrOLED-Photobioreactor: Design and Characterization of a milliliter-scale flat-panel-airlift-photobioreactor with optical process monitoring. *Algal Research*, **18**, 225–234. doi:10.1016/j.algal.2016.06.018.

Lane, T. W. (2022). Barriers to microalgal mass cultivation. *Current Opinion in Biotechnology*, **73**, 323–328. doi:10.1016/j.copbio.2021.09.013.

Lee, E., Jalalizadeh, M., & Zhang, Q. (2015). Growth kinetic models for microalgae cultivation: A Review. *Algal Research,* **12**, 497–512. doi:10.1016/j.algal.2015.10.004.

Lee, Y. K., Chen, W., Shen, H., Han, D., Li, Y., Jones, H. D. T., Timlin, J. A., & Hu, Q. (2013). Basic Culturing and Analytical Measurement Techniques. *Handbook of Microalgal Culture: Applied Phycology and Biotechnology: Second Edition*, 37–68. doi:10.1002/9781118567166.ch3.

Lee, Y., Shen, H. (2004). Basic culturing techniques. *Handbook of Microalgal Culture*, **3**, 40–56. doi:10.1002/9780470995280.

Legrand, J., Artu, A., & Pruvost, J. (2021). A review on photobioreactor design and modelling for microalgae production. *Reaction Chemistry & Engineering*, **6**, 1134–1151. doi:10.1039/d0re00450b.

Lehmuskero, A., Skogen Chauton, M., & Boström, T. (2018). Light and photosynthetic microalgae: A review of cellular- and molecular-scale optical processes. *Progress in Oceanography*, **168**, 43–56. doi:10.1016/j.pocean.2018.09.002.

Lehr, F., & Posten, C. (2009). Closed photo-bioreactors as tools for biofuel production. *Current Opinion in Biotechnology*, **20**, 280–285. doi:10.1016/j.copbio.2009.04.004.

Lindblad, P., Fuente, D., Borbe, F., Cicchi, B., Conejero, J. A., Couto, N., … Wünschiers, R. (2019). CyanoFactory, a European consortium to develop technologies needed to advance cyanobacteria as chassis for production of chemicals and fuels. *Algal Research*, **41**, 101510. doi:10.1016/j.algal.2019.101510.

López Muñoz, I., & Bernard, O. (2021). Modeling the influence of temperature, light intensity and oxygen concentration on microalgal growth rate. *Processes*, ***9***, 496. doi:10.3390/pr9030496

Lürling, M., Mackay, E., Reitzel, K., & Spears, B. M. (2016). Editorial – a critical perspective on geo-engineering for eutrophication management in Lakes. *Water Research,* **97**, 1–10. doi:10.1016/j.watres.2016.03.035.

Ma, S., Li, D., Yu, Y., Li, D., Yadav, R. S., & Feng, Y. (2019). Application of a microalga, scenedesmus obliquus PF3, for the biological removal of nitric oxide (NO) and carbon dioxide. *Environmental Pollution,* **252**, 344–351. doi:10.1016/j.envpol.2019.05.084.

Markou, G., Vandamme, D., & Muylaert, K. (2014). Microalgal and cyanobacterial cultivation: The supply of nutrients. *Water Research*, **65**, 186–202. doi:10.1016/j.watres.2014.07.025.

Maroneze, M. M., Zepka, L. Q., Lopes, E. J., Pérez-Gálvez, A., & Roca, M. (2019). Chlorophyll oxidative metabolism during the phototrophic and heterotrophic growth of Scenedesmus Obliquus. *Antioxidants*, **8**, 600. doi:10.3390/antiox8120600.

Masojídek, J., Torzillo, G., & Koblízek, M. (2013). Photosynthesis in Microalgae. *Handbook of Microalgal Culture: Applied Phycology and Biotechnology: Second Edition*, 21–36. doi:10.1002/9781118567166.ch2.

Masojídek, J., Ranglová, K., Lakatos, G. E., Silva Benavides, A. M., & Torzillo, G. (2021). Variables governing photosynthesis and growth in microalgae mass cultures. *Processes*, **9**, 820. doi:10.3390/pr9050820.

Masojídek, J., Sergejevová, M., Malapascua, J. R., & Kopecký, J. (2015). Thin-layer systems for mass cultivation of microalgae: Flat panels and sloping cascades. *Algal Biorefineries*, 237–261. doi:10.1007/978-3-319-20200-6_7.

Mastropetros, S. G., Pispas, K., Zagklis, D., Ali, S. S., & Kornaros, M. (2022). Biopolymers production from microalgae and cyanobacteria cultivated in wastewater: Recent advances. *Biotechnology Advances*, **60**, 107999. doi:10.1016/j.biotechadv.2022.107999.

Maxwell, D. P., Falk, S., & Huner, NPA. (1995). Photosystem II excitation pressure and development of resistance to photoinhibition (I. Light-harvesting complex II abundance and zeaxanthin content in chlorella vulgaris). *Plant Physiology*, **107**, 687–694. doi:10.1104/pp.107.3.687.

Metting, F. B. (1996). Biodiversity and application of microalgae. Journal of Industrial Microbiology & *Biotechnology*, **17(5–6)**, 477–489. doi:10.1007/bf01574779.

Mohammed, K., Ahammad, S. Z., Sallis, P. J., & Mota, C. R. (2014). Energy efficient stirred-tank photobioreactors for simultaneous carbon capture and municipal wastewater treatment. *Water Science and Technology*, **69**, 2106–2112. doi: 10.2166/wst.2014.123.

Monod, J. (1949). The growth of bacterial cultures. *Annu. Rev. Microbiol*., **3**, 371–94.

Moran, R., & Porath, D. (1980). Chlorophyll Determination in Intact Tissues Using N,N-Dimethylformamide. *Plant Physiology*, **65**, 478–479. doi: 10.1104/pp.65.3.478.

Moseley, J., & Grossman, A. R. (2009). Phosphate metabolism and responses to phosphorus deficiency. *The Chlamydomonas Sourcebook*, 189–215. doi:10.1016/b978-0-12-370873-1.00014-9.

Myers, J. A., Curtis, B. S., & Curtis, W. R. (2013). Improving accuracy of cell and chromophore concentration measurements using optical density. *BMC Biophysics*, **6**. doi:10.1186/2046-1682-6-4.

Nikolaou, A., Hartmann, P., Sciandra, A., Chachuat, B., & Bernard, O. (2016). Dynamic coupling of photoacclimation and photoinhibition in a model of microalgae growth. *Journal of theoretical biology*, **390**, 61-72. doi:10.1016/j.jtbi.2015.11.004.

Paladino, O., & Neviani, M. (2020). Scale-up of photo-bioreactors for microalgae cultivation by π-theorem. *Biochemical Engineering Journal*, **153**, 107398. doi:10.1016/j.bej.2019.107398.

Pancha, I., Chokshi, K., George, B., Ghosh, T., Paliwal, C., Maurya, R., & Mishra, S. (2014). Nitrogen stress triggered biochemical and morphological changes in the microalgae Scenedesmus sp. *Bioresource technology*, **1077**. doi:10.1016/j.biortech.2014.01.025.

Perez-Garcia, O., Escalante, F. M. E., de-Bashan, L. E., & Bashan, Y. (2011). Heterotrophic cultures of microalgae: Metabolism and potential products. *Water Research*, **45**, 11–36. doi: 10.1016/j.watres.2010.08.037.

Perner-Nochta, I., & Posten, C. (2007a). Simulations of light intensity variation in photobioreactors. *Journal of Biotechnology*, **131**, 276–285. doi:10.1016/j.jbiotec.2007.05.024.

Posten, C. (2009). Design principles of photo-bioreactors for cultivation of microalgae. *Eng Life Sci,* **9**, 165–177. doi:10.1002/elsc.200900003.

Procházková, G., Brányiková, I., Zachleder, V., & Brányik, T. (2013). Effect of nutrient supply status on biomass composition of eukaryotic green microalgae. *Journal of Applied Phycology*, **26**, 1359–1377. doi:10.1007/s10811-013-0154-9.

Pultz, O. (2001). Photobioreactors: Production systems for phototrophic microorganisms. *Applied Microbiology and Biotechnology*, **57**, 287–293. doi:10.1007/s002530100702.

Pulz, O., & Gross, W. (2004). Valuable products from biotechnology of microalgae. *Applied Microbiology and Biotechnology,* **65***,* 635–648. doi:10.1007/s00253-004-1647-x.

Qin, L., Alam, Md. A., & Wang, Z. (2019). Open pond culture systems and photobioreactors for Microalgal biofuel production. *Microalgae Biotechnology for Development of Biofuel and Wastewater Treatment*, 45–74. doi:10.1007/978-981-13-2264-8_3.

Ranglová, K., Lakatos, G. E., Manoel, J. A., Grivalský, T., & Masojídek, J. (2019). Rapid screening test to estimate temperature optima for microalgae growth using photosynthesis activity measurements. *Folia Microbiologica,* **64**, 615–625. doi:10.1007/s12223-019-00738-8.

Ras, M., Steyer, J.-P., & Bernard, O. (2013). Temperature effect on microalgae: A crucial factor for outdoor production. *Reviews in Environmental Science and Bio/Technology*, **12**, 153–164. doi:10.1007/s11157-013-9310-6.

Rezayian, M., Niknam, V., & Ebrahimzadeh, H. (2019). Oxidative damage and antioxidative system in algae. *Toxicology Reports*, **6**, 1309–1313. doi:10.1016/j.toxrep.2019.10.001

Rhee, G.-Y., & Gotham, I. J. (1981). The effect of environmental factors on phytoplankton growth: Temperature and the interactions of temperature with nutrient limitation. *Limnology and Oceanography*, **26**, 635–648. doi:10.4319/lo.1981.26.4.0635.

Roopnarain, A., Gray, V. M., & Sym, S. D. (2014). Phosphorus limitation and starvation effects on cell growth and lipid accumulation in Isochrysis galbana U4 for biodiesel production. *Bioresour.Technol.,* **156**, 408–411. doi:10.1016/j.biortech.2014.01.092.

Rubio, F. C., Camacho, F. G., Sevilla, J. M., Chisti, Y., & Grima, E. M. (2002). A mechanistic model of photosynthesis in microalgae. *Biotechnology and Bioengineering*, **81**, 459–473. doi:10.1002/bit.10492.

Sajjadi, B., Chen, W.-Y., Raman, Abdul. Aziz., & Ibrahim, S. (2018). Microalgae lipid and biomass for biofuel production: A Comprehensive Review on lipid enhancement strategies and their effects on fatty acid composition. *Renewable and Sustainable Energy Reviews*, **97**, 200–232. doi:10.1016/j.rser.2018.

Seidl, P. R., Diaz, G. C., Carliz, R. G., Fortes, M. M., … Paula, R. C. V. (2018). Cultivation Systems of microalgae for the production of biofuels. *Biofuels - State of Development*. doi:10.5772/intechopen.74957.

Sforza, E., Gris, B., De Farias Silva, C. E., Morosinotto, T., & Bertucco, A. (2014). Effects of light on cultivation of Scenedesmus obliquus in batch and continuous flat plate photobioreactor. *Chemical Engineering Transactions*, **38,** 211–216. doi:10.3303/CET1438036.

Sforza, E., Urbani, S., & Bertucco, A. (2015). Evaluation of maintenance energy requirements in the cultivation of Scenedesmus obliquus: effect of light intensity and regime. *Journal of Applied Phycology*, **27**, 1453–1462. doi:10.1007/s10811-014-0460-x.

Shaikh, R., Rizvi, A., Pandit, S., Desai, N., & Patil, R. (2022). Microalgae: Classification, bioactives, medicinal properties, industrial applications, and future prospectives. An Integration of Phycoremediation Processes in Wastewater Treatment, 451–486. doi:10.1016/b978-0-12-823499-0.00004-3.

Shen, Y., Yuan W., Pei, Z. J., Wu, Q., & Mao, E. (2009). Microalgae Mass Production Methods. *Transactions of the ASABE*, **52**, 1275–1287. doi:10.13031/2013.27771.

Sili, C., Torzillo, G., & Vonshak, A. (2012). Arthrospira (spirulina). *Ecology of Cyanobacteria II*, 677–705. doi:10.1007/978-94-007-3855-3_25.

Singh, R. N., & Sharma, S. (2012). Development of suitable photobioreactor for algae production – a review. *Renewable and Sustainable Energy Reviews*, **16**, 2347–2353. doi:10.1016/j.rser.2012.01.026.

Sivakaminathan, S., Hankamer, B., Wolf, J., & Yarnold, J. (2018). High-throughput optimisation of light-driven microalgae biotechnologies. *Scientific Reports*, **8.** doi:10.1038/s41598-018-29954-x.

Staehelin, A. (1986). Chloroplast Structure and Supramolecular Organization of Photosynthetic Membranes Chloroplast structure and supramolecular organization of photosynthetic membranes, in Photosynthesis III. *Photosynthetic membranes and light-harvesting systems*, **19**, 1-84. doi:10.1007/978-3-642-70936-4_1

Stanier, R.Y., J.Deruelles, R.Rippka, M.Herdman, and J.B. Waterbury (1979). Generic Assignments, Strain Histories and Properties of Pure Cultures of Cyanobacteria. Microbiology, **111**, 1–61. doi: 10.1099/00221287-111-1-1.

Steele, J. H. (1962). Environmental control of photosynthesis in the sea. *Limnology and Oceanography*, **7**, 137–150. doi:10.4319/lo.1962.7.2.0137Limnol. Oceanogr., 7, 137–50.

Tamiya, H., Hase, E., Shibata, K., Mituya, A., Iwamura, T., Nihei, T. (1953). Kinetics of growth of Chlorella, with special reference to its dependence on quantity of available light and on temperature. Algal. Cult. Lab. Pilot. Plant., 204–32.

Theodorou, M. E., Elrifi, I. R., Turpin, D. H., & Plaxton, W. C. (1991). Effects of phosphorus limitation on respiratory metabolism in the green alga *selenastrum minutum*. *Plant Physiology*, **95**, 1089–1095. doi:10.1104/pp.95.4.1089.

Torzillo, G.; Vonshak, A. Environmental Stress Physiology with Reference to Mass Cultures. In Handbook of Microalgal Culture: Applied Phycology and Biotechnology; Richmond, A., Hu, Q., Eds.; Wiley-Blackwell: Chichester, UK, 2013; pp. 90–113.

Tredici, M. R. (2010). Photobiology of Microalgae Mass Cultures: Understanding the Tools for the Next Green Revolution. Biofuels, **1**, 143–162.

Trentin, G., Barbera, E., Bertucco, A., Georgakis, C. (2022). Experimental Test of the Design of Dynamic Experiments and Dynamic Response Surface Methodologies: Growth of a Photosynthetic Microorganism. *Industrial & Engineering Chemistry Research*, **61**, 16141-16152. doi:10.1021/acs.iecr.2c01851.

Trentin, G., Lucato, V., Sforza, E., & Bertucco, A. (2021). Stabilizing autotrophic cyanophycin production in continuous photobioreactors. *Algal Research*, **60**, 102518. doi:10.1016/j.algal.2021.102518.

Udayan, A., Pandey, A. K., Sharma, P., Sreekumar, N., & Kumar, S. (2021). Emerging industrial applications of microalgae: Challenges and future perspectives. *Systems Microbiology and Biomanufacturing*, **1**, 411–431. doi:10.1007/s43393-021-00038-8.

Vecchi, V., Barera, S., Bassi, R., & Dall'osto, L. (2020). Potential and challenges of improving photosynthesis in algae. *Plants,* **9**. doi: 10.3390/plants9010067.

Veeramuthu, A., & Ngamcharussrivichai, C. (2021). Potential of microalgal biodiesel: Challenges and applications. *Renewable Energy - Technologies and Applications*. doi:10.5772/intechopen.91651.

Wang, B., Lan, C. Q., & Horsman, M. (2012). Closed photobioreactors for production of microalgal biomasses. *Biotechnology Advances*, **30**, 904–912. doi:10.1016/j.biotechadv.2012.01.019.

Wang, S.-K., Stiles, A. R., Guo, C., & Liu, C.-Z. (2014). Microalgae cultivation in photobioreactors: An overview of light characteristics. *Engineering in Life Sciences*, **14**, 550–559. doi:10.1002/elsc.201300170

Wellburn, A. R. (1994). The spectral determination of chlorophylls a and B, as well as total carotenoids, using various solvents with spectrophotometers of different resolution. *Journal of Plant Physiology*, **144**, 307–313. doi:10.1016/s0176-1617(11)81192-2.

Witt, H.T. (1996). Primary reactions of oxygenic photosynthesis. *Berichte der Bunsengesellschaft für physikalische Chemie*, **100**, 1923-1942. doi:10.1002/bbpc.19961001202.

Wolf, S., Teitge, J., Mielke, J., Schütze, F., & Jaeger, C. (2021). The European Green Deal — more than climate neutrality. *Intereconomics*, **56**, 99–107. doi:10.1007/s10272-021-0963-z.

Wu, Q., Guo, L., Wang, Y., Zhao, Y., Jin, C., Gao, M., & She, Z. (2021). Phosphorus uptake, distribution and transformation with chlorella vulgaris under different trophic modes. *Chemosphere*, **285**, 131366. doi:10.1016/j.chemosphere.2021.131366.

Xiaogang, H., Jalalah, M., Jingyuan, W., Zheng, Y., Li, X., & Salama, E.-S. (2020). Microalgal growth coupled with wastewater treatment in open and closed systems for advanced biofuel generation. *Biomass Conversion and Biorefinery*, **12**, 1939–1958. doi:10.1007/s13399-020-01061-w.

Xin, L., Hong-ying, H., Ke, G., & Ying-xue, S. (2010). Effects of different nitrogen and phosphorus concentrations on the growth, nutrient uptake, and lipid accumulation of a freshwater microalga scenedesmus sp.. *Bioresource Technology*, **101)**, 5494–5500. doi:10.1016/j.biortech.2010.02.016.

Xing, Y., Guo, L., Wang, Y., Zhao, Y., Jin, C., Gao, M. She, Z. (2021). An insight into the phosphorus distribution in extracellular and intracellular cell of Chlorella vulgaris under mixotrophic cultivation. *Algal Research*, **60**, 102482. doi:10.1016/j.algal.2021.102482.

Xu, L., Weathers, P. J., Xiong, X.-R., & Liu, C.-Z. (2009). Microalgal bioreactors: Challenges and opportunities. *Engineering in Life Sciences*, **9**, 178–189. doi:10.1002/elsc.200800111.

Xu, N., Zhang, X., Fan, X. *et al*. Effects of nitrogen source and concentration on growth rate and fatty acid composition of Ellipsoidion sp. (Eustigmatophyta). *Journal of Applied Phycology,* **13**, 463–469 (2001). doi:10.1023/A:1012537219198

Yaakob, M.A.; Mohamed, R.M.S.R.; Al-Gheethi, A.; Aswathnarayana Gokare, R.; Ambati, R.R. Influence of Nitrogen and Phosphorus on Microalgal Growth, Biomass, Lipid, and Fatty Acid Production: An Overview. *Cells 2021*, **10**, 393. doi:10.3390/cells10020393.

Yang, F., Xiang, W., Li, T., & Long, L. (2018). Transcriptome analysis for phosphorus starvation-induced lipid accumulation in Scenedesmus SP. *Scientific Reports*, **8**. doi:10.1038/s41598-018-34650-x.

Zainith, S., Saxena, G., Kishor, R., & Bharagava, R. N. (2021). Application of microalgae in industrial effluent treatment, contaminants removal, and biodiesel production: Opportunities, challenges, and future prospects. *Bioremediation for Environmental Sustainability*, 481–517. doi:10.1016/b978-0-12-820524-2.00020-1.

Zarmi, Y., Gordon, J. M., Mahulkar, A., Khopkar, A. R., Patil, S. D., Banerjee, A., … Sapre, A. (2020). Enhanced Algal Photosynthetic Photon Efficiency by pulsed light. *iScience*, **23**, 101115. doi:10.1016/j.isci.2020.101115.

Zarrinmehr, M. J., Farhadian, O., Heyrati, F. P., Keramat, J., Koutra, E., Kornaros, M., & Daneshvar, E. (2020). Effect of nitrogen concentration on the growth rate and biochemical composition of the microalga, Isochrysis Galbana. *The Egyptian Journal of Aquatic Research,* **46**, 153–158. doi:10.1016/j.ejar.2019.11.003.

Zhang, X. (2015). Microalgae removal of CO_2 from flue gas. doi:10.13140/RG.2.2.26617.77929.

Zhang, Y., L. Ren, H. Chu, X. Zhou, T. Yao, and Y. Zhang (2019). Optimization for Scenedesmus Obliquus Cultivation: The Effects of Temperature, Light Intensity and PH on Growth and Biochemical Composition. *Microbiology and Biotechnology Letters*, **47**, 614–20. doi: 10.4014/mbl.1906.06005.

Zhu, L. (2015). Microalgal culture strategies for biofuel production: A Review. *Biofuels, Bioproducts and Biorefining*, **9**, 801–814. doi:10.1002/bbb.1576.

Zuccaro, G., Yousuf, A., Pollio, A., & Steyer, J. P. (2020). Microalgae cultivation systems. *Microalgae Cultivation for Biofuels Production*, 11–29. doi: 10.1016/B978-0-12-817536-1.00002-3.